Critical properties of the Abelian Higgs model

a Monte Carlo study

by

Joakim Hove

Thesis submitted in partial fulfillment of the requirements for the Norwegian academic degree of *Doktor Ingeniør*

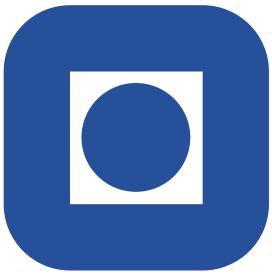

Department of Physics
Norwegian University of Science and Technology
Trondheim, Norway

URN:NBN:no-2110

URN:NBN:no-2110

Abstract

We have studied various aspects of the *critical* properties of the Abelian Higgs model. The initial motivation to study this model is its relation to superconductivity, but the results extend beyond the realms of superconductivity. This thesis contains an introductory part and three research papers, all related to different aspects of the Abelian Higgs model.

Paper 1: We have investigated the properties of the model using a dual vortex representation. By focusing on the propagators of the gauge field $\mathbf{A}$ and the dual gauge field $\mathbf{h}$ we find a nice demonstration of the fact that *the dual* of a neutral condensate is isomorphic to a charged condensate. Finally this also provides firm support for the existence of a stable charged fixed point in the theory, distinct from the 3DXY fixed point.

Paper 2: The critical fluctuations in the Abelian Higgs model are vortex loops. We have studied the geometrical properties of these loops, and by using duality we have obtained scaling relations between the fractal dimension D_{H} of the loops and the anomalous dimension η_ϕ of the dual field theory.

Paper 3: We have calculated the GL parameter κ_{tri} separating a first order metal to superconductor transition from a second order one, $\kappa_{\mathrm{tri}} = (0.76 \pm 0.04)/\sqrt{2}$. We also argue qualitatively that this κ_{tri} is the value separating type-I and type-II behavior, in contrast to the conventional value $1/\sqrt{2}$. The calculations have been done including fluctuations in the amplitude and the phase of the matter-field, as well as fluctuations in the gauge field.

paper 4: We have determined the effective interaction between vortices in the Ginzburg-Landau model from large-scale Monte-Carlo simulations. We find a change, in the form of a crossover, from attractive to repulsive effective vortex interactions in an intermediate range of Ginzburg-Landau parameters $\kappa \in [0.76, 1]/\sqrt{2}$, depending on temperature. We present a simple physical picture of the crossover, and relate it to observations in Ta and Nb elemental superconductors which have low-temperature values of κ in the relevant range.

URN:NBN:no-2110

URN:NBN:no-2110

Acknowledgment

Firstly I want to express my gratitude to Professor *Asle Sudbø*, who has been my supervisor. Asle approaches physics research with great energy and enthusiasm, and with an impressing ability to spot the interesting physics hidden under thick layers of functional integration. Asle has also been very important in promoting my numerical results to interesting physics.

During the last half of my PhD work I have cooperated closely with fellow PhD student *Sjur Mo*. Research can be a lonely game, and having Sjur down the hall has been a great asset, in addition we complement each other quite nicely in scientific terms, all in all I am very grateful for this cooperation.

The first year of my PhD studies I shared office with fellow PhD student *Anh Kiet Nguyen*, and during that year benefited greatly from Anh Kiets gentle introduction to large scale Monte Carlo simulations. In addition to Anh Kiet I have enjoyed the company of numerous other colleagues in the superconductivity group, Sai-Kong Chin, John Ove Fjærestad, Jørgen Nyhus, Professor Kristan Fossheim and Ulrik Thisted.

During the years several project and diploma students have been connected to the group. *Jo Smiseth* and *Eivind Smørgrav* have goneall the way from project students to beginning PhD students, I have enjoyedcontributing to the supervising of Jo and Eivind, and generally having them around. They are also acknowledged for critical reading of this manuscript.

In May 2001 Sjur Mo and myself spent a week with Dr. Kari Rummukainen at NORDITA in Copenhagen. Kari is an expert on lattice gauge theories, especially the computational details. The week spent with Kari was extremely helpful; we would not have been able to complete Paper III without the assistance from Kari.

My PhD work has been heavily based on numerical simulations, and reliable access to supercomputers has been essential. The supercomputing centers at UiB and NTNU are acknowledged for keeping `huge`,`ask` and `gridur` running at a steady pace. Finally *Norges Forskningsråd* is acknowledged for financial support to the supercomputing centers.

The PhD studies have been hard work, and at times I have felt uncertain whether I was really upto it. Atsuch times moral support from my dear wife Sonia, has been essential. Overall family happiness has been affected by the current progress of my PhD and I am very grateful to Sonia for loving me even those days.

My parents Knut and Veronicahave alwaysshowedgreat interest in my activities, and altough the details of my research have been beyond their comprehension this also applies to my PhD work. Their interest and long-distance moral support has been highly appreciated.

Trondheim, January 2002

Joakim Hove

URN:NBN:no-2110

URN:NBN:no-2110

Contents

List of scientific papers

Paper I: J. Hove and A. Sudbø, *Anomalous scaling dimensions and stable charge d fixed-point of typ e-II superconductors*, Phys. Rev. Lett., **84**, 3426 (2000).

Paper II: J. Hove, S. Mo and A. Sudbø, *Hausdorff dimension of critic al fluctuations in ab elian gauge the ories*, Phys. Rev. Lett., **85**, 2368 (2000).

Paper III: S. Mo, J. Hove and A. Sudbø, *The order of the metal to superconductortransition*, Phys. Rev B, **65**, 104501 (2002).

Paper IV: J. Hove, S. Mo and A. Sudbø, *Vortex Interactions and Thermally Induced Crossover from Type-I to Type-II Superconductivity* cond-mat/0202215, (submitted to Phys. Rev. B).

URN:NBN:no-2110

URN:NBN:no-2110

1 Introduction

The current chapter is a brief introduction to superconductivity in general; and to the contents of the thesis. Section 1.1 starts with an overview of the historical development, and continues to give an account of the macroscopic observable properties of superconductors. In section 1.2 the microscopic ingredients of superconductivity are briefly described. Finally section 1.3 is an introduction to coarse grained phenomenological theories of superconductivity.

The main focus of this thesis has been on the normal-superconductor transition. Many aspects of phase transitions are general, irrespective of the particular transition in question; chapter 2 contains a general introduction to phase transitions. All the original work in this thesis is based on different approaches to the Ginzburg Landau (GL) model, various aspects of this model are the topic of chapter 3. The main tool used in our investigations has been *Monte Carlo* (MC) simulations, and this technique is covered in chapter 4.

1.1 Macroscopic overview

In this section I will present superconductivity from a macroscopic point of view, i.e. the macroscopic phenomena that together constitute superconductivity.

Perfectconductivity (1911) Superconductivity was first discovered by H. Kamerlingh Onnes in 1911 [1]. What he discovered was what we can call *perfect conductivity*, i.e. that in certain metals such as mercury, lead and tin electric DC resistance vanishes *completely* below a certain temperature.

Perfectdiamagnetism (1933) The second ingredient of superconductivity was discovered in 1933; *perfect diamagnetism*. A magnetic field is not allowed to enter a superconductor. Furthermore, a magnetic field initially present in the sample will be expelled when the sample is cooled through the critical temperature[1]. This

[1] This view has later been modified; for type-II superconductors a field initially in the sample will freeze in and form a *flux line lattice*

is a fundamental property, and distinct from perfect conductivity[2]. Together the two concepts of *perfect conductivity* and *perfect diamagnetism* are the hallmarks of superconductivity.

Theoretical progress (1950 - 1960) For a long time the concept of superconductivity puzzled physicists, but during the 1950's there was great theoretical progress, and a seemingly complete understanding of the phenomenon emerged. Highlights from this period were the BCS [2] theory ,Gorkov's derivation of the GL model from the BCS theory [3], and Abrikosov's discussion of *type-II* superconductors [4], which in particular have significantly different properties in a magnetic field.

High T_c (1986) The field of superconductivity was revitalized with Bednorz and Müller's discovery of High-T_c superconductivity [5] in 1986. The superconductors known prior to Bednorz and Müller's discovery had to be cooled with liquid Helium, a procedure which is expensive and cumbersome. The High T_c superconductors can be cooled with liquid Nitrogen; a major simplification compared to Helium.

High T_c superconductivity was first found in the ceramic compound LaSrCuO, and has later been found in the similar compounds YBaCuO and BiSrCuO. Common to these materials is a *highly anisotropic* structure consisting of 2D CuO planes, high values for κ (i.e. they are all type II superconductors) and low carrier density. Ironically these superconductors are all very poor conductors, or even insulators, above the critical temperature.

As the name indicates, superconductors are perfect conductors, but from a theoretical point of view the properties in a magnetic field are even more interesting. Fig. 1.1 shows how the magnetic field lines are excluded from[3] into the interior of the superconductor.

At some magnetic field the excess energy from expelling the magnetic field will exceed the condensation energy of the superconducting condensate. At this stage the magnetic field enters the superconductor, and superconductivity is destroyed. This process can take place in two ways depending on whether it is a *type-I* or *type-II* superconductor[4]. A type-I superconductor will change abruptly to the normal phase when the magnetic field exceeds a critical field H_c. For a type-II superconductor the magnetic will enter the superconductor and form a *flux line lattice* for $H_{c_1} < H < H_{c_2}$, and then go completely normal for $H > H_{c_2}$.

In the intermediate state the superconductor is still superconducting, but the ability to carry a superconducting current is severely limited by the flux lines. The microscopic difference between type-I and type-II superconductors is whether the interaction between the flux lines is attractive or repulsive. This topic has been studied in Paper III.

[2] Consider for instance a gas of free fermions, there is no resistance in this gas, but it does not show the Meissner effect and is consequently *not* a superconductor.

[3] This is not entirely true; the magnetic field penetrates an outer layer of thickness λ which is of order 10^2 Å.

[4] In fact it is actually the other way around, the classification in type-I and type-II superconductors is based on their response to an external magnetic field.

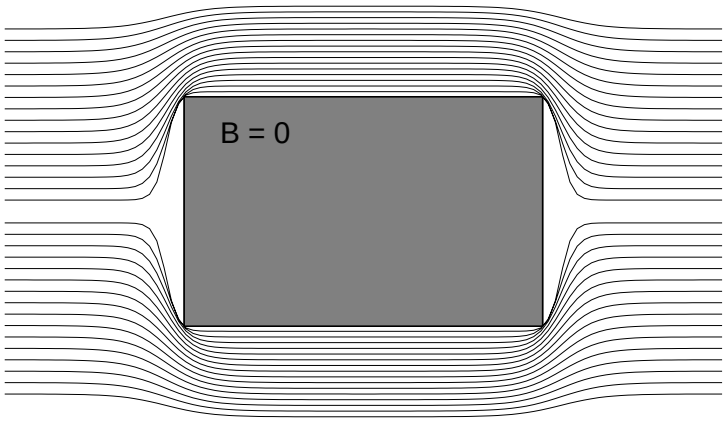

Figure 1.1: A superconductor in a weak magnetic field. The magnetic field lines go around the superconductor, and the induction in the interior of the superconductor is zero. This is a visual demonstration of the *Meissner* effect.

There are numerous industrial applications of superconductors: SQUIDs are extremely sensitive to magnetic field, High T_c superconductors are used in cellular filters to get sharp frequency response [6], in MRI superconductors are used to maintain a strong magnetic field, and in power applications superconductors are used both for distribution [7] and for transformers.

1.2 Microscopic aspects

Superconductivity is a highly nontrivial quantum mechanical problem. Due to some effective attractive electron-electron interaction a certain fraction of the electrons pair up in so called *Cooper-pairs*, forming a superconducting condensate. In *convential* superconductors like Aluminum, Tin and Lead this effective interaction is mediated by phonons [1]. Whereas in in the case of high T_c superconductors there is only limited knowledge of the pairing mechanism, however some important facts are:

d-wave: The gap function has *d*-wave symmetry [8,9] conventional *s*-wave symmetry.

AF/SC: The ground state is either a superconductor or an insulating *antiferromagnet*, depending on the doping level [10], see Fig. 1.2. This ground state is *highly exotic*, making high T_c superconductors a *regime of their own*.

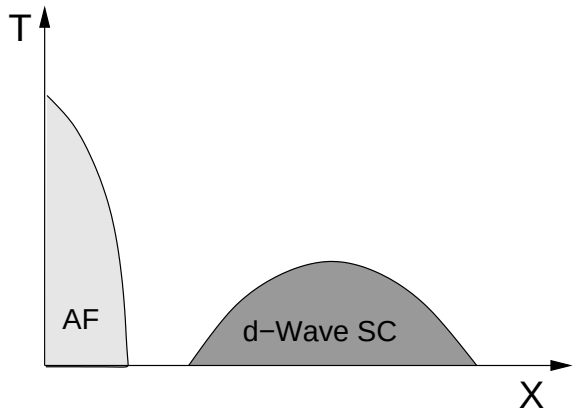

Figure 1.2: A generic phase diagram in the doping-temperature plane common for all high T_c superconductors, figure copied from [10].

Given that there is an effective attractive electron-electron interaction, the BCS [1] theory provides a very satisfying explanation of how superconductivity arises.

1.3 Phenomenological theories

The pairing of electrons into a superconducting condensate is a problem of quantum mechanics. But the question of what happens to the condensate when the temperature is increased, and more specifically: what are the properties of the superconducting $\rightarrow$ normal transition; this is generally a problem of statistical mechanics[5]. The problem is typically approached as follows:

1. Some, possibly unknown, mechanism leads to the formation of a condensate. In the case of superconductivity the universal properties of this condensate are
   (a) It is described by a *complex* field $\psi(\mathbf{r})$.
   (b) It is charged, and consequently there must be a *photon* mediating long range interactions.
   (c) The thermal properties are such that $|\psi(\mathbf{r})|$ is finite below the critical temperature, and vanishes above it.
2. A statistical mechanics model is formulated which captures the universal properties of the condensate, and this model is approached with the usual tools of statistical

[5]Of course - strictly speaking this is also a quantum mechanical problem, however at finite temperature the thermal fluctuations will by far dominate over the quantum fluctuations, and the latter are ignored.

mechanics. In our case the Ginzburg Landau model meets these requirements, but the requirements listed above are *very general* and as we shall see in chapter 3 the model can be applied to many other phase transitions as well.

In addition to superconductivity the lambda transition in ^{4}He has been treated in this fashion with *great success*[11].

URN:NBN:no-2110

2 Phase Transitions

Understanding the various phases of matter is one of the major problems in physics. We are all familiar with the phases H_2O go through upon heating; from the solid ice phase, to the liquid phase and finally to the vapor phase. Phase transitions take place in *many* different areas of physics. The topic of this thesis has been the superconductor to normal metal[1] phase transition. Important questions to consider when studying a phase transition are:

1. What is the symmetry of the disordered state, and is this symmetry broken in the ordered state.
2. What is the order of the phase transition, and in the case of second order transitions what are the critical exponents, i.e. the universality class.
3. What is the mechanism behind the transition. This is specially applies to continuous transitions, where the universal properties are determied by *critical fluctuations*.

The underlying principle, that the equilibrium state minimizes free energy, and the resulting competition between entropy and energy is considered in section 2.1. Section 2.2 is devoted to the important concept of symmetries, and broken symmetries. In section 2.3 we will present the difference between first order and second order transitions. The last two sections, 2.4 and 2.5 are devoted to critical phenomena.

2.1 Phase transitions and Free Energy

The concept of an order parameter is very important when studying phase transitions. Most[2] phase transitions can be formulated as *order/disorder* transitions. The low tem-

[1] Will use the term "metal", although at least some of the High-T_c materials have very exotic normal states, quite different from ordinary metals.

[2] Theories with *local symmetries*, the GL model being the prime example, are exceptions. For these theories it is impossible to define a local order parameter, also global order parameters are fraught with difficulties, and the whole concept of an order parameter is less useful. Nevertheless it still makes sense to speak of an ordered and a diordered state in the sense that the ordered state has *low entropy* and the disordered state has *high entropy*.

perature state is *ordered*, indicated by a finite value for the order parameter, andthe high temperature state is *disordered*with a vanishing order parameter. The Helmholtz Free energy very clearly reveals the main principles in a transition between order and disorder

$$F = E - TS. \tag{2.1}$$

The equilibrium state minimizes F, and as we can we see from Eq. 2.1 this is achieved by minizing E and maximizing S. However these two are conflicting goals. Generally the internal energy is minimized by forming an ordered state with low entropy. On the other hand the entropy is maximized by forming a completely random state, which leads to an increase in energy with respect to the ordered state. The results is that for low temperatures the energy dominates over entropy leading to an *ordered* state, whereas for high temperatures the situation is opposite. Clearly the transition occurs when the equilibrium state changes from an energy dominated state to an entropy dominated one. For some models, like the 1D ising model there is no finite temperature transition; for these model the disordered state will be favored for any $T > 0$.

2.2 Broken symmetries

Most models in statistical physics have *symmetries*, i.e. the microscopic state ψ can be transformed, while the configurational energy $H(\psi)$ remains invariant. Let Λ be a *faithful* representation of the symmetry group $\mathcal{G}$, then $H(\psi)$ has a $\mathcal{G}$ symmetry if

$$H(\Lambda\psi) = H(\psi). \tag{2.2}$$

The *Ising* and XY models have a Z_2 and $U(1)$ symmetry respectively. The configuration energy for these two models, along with representations of the Z_2 and $U(1)$ symmetries are shown in Eq. 2.3 and 2.4:

$$H_I = -\sum_{\langle i,j\rangle} s_i s_j \qquad s_i \to -s_i \qquad Z_2, \tag{2.3}$$

$$H_{XY} = -\sum_{\langle i,j\rangle} \cos(\theta_i - \theta_j) \qquad \theta_i \to \theta_i + \varphi \qquad U(1). \tag{2.4}$$

Let us consider the order parameter for the Ising model,

$$\langle m(\psi)\rangle = \frac{1}{V}\sum_{\mathbf{x}} s(\mathbf{x}). \tag{2.5}$$

In the disordered state $\langle m(\psi)\rangle = \langle m(\Lambda\psi)\rangle = 0$ and $\langle m(\psi)\rangle$ has the same symmetry has

the configuration energy[3]. However in the ordered state the system has chosen a value[4] for $\langle m(\psi)\rangle$ spontaneously, and $\langle m(\psi)\rangle \neq \langle m(\Lambda\psi)\rangle$. In this case the state of the system no longer possesses the symmetry of the Hamiltonian, and we say that the symmetry has been *spontaneously broken*.

To see how a spontaneous symmetry breaking can take place we consider the two Ising states ψ_A and ψ_B which are related by spin reversal. The magnetization of the two states is M_0 and $-M_0$ respectively. In zero field the probability to find the system in the two states is equal, i.e. $P_A = P_B$. When we couple the spins to a symmetry breaking magnetic field h this degeneracy is lifted, and the probability to find the system in state ψ_A is given by

$$P_A = \frac{e^{\beta M_0 h N}}{e^{\beta M_0 h N} + e^{-\beta M_0 h N}}. \tag{2.6}$$

Here N is the number of spins in the system. If we now *first* consider the limit $N \to \infty$ and then subsequently the limit $h \to 0^+$ Eq. 2.6 yields $P_A = 1$. By going to the $N \to \infty$ limit with a finite H, we effectively ban the system from part of phase space[5], and when we later let $h \to 0^+$ the system is still confined to this part of phase space. The end result is that $\langle m(\psi)\rangle$ has been spontaneously chosen[6] to the value M_0.

It is crucial to understand that:

1. The $N \to \infty$ limit is *required* to get spontaneous symmetry breaking. Mathematically the spontaneous loss of symmetry is singular behaviour, i.e. the ordered and disordered state are seperated by a singularity. For any finite N the ordered and disordered states can be analytically connected.

2. The limits $N \to \infty$ and $h \to 0^+$ do *not* commute; the limit $N \to \infty$ *must* be taken first.

Both the symmetries in Eq. 2.3 and 2.4 are *global*, in the sense that we must transform *all* the spins to leave the action invariant. If we couple the matter field to a gauge field, we can make the symmetry *local*, in the sense that a transformation involving only a finite number of spins can leave the action invariant. The Ginzburg Landau model has a *local* $U(1)$ symmetry, local symmetries can never be spontaneously broken [12]. This means that non gauge-invariant quantities are bound to zero by symmetry.

[3] We say that the *state* ψ has the full symmetry of $H(\psi)$, and for this reason the disordered state is also called the *symmetric* state. At the level of individual spins the state of the system is clearly *not* invariant, but the statistical properties are invariant.

[4] In the case of the ising model this is just a choice between $+m_0$ and $-m_0$.

[5] For this reason spontaneous symmetry breaking is also described as ergodicity breaking.

[6] Of course in this case the choice was facilitated by the limit $h \to 0^+$, $h \to 0^-$ would have given the opposite result. In nature this is accomplished by infinitesimal fields from an inevitable imperfection of some kind.

2.3 The order of a phase transition

The most common classification of the order of phase transitions is that transitions with a finite latent heat are *first order*, and the remaining are *continuous*[7] [13]. When we go through a first order transition from disordered side, we change to a "fully developed" ordered state, whereas for a second order transition the ordering *starts* at the critical point.

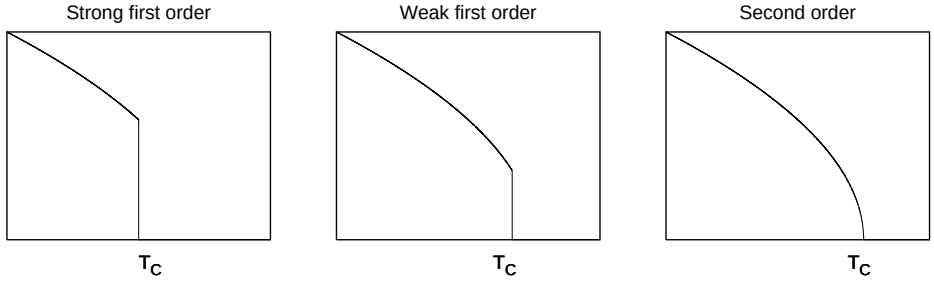

Figure 2.1: A schematic illustration of the order parameter behavior with temperature for a strong first order, weaker first order, and continuous transition.

The vertical jumps indicated in Fig. 2.1 are between two distinct phases with the same free energy. If we go to the right in Fig. 2.1, i.e. to weaker and weaker first order transitions, we eventually come to a *critical point*, where the phases which were distinct coalesce into one. At this point the transition has changed to second order, or continous.

2.4 Critical phenomena

When the ordered state and the disordered state can no longer be distingushed we have a critical point. For the remaining part of of this chapter we will consider spin models like Eq. 2.3 and 2.4, but with an additional symmetry breaking field $\mathbf{h}$ conjugate to the order parameter. In what follows m is the order parameter, and $t = |T - T_c|$ is the distance from the critical point. For a system to be critical both t and h must be tuned to $(0, 0)$.

2.4.1 Scaling and critical exponents

The spesific heat diverges at the critical point. This is not just any divergence, it is a *power law* governed by the *critical exponent* α, i.e. $C_V \propto |T - T_c|^{-\alpha}$. Many

[7] In most cases the continuous are *second* order, but we can also have anomalies like the KT transition which can be considered as infinite order.

other thermodynamical quantities also diverge as pow er laws with accompanying critcial exponents, they are listed in table 2.1.

Quantity			Definiton	Critical point	
C_V	$\propto$	$\frac{\partial^2 f}{\partial T^2}$	$\lvert T-T_c\rvert^{-\alpha}$	$T \to T_c^{\pm}$	$h=0$
χ	$\propto$	$\frac{\partial^2 f}{\partial h^2}$	$\lvert T-T_c\rvert^{-\gamma}$	$T \to T_c^{\pm}$	$h=0$
m	$\propto$	$\frac{\partial f}{\partial h}$	$\lvert T-T_c\rvert^{\beta}$	$T \to T_c^{-}$	$h=0$
m	$\propto$	$\frac{\partial f}{\partial h}$	$\lvert h\rvert^{1/\delta}$	$T = T_c$	$h \to 0^{\pm}$
$G(r)$	$\propto$	$\langle m(0)m(r)\rangle - \langle m\rangle^2$	$r^{-(d-2+\eta)}$	$T = T_c$	$h=0$
$G(r)$	$\propto$	$e^{-r/\xi}, \quad \xi \propto \lvert T-T_c\rvert^{-\nu}$		$T \to T_c^{\pm}$	$h=0$

T able 2.1: Critical exponents along with their definition.

The six critical exponents listed in table 2.1 are *not* independent, in 1963 Rushbrooke used basic thermodynamics, along with some quite reasonable assumptions to show that the six exponents must satisfy four inequalities [13,14]. Experiments indicated that the inequalities were indeed satisfied as equalities, and in 1965 Widom [15] put forward the generalized homogeneity assumption

$$f_s(|t|,h) \propto b^{-d} f_s(|t|b^{1/\nu}, hb^{\lambda_h}) \tag{2.7}$$

assumed to be valid close to the critical point $(t,h) = (0,0)$. In Eq. 2.7, f_s is the *singular* part of the free energy densit y,and b is an arbitrary scaling factor. From this h ypothesis it is quite simple to derive scaling relations relating the six exponents, reducing the number of independent exponents to two. The scaling relations are derived b y differentiation according to table 2.1, combined with a suitable choice of the scaling factor b. F or the exponent α the derivation is as follows:

$$C_V \propto \frac{\partial^2 f}{\partial t^2} = b^{2/\nu - d} f^{(2)}(|t|\, b^{1/\nu}, hb^{\lambda_h}). \tag{2.8}$$

The next step is to set $h = 0$ and *choose* $b = |t|^{-\nu}$, this gives

$$C_V \propto |t|^{d\nu-2}\, f^{(2)}(1,0), \tag{2.9}$$

and we can identify $\alpha = 2 - d\nu$. If w e proceed in the same manner for the other exponents w e can express*all* of them in terms of the unknown exponents ν and λ_h

$$\alpha = 2 - d\nu \quad \gamma = \nu(2\lambda_h - d) \quad \delta = \frac{1}{d/\lambda_h - 1} \quad \beta = \nu(d - \lambda_h). \tag{2.10}$$

From Eq. 2.10 we can eliminate the dependence on λ_h and ν, and we find the following relations relating the remaining four exponents

$$\alpha + 2\beta + \gamma = 2, \tag{2.11}$$
$$\alpha + \beta(\delta + 1) = 2, \tag{2.12}$$

these scaling laws are called Rushbrook and Griffiths laws. The four exponets α, β, γ and δ can all be derived from the free energy, and are also called the *thermodynamic exponents* Kadanoff [16] pointed out that two further relations, which were already seen to be satisfied by experiments, could be understood if we assume the form

$$G(r,t) = \frac{\Phi(rt^{\nu})}{r^{d-2+\eta}} \tag{2.13}$$

for the two-point correlation function. In Eq. 2.13 $\Phi(z)$ is a scaling function with the properties

$$\Phi(z) \propto \begin{cases} C & z \ll 1 \\ z^{d-2+\eta} e^{-z} & z \gg 1. \end{cases} \tag{2.14}$$

From the *Fluctuation Dissipation* theorem we know that the susceptibility χ is equal to the spatial integral of $G(r,t)$, and sufficiently close to the critical point this gives

$$\chi \propto \int \mathrm{d}\mathbf{r} G(r,t) = \int \mathrm{d}\mathbf{r} \Phi(rt^{\nu}) r^{1-\eta}. \tag{2.15}$$

We introduce $z = rt^{\nu}$ and rewrite Eq. 2.15 as

$$\chi \propto t^{-\nu(2-\eta)} \underbrace{\int \mathrm{d}z \Phi(z) z^{1-\eta}}_{I}. \tag{2.16}$$

In Eq. 2.16 I is a numerical integral without temperature dependence, and we can identify the scaling of the prefactor with γ.

$$(2-\eta)\,\nu = \gamma \tag{2.17}$$
$$\nu d = 2 - \alpha \tag{2.18}$$

The two equations Eq. 2.17 and 2.18 are called Fishers and Josephons scaling relations respectively. Josephons scaling relation is also called *hyperscaling*, and is the only scaling relation with explicit dependence on d. For $d > d_c$ it breaks down.

Grouping the exponents

The description of phase transitions in terms of an order parameter, and a configuration energy is not unique. For instance both of the models

$$Z = \int \mathcal{D}\theta e^{\beta \sum_{\langle i,j \rangle} \cos(\theta_i - \theta_j)} \tag{2.19}$$

and

$$Z = I_0(\beta)^{3N} \sum_{\{\mathbf{b}(\mathbf{x})\}} \delta_{\nabla \mathbf{b}(\mathbf{x}),0} e^{-\sum_{\mathbf{x},i} \ln\left(I_{b_i(\mathbf{x})}(\beta)/I_0(\beta)\right)} \tag{2.20}$$

describe the phase transition in a $3D$ magnetic model of planar spins[8]. Since Eq. 2.19 and 2.20 are such *widely different* parameterisations there is no reason why the critical exponents should be the same. On the other hand an experimentalist can *measure* both C_V and α, and both representations Eq. 2.19 and 2.20 should reproduce the correct value of α. Consequently it seems fruitful to split the exponents in two groups:

α, ν	*Universal* exponents spesific for the particular transition.
$\eta, \beta, \delta, \gamma$	Exponents that depend on the description chosen.

The exponents in the last group "transform as a subgroup", i.e. they can change numerical value *without* affecting the value of α or ν. By expressing α and ν in terms of the other exponents we find that the following combinations of exponents must be invariant

$$\frac{\gamma}{2-\eta} \qquad 2\beta + \gamma \qquad \beta(\delta + 1) \tag{2.21}$$

when the *same transition* is described with different representations. This is what happens in both Paper I and Paper II where the same transition is described with two different theories which have different stable fixed points.

2.4.2 Limits of critical exponents $\to$ 1. order transitions

The diverging correlation length, and the resulting scale-invariance and critical exponents is a property of second order phase transitions. For first order transitions the correlation length stays finite, and consequently there is no scale-invariance nor critical exponents. From quite simple principles it is possible to calculate bounds for some of the critical exponents, and as we shall see below these limits correspond to the critical exponents we obtain if we formally consider first order transitions.

[8] Eq. 2.20 is the *character representation* of the XY model [17].

Lower bound for η

We go back to the integral in Eq. 2.15 and insert the scaling ansatz Eq. 2.14 explicitly. Right at the critical point $t = 0$, and we insert $\Phi(rt^\nu) = C$. The spatial dependence is a pure power law

$$\chi \propto \int_0^L \mathrm{d}r r^{1-\eta} \propto L^{2-\eta}. \tag{2.22}$$

Clearly χ can *not* divergefaster with system size than $\chi \propto L^d$, and consequently we must have $\eta \geq 2 - d$.

Lower bound for β

The order parameter should vanish at the critical point, i.e.

$$\lim_{|t|\to 0} |t|^\beta = 0 \quad \Rightarrow \beta > 0, \tag{2.23}$$

on the other hand a discontinuous jump, i.e. a first order transition, would correspond to $\beta = 0$.

Upper bound for α

There is no latent heat ΔE for a continous phase transition, i.e.

$$\Delta E = \int_{-\Delta t}^{\Delta t} \mathrm{d}t\, |t|^{-\alpha} \propto 2\Delta t^{1-\alpha}, \tag{2.24}$$

must vanish in the limit $\Delta t \to 0$. Consequently we must have $\alpha < 1$. For a first order transition there is a *finite* latent heat, which corresponds to $\alpha = 1$. All in all this gives the following bounds on the critical exponents

$$\alpha < 1, \quad \eta > 2 - d, \quad \nu > \frac{1}{d}, \quad \beta > 0, \quad \gamma > 1, \quad \frac{1}{\delta} > 0. \tag{2.25}$$

Especially the bounds in Eq. 2.22 and 2.23 along with the formal continuation to first order transitions was used in Paper II and Paper III.

2.5 Renormalization

The divergencies at the critical point are *not* just any arbitrary divergence, they are governed by *critical exponents*, i.e they are *power laws*. The important aspect of power laws is that they are *scale free*, meaning that there is no natural intrinsic length scale in the system. This qualitative insight is the foundation of *Renormalization Group*

(RG) theory. The idea is to to study how the system transforms under a length scale transformation, and then find a fixed point for this transformation. At the fixed point the system is self-similar, i.e. critical. RG is *not* a canned method, it is more a way of thinking, and the actual implementation must be carefully adapted to the problem at hand[9]. It is used in many different fields of physics, and there is an extensive literature on the topic [13, 19–23]. Below I will just sketch two situation where RG is applied, the first is quite simple and intuitive, the second is important to understand the field theories we have considered in Paper III.

Real space RG

The real space RG technique consists of summing out short distance fluctuations, and then subsequently rescaling the lattice constant with a factor b^{-1} to recover the original lattice. It is not the most frequently used approach for actual computations of critical exponents, but demonstrates the underlying principles nicely. The formation of *block spins* is shown schematically in Fig. 2.2.

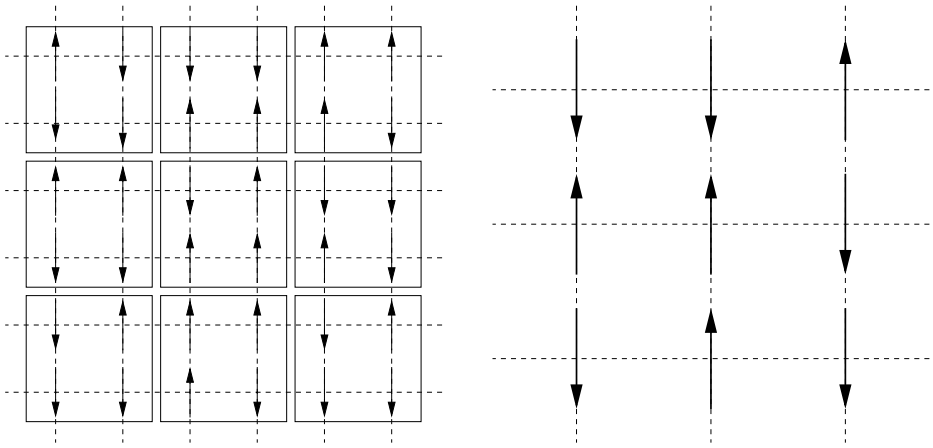

Figure 2.2: The left part shows a 2D lattice of ising spins, in the right part the lattice has been coarse grained, and the direction of each *block spin* is given by the net direction of the spins in 2×2 block to the left. In the case of a draw, the value of the upper left spin is used.

The transformation shown in Fig. 2.2 is straightforward to implement "visually", but to actually calculate nontrivial critical properties in this manner is cumbersome. One approximate method is the Migdal-Kadanoff procedure [24]. From the simple algorithm demonstrated in Fig. 2.2 it is evident that the method lends itself quite naturally to Monte Carlo simulations [25].

[9] In [18] there is an entertaining banter over the unfortunate use of the definite article "the" in conjunction with renormalization theory.

For the remaining part of this section we will consider a general situation, where the system has been transformed by summing out fluctuations on a length scale $< b$, and then see what general results we get from this. Actual calculations are quite complicated and outside the scope of this introduction.

We start very generally with an action S which is parametrized by the couplings $\{K\}$

$$S = K_1 O_1 + K_2 O_2 + K_3 O_3 + \cdots, \quad Z = \mathsf{Tr} e^{-S(\{K\})}. \tag{2.26}$$

In Eq. 2.26 O_i are general operators[10]. Observe that there is no explicit temperature dependence in Eq. 2.26, i.e. for simple spin models a factor β^{-1} has been absorbed in the couplings. Furthermore, we assume that the model has a continuous phase transition[11], and that there exists a transformation

$$\{K'\} = \mathcal{R}(\{K\})$$

in the space of couplings, and further that this transformation has a fixed point

$$\{K^*\} = \mathcal{R}(\{K^*\}),$$

corresponding to the critical point. Close to the fixed point we assume that the transformation can be *linearized* about the fixed point

$$K'_i - K^*_i = \sum_i T_{ij} \left(K_j - K^*_j\right), \quad T_{ij} = \left.\frac{\partial K'_i}{\partial K_j}\right|_{\{K\}=\{K^*\}}. \tag{2.27}$$

We *assume* that T can be diagonlized and denote the eigenvalues λ^μ and the *left* eigenvectors by e^μ, we can then form the linear combinations

$$u_\mu = \sum_i e^\mu_i \left(K_i - K^*_i\right) \tag{2.28}$$

which transform as

$$u'_\mu = \sum_{i,j} e^\mu_i T_{ij} \left(K_j - K^*_j\right) = \lambda^\mu u_\mu = b^{y_\mu} u_\mu. \tag{2.29}$$

As indicated in Eq. 2.29 it is convenient to write λ^μ as b^{y_μ}, where y_μ are called RG eigen values. We group scaling fields u_μ and RG eigenvalues y_μ together, and determine whether u_μ is *relevant* depending on the sign of y_μ:

$y_\mu > 0$: u_μ is a *relevant* scaling field, in the sense that u_μ according to Eq. 2.29 grows under rescaling, a coupling K_μ which deviates only slightly from the critical value will then flow *away* from K^*_μ, and the system as a whole is *not* critical. The reduced temperature and conjugated field are always examples of *relevant* scaling fields.

[10] In the case of spin models O_i typically correspond to nearest-neighbor interaction, next-nearest-neighbour interactions, multi-spin interactions and so on.

[11] The RG theory can not be used to determine whether there is a continous phase transition; this must be given.

$y_\mu < 0$: u_μ is a *irrelevant* scaling field, the deviation from the critical value will vanish upon continued rescaling. An example of an irrelevant variabel is the (finite) anisotropy parameter Γ in a spin model; although the critical state is generally isotripic we will *not* destroy criticality by starting out with $\Gamma \neq 1$.

Irrelevant scaling fields may give rise to *corrections* to scaling which apply some distance from the critical point [18], finally *dangerous* irrelavant variables indeed affect the fixed point properties [18, 26].

$y_\mu = 0$: u_μ is a *marginally* relevant scaling field, which may, or may not, be of interest.

A physical way explaining the distinction between relevant and irrelevant scaling fields is that the relevant scaling fields correspond[12] to variables which the experimentalist must carefully tune to find a critical point, whereas she can simply ignore the irrelevant. One of the properties of the RG is that the partition function is preserved [18]. Close to the fixed point we can ignore all the irrelevant scaling fields, and the *singular* part of the free energy density satisfies

$$f_s(u_t, u_h) = b^{-d} f_s(b^{y_t} u_t, b^{y_h} u_h). \tag{2.30}$$

If we identify the scaling fields u_t and u_h with t and h respecitively[13], and $\lambda_t = 1/\nu$ we immediately recognize Widoms homogeneity assumption Eq. 2.7. That the homogeneity assumption and scaling laws follow as a natural consequence, are one of the great successes of RG theory [13].

RG applied to field theories

A *very* different application of RG is on continuum field theories like the Ginzburg Landau theory, and ϕ^4 theory .The partition function for these theories is defined by a functional integral

$$Z = \int \mathcal{D}\phi e^{-S(\phi)}, \quad S(\phi) = \int \mathrm{d}\mathbf{x} \left[\frac{1}{2} |\nabla\phi|^2 + m^2 |\phi|^2 + u |\phi|^4 \right], \tag{2.31}$$

i.e. the sum of all possible values of ϕ at all points in space with the weight given by $S(\phi)$. Now clearly it does not make sense to sum over all paths $\phi(\mathbf{x})$, the system of interest has an inherent microscopic scale, and we must limit the set of functions $\{\phi(\mathbf{x})\}$ to those which are smooth on this distance. To facilitate this we introduce an *arbitrary* length scale Λ^{-1}, and only consider functions that can be expressed as

$$\phi(\mathbf{x}) = \int_0^\Lambda \mathrm{d}\mathbf{k} e^{i\mathbf{k}\mathbf{x}} \tilde{\phi}(\mathbf{k}), \tag{2.32}$$

[12] Observe that due to the coupling Eq. 2.28 the scaling fields will generally be linear *combinations* of the original variables like pressure and temperature.

[13] The spin models, which we have adopted as example here, are particularly simple because T is diagonal, at least for the relevant eigenvalues.

i.e. functions which are smooth on length scales $\lesssim \Lambda^{-1}$. This process of "controlling" the functional integral is called *regularization*. The regularization introduces an arbitray parameter Λ, which is clearly unsatisfactory. It is desirable to reexpress the theory in such a manner that measurable quantities are independent of this arbitrariness, this is achieved by *renormalization*.

3 The Ginzburg Landau model

The Ginzburg Landau (GL) model, or Abelian Higgs model as it is called in particle physics, is a *metamodel* which is used to describe *many* [27] different phase transitions at a phenomenological level. In its most general form it consists of a matter-field ϕ coupled to a gauge field $\mathbf{A}$ which mediates long range interactions.

Depending on the properties of the matter, ϕ can be for instance complex scalar (Superconductivity) or a tensor (Liquid Crystals).

This thesis is entirely based on various approaches to the critical properties of the GL model. In this chapter we will present various aspects which have been important in our approach. Section 3.1 is a presentation of the model, and we performe a naive saling analysis to obtain a dimensionless description. Section 3.2 is a brief historical account of the *order* of the phase transition in the GL model. Topological defects in the form of vortex lines and loops are very important excitations in the GL model, they are the topic of section 3.3 and in section 3.4 we construct a *dual* theory which has these vortices as the primary objects. Section 3.5 deals with an interacting *gas of loops*, the GL model can be used as an effective theory for this gas. Section 3.6 contains a discussion the the RG flow diagram, and finally section 3.7 contains the discrete model used for simulations in Paper III.

3.1 Representation of the model

The model was first written down in 1950 by Ginzburg and Landau [35], their approach was based purely on physical intution [36], with no detailed knowledge of the superconducting state. Although it is now to *some extent* possible to *derive* [3, 37] the GL equations from the microscopical BCS theory we will generally consider the parameters of theory as *free*.

The GL model can be written in *many* different ways, in the superconductivity littera-

ture it is customarily written as an energy-functional with dimensional quantities

$$H(\psi,\mathbf{A}) = \int \mathrm{d}\mathbf{r}\left[\alpha(T)\left|\psi\right|^2 + \frac{u}{2}\left|\psi\right|^4 + \frac{\hbar^2}{2m^*}\left|\left(\nabla - ie^*\mathbf{A}\right)\psi\right|^2 + \frac{1}{2\mu_0}\left(\nabla\times\mathbf{A}\right)^2\right]$$
$$Z = \int \mathcal{D}\psi\mathcal{D}\mathbf{A}e^{-\beta H(\psi,\mathbf{A})}. \tag{3.1}$$

Here $\alpha(T) = \alpha_0\tau, \tau = (T - T_{\mathsf{MF}})/T_{\mathsf{MF}}$ is a temperature dependent parameter which drives the system through a phase transition. T_{MF} is the mean-field critical temperature where the superconducting condensate is formed[1]. m^* and e^* are effective mass and charge for a cooper pair[2], and u is a self-coupling, to have $u > 0$ is essential to stabilize the low-temperature properties of the theory

If we ignore spatial fluctuation in the fields in Eq. 3.1 the integrand in $H(\psi,\mathbf{A})$ becomes a *free energy* density, and $\psi(T)$ can found as the value maximizing f,

$$\left|\psi(T)\right| = \begin{cases}\psi_0\left|\tau\right|^{\frac{1}{2}} & T < T_{\mathsf{MF}}\\ 0 & T > T_{\mathsf{MF}}\end{cases}, \quad \psi_0 = \sqrt{\frac{\alpha_0}{u}}. \tag{3.2}$$

For $T < T_{\mathsf{MF}}$ we see from Eq. 3.2 that ψ attains a finite value. When ψ has a finite value, the gauge field $\mathbf{A}$ acquires a *dynamical* mass $m_{\mathbf{A}}$ through the *Higgs mechanism* [38–40]. In terms of interactions the Higgs mechanism means that the the electromagnetic interactions are *screened* with a screening length $\lambda \sim m_{\mathbf{A}}^{-1}$[3].

In addition to the length scale λ, the order parameter varies spatially on a length scale ξ, the correlation length. At the mean field level λ and ξ are given by

$$\lambda(T) = \underbrace{\sqrt{\frac{m^*u}{4(e^*)^2\mu_0\alpha_0}}}_{\lambda_0}\left|\tau\right|^{-\frac{1}{2}}, \quad \xi(T) = \underbrace{\sqrt{\frac{\hbar^2}{2m^*\alpha_0}}}_{\xi_0}\left|\tau\right|^{-\frac{1}{2}}, \tag{3.3}$$

i.e. they both diverge at the critical point with critical exponents $1/2$. The fraction $\kappa = \lambda/\xi$ is a material parameter which determines the superconductors response to an external magnetic field. At the mean field level the separation between type-I and type-II superconductors is at the value $\kappa = 1/\sqrt{2}$, however we argue in Paper III that fluctuations reduce this value to $\kappa \approx 0.76/\sqrt{2}$. Although the spesific values, and in

[1] In conventional superconductors thermal fluctuations are not important. Then Eq. 3.1 might be approximated with the saddle point approximation, and T_{MF} coincides with the true critical temperature. For high T_c superconductors an *incoherent* condensate is formed at T_{MF}, whereas superconductivity is not realized until this condensate is *coherent* at $T_C < T_{\mathsf{MF}}$. This intermediate regime is called the *pseudogap regime*, and T^* is often used to denote T_{MF}.

[2] It is actually possible to derive the GL equations [1] from BCS theory in a suitable limit [3, 37], and in that way give more precise values for e^* and m^*. However the real strength of the GL model is nevertheless to predict *universal* properties.

[3] Of course the Higgs mechanism is the underlying effect for the *Meissner effect*.

particular the critical exponents of 1/2 in Eq. 3.3 are wrong, the defintion of λ and ξ as the length scales of the magnetic field and order parameter variations, and the ratio κ, will still be used when fluctuations are included.

To reduce the number of parameters in Eq. 3.1 it is convenient to define rescaled fields and couplings through the following *replacements*

$$\mathbf{A} \to \sqrt{\frac{\mu_0}{\beta}}\mathbf{A}, \quad e^* \to \sqrt{\frac{\beta}{\mu_0}}e, \quad \psi \to \sqrt{\frac{2m^*}{\beta\hbar^2}}\psi, \quad \frac{m^*\alpha(T)}{2\beta\hbar^2} \to m^2, \quad u \to \frac{\beta\hbar^4}{2\left(m^*\right)^2}u. \tag{3.4}$$

Then Eq. 3.1 is replaced by the expression

$$\begin{aligned} Z &= \int \mathcal{D}\mathbf{A}\mathcal{D}\psi \exp(-S(\mathbf{A},\psi)) \\ S &= \int \mathrm{d}\mathbf{r}\left[\left|(\nabla - ie\mathbf{A})\,\psi\right|^2 + m^2|\psi|^2 + u|\psi|^4 + \frac{1}{2}\left(\nabla\times\mathbf{A}\right)^2\right]. \end{aligned} \tag{3.5}$$

In Eq. 3.5 we have a dimensionless *action* $S(\psi,\mathbf{A})$ instead of the dimensionful *energy function* $H(\psi,\mathbf{A})$ in Eq. 3.1. All the individual terms in the integrand of $S(\psi,\mathbf{A})$ carry dimension L^{-d}, and the individual *naive* scaling dimensions of fields and couplings are as follows

$$[\psi] = L^{\frac{1-d}{2}}, \quad [\mathbf{A}] = L^{1-\frac{d}{2}}, \quad [u] = L^{d-2}, \quad \left[m^2\right] = L^{-1}, \quad [e] = L^{\frac{d}{2}-2}. \tag{3.6}$$

If we express all dimensionful quantities in terms of the coupling q, we can introduce dimensionless fields and couplings by making the following replacements,

$$\psi \to \psi e^{-1}, \quad \mathbf{A} \to \mathbf{A}e^{-1}, \quad \mathbf{r} \to \mathbf{r}e^2, \quad m^2 \to ye^4, \quad u \to xe^2. \tag{3.7}$$

Then we get the final action

$$S = \int \mathrm{d}\mathbf{r}\left[\left|(\nabla - i\mathbf{A})\,\psi\right|^2 + y\left|\psi\right|^2 + x\left|\psi\right|^4 + \frac{1}{2}\left(\nabla\times\mathbf{A}\right)^2\right]. \tag{3.8}$$

with the dimensionless coupling constants x and y, and where all fields are dimensionless.

3.2 The transition

In the original expression Eq. 3.1 the transition was driven by $\alpha(T)$ which changes sign at T_{MF}, in Eq. 3.8 the whole concept of a mean-field critical temperature does not make sense any more. However the transition is still driven by the term in front of $|\psi|^2$, i.e. y. At the mean field level this means that the transition is at $y = 0$, fluctuations will modify this value, the value of y_c depends on x, and is a decreasing function of x [41]. The parameter x corresponds to κ^2, and we will use x and κ interchangeably.

The GL model is complex, and even the question of the *order* of the transition has been nontrivial to settle. At the mean field level the effect of the gauge field vanishes, and Eq. 3.5 reduces to $|\phi|^4$ theory. This theory has a continuous transition both at the mean field level and also when fluctuations are taken into account. When considering the various approximate approaches to the transition it is convenient to divide the degrees of freedom in three categories: gauge field $\mathbf{A}$, amplitude $|\psi|$ and phase $\arg[\psi]$. The various approximations then consist of including the fluctuations in only *some* of these fields, this is summarized in table 3.1.

From table 3.1 one can conclude that *there is* a $\kappa_{\rm tri}$ separating the first order and second order transistion, and the next question is the numerical value of this κ. In 1982 Hagen Kleinert [46] calculated $\kappa_{\rm tri} \approx 0.80/\sqrt{2}$ using a dual approach, and in 1983 John Bartholomew [47] found $\kappa_{\rm tri} \approx 0.4/\sqrt{2}$ with Monte Carlo simulations. A short review of this question can be found in [48], finally our Paper III is devoted to calculating $\kappa_{\rm tri}$. We find $\kappa_{\rm tri} \approx 0.76/\sqrt{2}$ using Monte Carlo simulations.

3.3 Vortices and flux lines

Vortices and flux lines are essential elements of superconductivity. In type-II superconductors the magnetic field penetrates the superconductor in terms of *flux lines* or flux tubes. Vortices are singular phase fluctuations, and determine the critical properties of the theory.

3.3.1 Vortices in neutral theories

To introduce vortices we will start with the simpler $|\phi|^4$ theory, which has the Hamiltonian density

$$\mathcal{H} = \frac{1}{2}|\nabla\phi|^2 + \underbrace{m^2|\phi|^2 + u|\phi|^4}_{V(|\phi|)}. \tag{3.9}$$

Eq. 3.9 has a global $U(1)$ symmetry, i.e. $\mathcal{H}$ is invariant under the transformation

$$\phi(\mathbf{x}) \to e^{i\Lambda}\phi(\mathbf{x}). \tag{3.10}$$

The vacuum state is the one which minimizes the potential energy $V(|\phi|)$ and is constant in space. For $m^2 > 0$ this is the solution $|\phi_0| = 0$, but for $m^2 < 0$ there is an infinite set of vacuum states $|\phi_0| = \sqrt{-m^2/2u}$ which are related by the symmetry transformation Eq. 3.10. This set $\mathcal{M}$ of vacua is called the *vacuum manifold*, in the case of $U(1)$ symmetry $\mathcal{M} \sim S^1$.

Let us now consider a classical solution[4] where ϕ approaches different points in $\mathcal{M}$ in different spatial directions:

[4] To be a solution the field configuration must approach the vacuum asymptotically at spatial infinity [49].

Description	Fluctuations	Order
1: A t the pure mean-field lev el the model reduces to the $\|\psi\|^4$ theory, i.e. the effect of the gauge field vanishes completely.	None	2. order
2: $\|\psi\|^4$ theory is a well known theory, which is muc h studied [42].	$\|\psi\|, \arg[\psi]$	2. order
3: T o study the effect of the gauge field Halperin, Lubensky and Ma [43] integrated out the gauge field exactly, this giv es a cubic term in the remaining effective ϕ theory .This is a sound approach in the $\kappa \ll 1$, i.e. strongly type-I regime.	$\mathbf{A}$	1. order
4: In 1981 Dasgupta and Halperin [44] studied the combined effects of phase and gauge field fluctuations, *excluding* amplitude fluctuations. They deriv ed various duality relations, and introduced the concept of an *inverte d*XY transition. Excluding the amplitude fluctuations is a valid approximation in the $\kappa \gg 1$, i.e. strongly type-II regime.	$\arg[\psi], \mathbf{A}$	2. order
5: For the superconductors present at the beginning 1980's the critical region is extremely narrow, and the predicted jump across the first order transition very small. Consequently the question was difficult to settle experimentally . However there is an isomorphism betw eensuperconductors and liquid crystals [30, 43], and on this system experiments can be done [45].	$\|\psi\|, \arg[\psi], \mathbf{A}$ (Experiment)	1. **and** 2. order

Table 3.1: A schematic view of some important results regarding the *order* of the phase transition in the GL model. Especially from cases 3 and 4 one can conclude that there must be a κ_{tri} sepa rating first order and second order transitions. It is also important to realize that a correct description of this feature of the GL model requires a *full descprition*, including fluctuations in $|\psi|, \arg[\psi]$ and $\mathbf{A}$.

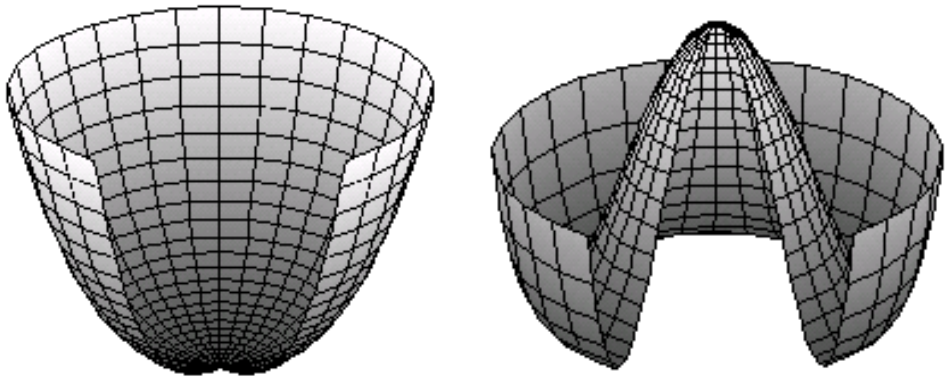

Figure 3.1: The potential $V(|\phi|)$ for $m^2 > 0$ and $m^2 < 0$. In the first case the minimum is unique, whereas in the second case there is an infinite number of equivalent minimum characterized by different values of $\arg[\phi_0]$. These different minima can be transformed into each other by Eq. 3.10.

$$\phi(r,\theta) = |\phi(r)|\, e^{i\theta} \tag{3.11}$$

This solution is everywhere continuous except in a subspace of dimensionality $d_s = d - d_\phi$, where d_ϕ is the "dimensionality" of ϕ, i.e 2 in our case, the subspace with a singular $\phi(r)$ is then a point in $d = 2$ and a line in $d = 3$. If we encircle the singular point/line the phase of ϕ changes by 2π, this phase change is *topologically stable*, in the sense that we must make *global* changes in ϕ to recover the true vacuum state, and it is called a *vortex*. The amplitude $|\phi(r)|$ is left unspecified in Eq. 3.11, but to avoid divergences we must require $|\phi(r)| \to 0$ in the core of the vortex [17]. The size of the vortex core is given by ξ, and for $r \gg \xi$ $|\phi(r)|$ approaches a constant. In lattice theories the vortices will live on the *dual lattice* where the original variables are not defined, and hence the vanishing amplitude in the vortex core is not an issue. Since vortices are mostly a phase phenomena, pure phase models capture this degree of freedom perfectly.

The energy a single vortex diverges linearly with system size, and is consequently not a particularly relevant excitation[5]. However *vortex-pairs* with opposite charge have much lower energy and are very important[6]. The famous Kosterlitz-Thouless [50] transition in the 2DXY model is an unbinding of vortex pairs, whereas the 3D transition is a

[5] It should be noted that *periodic boundary conditions*, which are the most commonly used boundary conditions in simulations, explicitly rule out the possibility of single vortices in 2D, or vortex lines which end in the interior of the sample in 3D.

[6] The 3D generalization of two point charges is a unit loop.

vortex-loop *blowout* [51, 52]. The difference between a single vortex and a pair with opposite charge is illustrated in Fig. 3.2. That the energy density of a single vortex only decays algebraically also means the vortices interact through *long range* interactions.

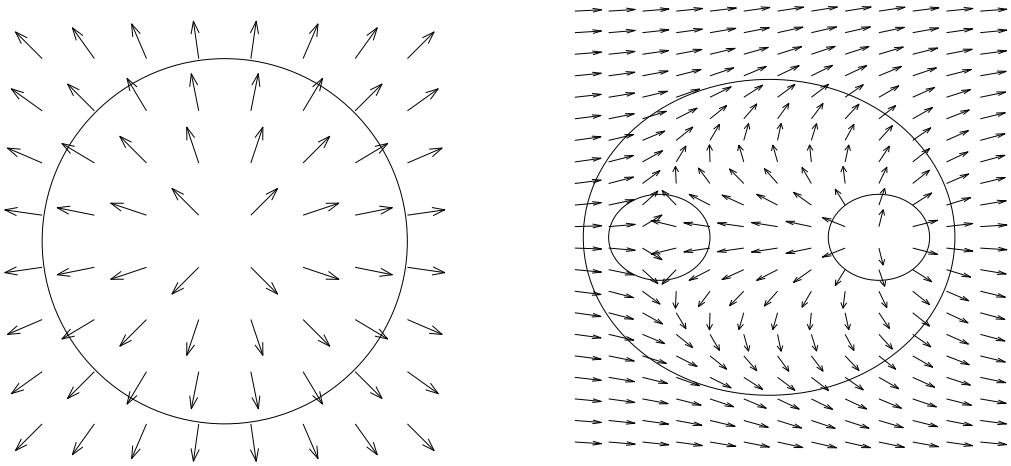

Figure 3.2: To the left is a single vortex of charge $+1$, if we integrate the phase along the circle we pick up a phase change of 2π, furthermore we observe that the effect of the vortex in the interior is felt all the way to the edges. To the right is a pair of vortices of charge ± 1, if we encircle *one* of these vortices along one of the small paths we pick up a phase change of $\pm 2\pi$, wheras the phase change along the large path is zero. Finally, outside of the large circle the effect of the vortex pair is not felt.

3.3.2 Vortices in charged theories

The GL model is a gauge theory with a *local symmetry* also for these models topological excitations in the form of vortices are important, but due to the local gauge symmetry the interpretation in terms of a phase field is more subtle; for instance it is always possible to carry out a transformation into the *unitary gauge*, where $\arg[\phi]$ is a constant everywhere in space [49]. The natural generalization of the $U(1)$ vortices to gauge theories are Abrikosov flux tubes [4] or Nielsen-Olesen vortices as they are called in the particle physics community [53]

$$\phi(r,\theta,z) = |\phi_0|\, e^{iN_W\theta} f(\lambda/e^2, e\,|\phi_0|\, r), \quad A_\mu(r,\theta,z) = -\frac{N_W}{er}\hat{\theta}_\mu a(e\,|\phi_0|\, r). \tag{3.12}$$

N_W is an integer, and $a(z)$ and $f(z)$ are functions which must be determined numerically, they vanish for $z \to 0$ and approach unity for $z \to \infty$. In addition to the phase singularity, and vanishing order parameter along the core, these vortices also *carry*

magnetic flux,

$$\Phi = \lim_{R\to\infty} \oint_{|\mathbf{r}|=R} \mathrm{d}\mathbf{r}\mathbf{A} = -N_W \frac{2\pi}{e}. \tag{3.13}$$

In the context of superconductivity they are called *Abrikosov flux tubes*, and they are the object responsible for the magnetic flux penetrating type-II superconductors. The magnetic field decays with a characteristic length λ away from the vortex. The two chracteristic lengths ξ and λ are illustrated in Fig. 3.3.

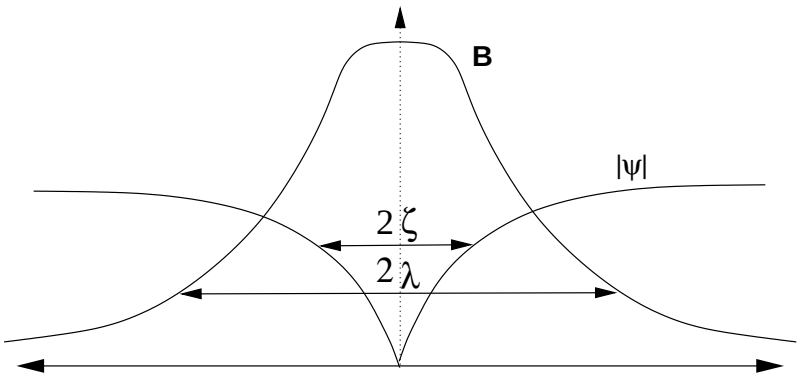

Figure 3.3: Schematic figure of a $|\psi(r)|$ and $\mathbf{B} = \nabla \times \mathbf{A}$ around a vortex, along with the characteristic lengths ξ and λ.

Due to the fluctuating gauge field the energy density of Nielsen-Olesen vortex decays exponentially, and consequently the vortex-vortex interactions are *screened* with a characteristic length λ. The origin of this screening is the Higgs mechanism, which renders the gauge field massive, i.e. $m_{\mathbf{A}} \sim 1/\lambda$[7]. Note the somewhat paradoxical situation that vortices in a neutral theory interact with long-range interactions, whereas the vortices in a charged theory have short range interactions. This will be a recurring theme which we will meet again several times when we discuss charged and neutral theories in relation to duality in sections 3.4 and 3.5.

In the remaining part of the chapter we will present various approximations to the GL model, common for all these approaches is that the vortices, and their properties, are correctly retained.

[7] In the superconductivity literature it is usually called the *Meissner* effect due to Meissner who discovered perfect diamagnetism. But the origin of the perfect diamagnetism is the Higgs mechanism, which is a general mechanism for dynamic mass creation.

3.4 Duality

In 1941 Kramers and Wannier [54] formulated a *dual* version of the 2D Ising model on a square lattice by constructing a set of new variables living on the *links* of the original lattice, this particular model turns out to be *self-dual* and it is a simple exercise both to derive the dual model, and the critical coupling β_c [55]. The generalization to different lattices and interactions, was carried out by F. Wegner [56].

In general a dual model has the following features:

1. The dual variables live on a lattice which is dual to the original, see Fig. 3.4
2. The strong coupling and weak coupling states are interchanged, in terms of conventional statistical mechanics. This means that the dual theory will have an effective *dual temperatur* $e \beta_d(\beta)$ with the properties $\lim_{\beta\to\infty} \beta_d(\beta) = 0$ and $\lim_{\beta\to 0} \beta_d(\beta) = \infty$.

   One consequence of this property is that a strongly coupled problem which is difficult to attack with perturbative methods might be more manageable in the dual weak-coupling formulation.

The dual theory is generally constructed by identifying the important fluctuations which *destroy order* in the original theory. These excitations are the primary objects of the dual theory, in the ordered state, the density of these excitations is low, whereas in the disordered state they proliferate. On this background one can also consider the dual theory as a *disorder* theory , and the dual order parameter as a *disorder-parameter*[8] in contrast to a conventional order parameter.

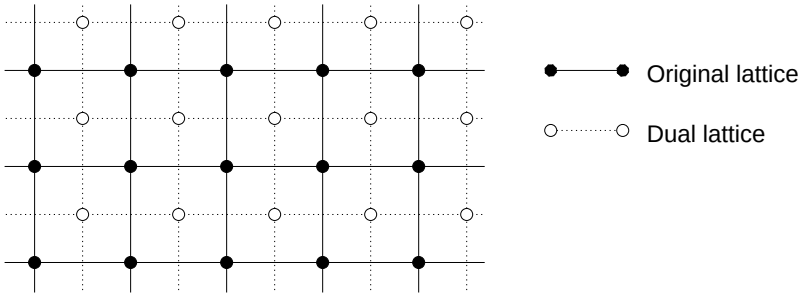

Figure 3.4: A superposition of a 2D square lattice and its dual counterpart. The dual lattice is made by translating every lattice point half a lattice constant in all directions. Clearly a second duality transformation will lead back to the original lattice.

As described in section 3.3 vortices are very important fluctuations in the GL model. Reformulating the theory so that these highly non local excitations become the primary

[8] This of course only applies when the dual theory is expressed in terms of original coupling constants.

objects is the foundation of the dual approach. This transformation has been performed in many different ways in the literature [57–60].

3.4.1 Lattice transformation

The actual duality transformation is exact, but some approximations must be done before we can make analytical headway. Starting with Eq. 3.5 the first approximation is in defining the model on a lattice and replacing all derivative with finite-difference operators[9], this gives us:

$$S(\psi, \mathbf{A}) = a^3 \beta \sum_{\mathbf{x}} \left[\alpha(T) \left|\psi\right|^2 + \frac{u}{2} \left|\psi\right|^4 + \frac{\hbar^2}{2m^* a^2} \left|\left(\Delta - ie^* \mathbf{A}\right) \psi\right|^2 + \frac{1}{2\mu_0 a^2} \left(\Delta \times \mathbf{A}\right)^2 \right] \tag{3.14}$$

We then make the *London approximation*

$$\psi \to \left|\psi_0\right| e^{i\phi}, \quad \left|\psi_0\right| \text{ is uniform in space.} \tag{3.15}$$

There are two important limitations arising from this approximation:

1. For small x values the GL model has a first order transition between the normal state and the superconducting state. Amplitude fluctuations are an essential ingredient in this transition, and consequently the dual theory can *not* give correct predictions in this part of the phase diagram[10] [44, 61].

2. To have a superconducting condensate two requirements must be met:

   (a) We must have a finite amplitude $|\psi(r)|$, i.e. a condensate of Cooper-pairs must exist.

   (b) This condensate must be *coherent*.

   By fixing the amplitude we ignore the requirement in point 2a, and take the existence of a condensate as given. This is generally a valid approximation as superconductivity is destroyed when the condensate is *incoherent*, and not when the amplitude vanishes [51].

[9] We will initially keep a finite lattice constant a, i.e.

$$\partial_\mu f(\mathbf{x}) \to \frac{1}{a} \left(f(\mathbf{x} + a\hat{\mu}) - f(\mathbf{x})\right) = \frac{1}{a} \Delta_\mu f(\mathbf{x})$$
$$\int \mathrm{d}\mathbf{r} \to a^3 \sum_{\mathbf{x}}$$

, but the a will eventually be set to unity.

[10] Actually Hagen Kleinert does this [46], however this requires additional approximations.

Furthermore we replace $\mathbf{A}$ and e^* according to Eq. 3.4

$$S(\psi, \mathbf{A}) = \sum_{\mathbf{x}} \left\{ \frac{\beta J}{2} \left| (\Delta - ie\mathbf{A}) e^{i\phi} \right|^2 + \frac{1}{2} (\Delta \times \mathbf{A})^2 \right\}, \quad J = \frac{a\psi_0^2 \hbar^2}{m^*}. \tag{3.16}$$

The final step is to expand the kinetic term in Eq. 3.16,

$$\left| (\Delta_\mu - ie\mathbf{A}) e^{i\phi} \right|^2 \to \left| e^{i\phi(\mathbf{x}+a\hat{\mu}) - iaA_\mu} - e^{i\phi(\mathbf{x})} \right|^2 = 2 \left[1 - \cos \left(\Delta_\mu \phi(\mathbf{x}) - eaA_\mu(\mathbf{x}) \right) \right]. \tag{3.17}$$

This way we are guaranteed that the lattice model has the same local $U(1)$ symmetry as the continuum model. We ignore the the constant term from Eq. 3.17, and set $J = 1$. Then the model is the 3DXY model coupled to a gauge field

$$S = -\beta \sum_{\mathbf{x},\mu} \cos \left(\phi(\mathbf{x} + \hat{\mu}) - \phi(\mathbf{x}) - eaA_\mu(\mathbf{x}) \right) + \frac{1}{2} (\nabla \times \mathbf{A})^2. \tag{3.18}$$

Now the remaining part of the duality transformation is explained in great detail in Appendix A, here I will just sketch some essential elements in the transformation:

1. The cos - function is replaced with a quadratic form and an auxiliary integer using the Villain approximation.

2. The kinetic energy is decoubled using the Hubbard Stratonovich decoubling.

3. The Poisson summation formula, along with the curl identity $\nabla \cdot (\nabla \times \mathbf{G}) = 0$ is used several times.

The end-result is the following theory of interacting vortex loops

$$Z(\beta) = \int \mathcal{D}\mathbf{h} \sum_{\mathbf{m}}{}' \exp \left[- \sum_{\mathbf{x}} \left\{ 2\pi i \mathbf{m} \cdot \mathbf{h} + \frac{1}{2\beta} (\nabla \times \mathbf{h})^2 + \frac{e^2}{2} \mathbf{h}^2 \right\} \right], \tag{3.19}$$

Here the $\mathbf{m}$ field is a set of integer valued vortex segments forming closed loops, and $\mathbf{h}$ is a *dual gauge field* mediating interactions betw eenthe vortex segments. The $\mathbf{h}$ was originally introduced as an auxiliary field, but in the dual theory it appears as a gauge field in the same manner as the $\mathbf{A}$ field appears in the original theory. This identification will be clear when we have discussed the continuum dual model and properties of charged and neutral theories in general in sections 3.4.2 and 3.4.3. Again we see that an originally charged theory (with $e \neq 0$) will have a *massive* $\mathbf{h}$ field, and consequently screened interactions, whereas the interactions will be *long-r ange*in a originally neutral theory. The dual gauge field can be integrated out exactly to yield an effective vortex theory Eq. A.20 and A.21, in this form the model has been extensively used for simulations [62–66].

By adding source terms $\mathbf{J_A}$ and $\mathbf{J_h}$ which couple to $\mathbf{A}$ and $\mathbf{h}$ respectively, we can also calculate the correlation functions $\langle \mathbf{A_q A_{-q}} \rangle$ and $\langle \mathbf{h_q h_{-q}} \rangle$. The derivations are sketched in Appendix A, and the we find

$$\langle \mathbf{A_q A_{-q}} \rangle = \frac{1}{|\mathbf{Q}|^2 + m_0^2} \left(1 + \frac{4\pi^2 \beta m_0^2 \langle \mathbf{m_q m_{-q}} \rangle}{|\mathbf{Q}|^2 \left(|\mathbf{Q}|^2 + m_0^2 \right)} \right), \tag{3.20}$$

$$\langle \mathbf{h_q h_{-q}} \rangle = \frac{2\beta}{|\mathbf{Q}|^2 + m_0^2} \left(1 - \frac{2\beta\pi^2 \langle \mathbf{m_q m_{-q}} \rangle}{|\mathbf{Q}|^2 + m_0^2} \right) \tag{3.21}$$

where $m_0 = \lambda^{-1}$ and $Q_\mu = 1 - e^{-i\mathbf{q}\cdot\hat{\mu}}$. These correlation functions were studied in Paper I. All correlation functions have been calculated in the *transverse gauge* $\nabla \cdot \mathbf{A} = \nabla \cdot \mathbf{h} = 0$. Both of the fields $\mathbf{h}$ and $\mathbf{A}$ are renormalized by vortex fluctuations, albeit in quite different ways. The correlation functions Eq. 3.20 and 3.21 will be studied in more detail at the end of Section 3.4.3. The vortex-vortex correlator $\langle \mathbf{m_q m_{-q}} \rangle$ can be calculated quite simply from a simulation of the vortex model, and then Eq. 3.20 and 3.21 can be used to calculate $\langle \mathbf{A_q A_{-q}} \rangle$ and $\langle \mathbf{h_q h_{-q}} \rangle$.

3.4.2 Continuum dual model

In the previous section we have performed a lattice duality transformation from Eq. A.5 to Eq. A.20 and A.21, ultimately we would like a *continuum* dual model, i.e. the dual of Eq. 3.5. Based on the lattice derivation this can be achieved by "a backward identification" and one additional (uncontrolled) approximation, the presentation below is mostly based on [67, 68]. The key point is to compare the equations

$$Z(\beta) = \int \mathcal{D}\mathbf{A} \sum_{\mathbf{b}}{}' \exp\left[-\sum_{\mathbf{x}} \left\{ \frac{1}{2\beta}\mathbf{b}^2 - i\mathbf{b}\mathbf{A} + \frac{1}{2}\left(\nabla \times \mathbf{A}\right)^2 \right\} \right] \tag{3.22}$$

and

$$Z(\beta) = \int \mathcal{D}\mathbf{h} \sum_{\mathbf{m}}{}' \exp\left[-\sum_{\mathbf{x}} \left\{ 2\pi i \mathbf{m}\cdot\mathbf{h} + \frac{1}{2\beta}\left(\nabla \times \mathbf{h}\right)^2 + \frac{e^2}{2}\mathbf{h}^2 + \frac{\Gamma}{2}\mathbf{m}^2 \right\} \right]. \tag{3.23}$$

Here Eq. 3.22 corresponds to Eq. A.8, but with the $\mathbf{A}$ field included, and Eq. 3.22 is just Eq. 3.19 with an additional term $\Gamma/2\mathbf{m}^2$ in the action. Formally the subsequent analysis should be performed in the limit $\Gamma \to 0$, but we need to retain a finite Γ to identify the continuum dual model[11]. The gauge field $\mathbf{h}$ in Eq. 3.23 is *massive*, but if

[11] This is essentially an uncontrolled approximation [67], but as long as $\Gamma\mathbf{m}^2$ is *short ranged* it should be irrelavant at least in the RG sense [44]. Furthermore results from simulations indicate that it is a valid approximation [51, 62].

we ignore this additional term the action of Eq. 3.22 and Eq. 3.23 can be compared term by term,

$$\frac{1}{2\beta}\mathbf{b}^2 \to \frac{\Gamma}{2}\mathbf{m}^2$$
$$\frac{1}{2}\left(\nabla \times \mathbf{A}\right)^2 \to \frac{1}{2\beta}\left(\nabla \times \mathbf{h}\right)^2$$
$$-\mathbf{b}\cdot\mathbf{A} \to 2\pi\mathbf{m}\cdot\mathbf{h}.$$

With this identification we observe that the role of the integer loop fields $\mathbf{b}$ and $\mathbf{m}$ can be interchanged, and if we interpret Eq. 3.23 as Eq. A.8 in the original duality transformation, and then *go backwards* to a field theoretical description, we find the continuum dual action

$$S(\mathbf{h},\phi) = \frac{1}{2}\left(\nabla \times \mathbf{h}\right)^2 + \frac{e^2}{2}\mathbf{h}^2 + \left|\left(\nabla - ie_d\mathbf{h}\right)\phi\right|^2 + m_\phi^2\left|\phi\right|^4 + u_\phi\left|\phi\right|^4. \tag{3.24}$$

In Eq. 3.24 ϕ is the dual field, this is a field for the vortices of the original theory. Observe how the original local gauge symmetry has been reduced to a global $U(1)$ symmetry due to the mass term $e^2/2\mathbf{h}^2$. From [68] we have the following *exact* RG identities:

$$m_\phi \frac{\partial e^2}{\partial m_\phi} = \eta_{\mathbf{A}} e^2 \tag{3.25}$$
$$\eta_{\mathbf{A}} = 1 \tag{3.26}$$

The identity $\eta_{\mathbf{A}} = 1$ has also been shown with simulations [62, 63]. From Eq. 3.25 we infer that in the long distance limit, any finite e will flow to infinity, this corresponds to making the gauge field in Eq. 3.24 infinitely massive and it effectively drops out of the theory. Then Eq. 3.24 reduces to the *neutral* theory

$$S(\phi) = \left|\nabla\phi\right|^2 + m_\phi^2\left|\phi\right|^4 + u_\phi\left|\phi\right|^4. \tag{3.27}$$

3.4.3 Charged and neutral theory

In case of the theories we consider there are long range interactions mediated by a gauge field in the charged case, whereas in the neutral case there are only short range interactions. The gauge field present in charged theories also provides ample amounts of entropy.

From the identities Eq. 3.25 and 3.26 we saw that a finite e would flow to infinity reducing the originally charged theory Eq. 3.24 to the neutral theory Eq. 3.27. If, on

$S(\mathbf{A},\psi) = m_\psi^2 \lvert\psi\rvert^4 + u_\psi \lvert\psi\rvert^4 + \frac{1}{2}(\nabla\times\mathbf{A})^2 + \lvert(\nabla - ie\mathbf{A})\,\psi\rvert^2$	$S(\phi) = m_\phi^2 \lvert\phi\rvert^4 + u_\phi \lvert\phi\rvert^4 + \lvert\nabla\phi\rvert^2$
$S(\psi) = m_\psi^2 \lvert\psi\rvert^4 + u_\psi \lvert\psi\rvert^4 + \lvert\nabla\psi\rvert^2$	$S(\mathbf{h},\phi) = m_\phi^2 \lvert\phi\rvert^4 + u_\phi \lvert\phi\rvert^4 + \frac{1}{2}(\nabla\times\mathbf{h})^2 + \lvert(\nabla - ie_d\mathbf{h})\,\phi\rvert^2$

Table 3.2: The various charged and neutral theories related by duality.

the other hand, the original is neutral, i.e. $e = 0$, the dual will be Eq. 3.24 with a massless gauge-field, i.e. a *charged* theory , and we can set up a table relating charged and dual theories.

The essential content of table 3.2 is also shown in Fig. 3.5. Observe the isomorphism along both the diagonals. These properties have been studied, and exploited, in Paper I and Paper II. Of course what is *dual*, and what is *original* theory eventually becomes a *relative* notion.

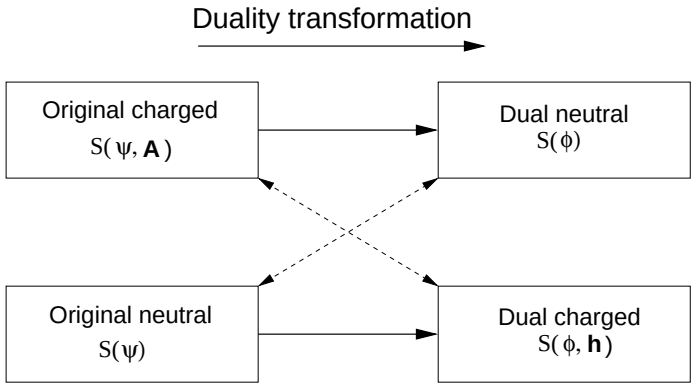

Figure 3.5: Figure showing the relations between charged and neutral versions of the original and dual theory, the various actions $S(\cdot)$ refer to table 3.2. The dashed lines indicate isomorphism.

The dual theory is a theory for the vortices, consequently we can study the properties of a particular theory by considering the vortices in a suitably chosen original theory. By considering the vortices of the 3DXY model (original neutral/dual charged), we have

calculated anomalous dimension of the full GL model. This exponent is difficult to calculate, and although our method is quite *indirect* our result $\eta_\psi \approx -0.30$ agrees with other methods [48].

Now when we have completed the duality picture, and introduced the concepts of charged and neutral theories, it is instructive to go back to the correlation functions Eq. 3.20 and 3.21. From the simulations we measure $\langle \mathbf{m_q m_{-q}} \rangle$, and spesifically how this correlation function behaves in the $q \to 0$ limit. For a charged system we find the following behavior [62]:

$$T < T_c: \quad \langle \mathbf{m_q m_{-q}} \rangle \propto q^2 \quad \Rightarrow \quad \langle \mathbf{A_q A_{-q}} \rangle \propto C \tag{3.28A}$$

$$T = T_c: \quad \langle \mathbf{m_q m_{-q}} \rangle \propto q^{\eta_\mathbf{A}} \quad \Rightarrow \quad \langle \mathbf{A_q A_{-q}} \rangle \propto q^{\eta_\mathbf{A}-2} \tag{3.28B}$$

$$T > T_c: \quad \langle \mathbf{m_q m_{-q}} \rangle \propto C \quad \Rightarrow \quad \langle \mathbf{A_q A_{-q}} \rangle \propto q^{-2} \tag{3.28C}$$

In Eq. 3.28B we have identified the scaling of $\langle \mathbf{m_q m_{-q}} \rangle$ at the critical point with the anomalous dimension of $\mathbf{A}$. We found $\eta_\mathbf{A} = 1$ in Paper I, but this is actually an exact result due to gauge invariance, which dates all the way back to Halperin, Lubensky and Ma [43, 68]. If we invoke the standard scaling form

$$\langle \mathbf{A_q A_{-q}} \rangle = \frac{1}{m_\mathbf{A}^2 + q^2}, \tag{3.29}$$

and insert the scaling behavior from Eqns. 3.28A - 3.28C we find that $m_\mathbf{A}$ is finite for $T < T_c$ and vanishes for $T \geq T_c$, i.e. an explicit demonstration of the Meissner effect.

From the preceding discussion of duality and charged versus neutral theories, we know that the dual of a *neutral* theory is isomorph to a charged theory, with inverted temperature axis. This is clearly demonstrated if we consider the *dual* gauge field correlator $\langle \mathbf{h_q h_{-q}} \rangle$ for a *neutral* theory .In this case $\langle \mathbf{m_q m_{-q}} \rangle$ will scale as q^2 for all T, but with different coefficients, and a careful calculation [62] gives similar behavior for $\langle \mathbf{h_q h_{-q}} \rangle$ as $\langle \mathbf{A_q A_{-q}} \rangle$ in Eqns. 3.28A - 3.28C, but with inverted temperatur axis, see Fig. 3.6, and Fig. 1 and 3 in Paper I.

3.5 Loop gas

In this section we will consider a gas of interacting loops, and eventually show that the GL model is an effective field theory for this gas. Although very different from the duality transformation in the preceding section; the final result is effectively the same. However the geometric approach of this derivation allows to establish a connection between the *geometric properties* of the loop(vortex)-tangle and the dual field theory. Something like this does *not* follow from the more direct duality transformation of the previous section. All of section 3.5 follows the derivations given in chapter 6 of [17] quite closely.

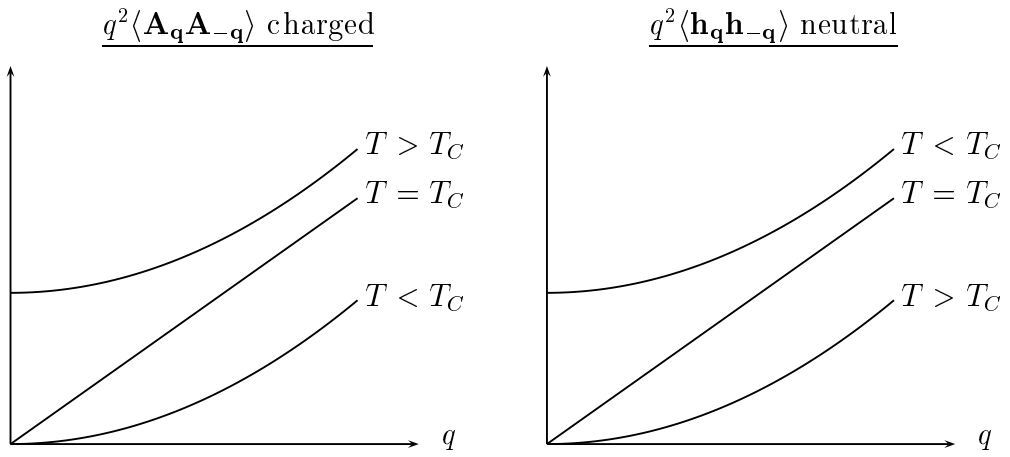

Figure 3.6: Schematic behavior of $q^2\langle \mathbf{A_q A_{-q}} \rangle$ and $q^2\langle \mathbf{h_q h_{-q}} \rangle$ for charged and neutral models respectively.

3.5.1 Random walk $\rightarrow$ Gaussian field theory

We start with random loops, i.e. random walkers which close on themselves, and then show that a Gaussian field theory can be used to describe these loops. We start by considering a random walker as shown in Fig. 3.7, and the probability $P(\mathbf{x}, \mathbf{y}, N)$, to get from $\mathbf{x}$ to $\mathbf{y}$ in a total of N steps.

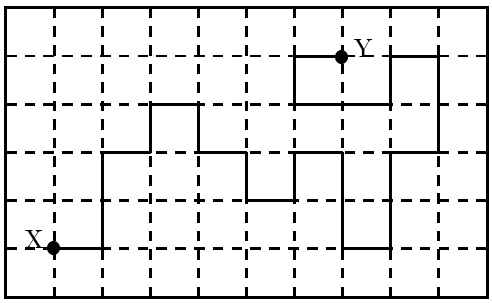

Figure 3.7: Random walker, starting in $\mathbf{x}$ and going to $\mathbf{y}$ in a total of $N = 26$ steps, lattice constant a.

$P(\mathbf{x},\mathbf{y},N)$ satisfies the following discrete diffusion equation,

$$\bar{\Delta}_N P(\mathbf{x},\mathbf{y},N) = \frac{a}{2D}\sum_\mu \bar{\Delta}_\mu \Delta_\mu P(\mathbf{x},\mathbf{y},N-1) \tag{3.30}$$
$$P(\mathbf{x},\mathbf{y},0) = \delta_{\mathbf{x},\mathbf{y}},$$

where Δ_μ and $\bar{\Delta}_\mu$ are forward and backward finite difference operators respectively, a is lattice constant and D is the spatial dimensionality. By using the Fourier ansatz $P(\mathbf{k},N) = P(\mathbf{k})^N$ we find that

$$P(\mathbf{k}) = 1 - \frac{a^2}{2D}\sum_\mu K_\mu(\mathbf{k})K_\mu^*(\mathbf{k}), \quad K_\mu(\mathbf{k}) = \frac{1}{ai}\left(e^{ik_\mu a}-1\right) \tag{3.31}$$

solves Eq. 3.30. We will mostly ignore the explicit N dependence and sum over all N, long paths will be suppressed with the Boltzmann factor $e^{-\beta N\varepsilon}$. In addition we will specialize on closed loops, i.e. $\mathbf{x}=\mathbf{y}$ and consider a *partition function* for one loop

$$Z_1 = \sum_{\mathbf{x},N}\frac{1}{N}e^{N(\ln(2D)-\beta\epsilon)}P(\mathbf{x},\mathbf{x},N), \tag{3.32}$$

$$Z_1 = -\sum_{\mathbf{k}}\ln\left(1-2DP(\mathbf{k})e^{-\beta\epsilon}\right). \tag{3.33}$$

The factor $(2D)^N$ in Eq. 3.32 and 3.33 accounts for the number of spatial configurations of a chain of length N, and the factor N^{-1} ensures that one particular loop is only counted once in the partition function[12]. The final step is to consider a grand canonical ensemble of such loops, by exponentiation of Eq. 3.33 we find the grand canonical partition function

$$\Xi = e^{Z_1} = \prod_{\mathbf{k}} G_0(\mathbf{k}) \tag{3.34}$$

$$G_0(\mathbf{k})^{-1} = 1 - e^{-\beta\varepsilon}2DP(\mathbf{k}) = \frac{m^2+\mathbf{K}\cdot\mathbf{K}^*}{m^2+2D/a^2}. \tag{3.35}$$

In Eq. 3.35 we have introduced the mass parameter $m^2 = a^{-2}\left(e^{\beta\varepsilon}-2D\right)$. The factors $G_0(\mathbf{k})$ in Eq. 3.34 can be produced by Gaussian integrals over real variables $\phi(\mathbf{k})$

$$\prod_{\mathbf{k}} G_0(\mathbf{k}) = \prod_{\mathbf{k}}\left[\int\frac{\mathrm{d}\phi_1(\mathbf{k})}{\sqrt{2\pi}}\frac{\mathrm{d}\phi_2(\mathbf{k})}{\sqrt{2\pi}}\right]e^{-\frac{1}{2}\sum_{i=1}^2\phi_i(\mathbf{k})G_0^{-1}(\mathbf{k})\phi_i(\mathbf{k})}. \tag{3.36}$$

[12]The summation over N going from Eq. 3.32 to Eq. 3.33 is done using the identity

$$\sum_{N=1}^{\infty}\frac{1}{N}x^N = -\ln(1-x).$$

Observe that we for the moment have *no physical interpretation of* $\phi(\mathbf{k})$, *its only purpose* is to bring down factors of $G_0(\mathbf{k})$ through Gaussian integration. We are mainly interested in the the continuum limit $a \to 0$, and then we can approximate $G_0(\mathbf{k})$ to a free propagator, and we get the final field theory:

$$\boxed{\Xi = \int \mathcal{D}\phi e^{-\frac{1}{2}\int \mathrm{d}\mathbf{r}\phi^*(\mathbf{r})\left(-\partial^2+m^2\right)\phi(\mathbf{r})}.} \tag{3.37}$$

Eq. 3.37, that a set of random loops can be described by a Gaussian field theory, concludes this section. In the next section we will see how the free field theory can be modified to include interactions between the loop segments.

3.5.2 Adding interactions

The goal of this section is to add interactions between the loop segments, and see how the field theory Eq. 3.37 can be modified to accommodate these interactions. First we will add a steric repulsion term between the loop segments, and then subsequently we will see how to add long range interactions.

Steric repulsion

If we consider the continuum limit of Eq. 3.30, with imaginary time $t = -is$ substituted for the step variable, we get the Schrödinger equation

$$i\partial_t\psi(\mathbf{x},t) = -\frac{1}{2M}\partial^2\psi(\mathbf{x},t) \tag{3.38}$$

for a particle of mass $M = D/a$. Consequently we can consider Eq. 3.37 as second quantized version of the same theory. In terms of second quantized field theories we know how to add two-particle interactions [69],

$$E = \frac{1}{2}\int \mathrm{d}\mathbf{x}\mathrm{d}\mathbf{y}\phi(\mathbf{x})\phi^*(\mathbf{x})V(\mathbf{x}-\mathbf{y})\phi(\mathbf{y})\phi^*(\mathbf{y}). \tag{3.39}$$

If we assume that $V(\mathbf{x}-\mathbf{y})$ is a pure contact interaction, i.e. $V(\mathbf{x}-\mathbf{y}) = u\delta(\mathbf{x}-\mathbf{y})$ we find that steric repulsion between the loop segments can be included by adding a $|\phi|^4$ term to the free action in Eq. 3.37.

Long range interactions

The vortex loops which are interested in are excitations which destroy the order in the system, and hence couple to the soft modes of the system. Unless screened, this coupling will give rise to long range interactions, and it is essential to find a way to include such

interactions to the loop-gas formulation. We want to include $1/R$ interactions between the loop segments in a manner which mimicks the electromagnetic interaction between *current* loops, i.e. we want a Boltzmann weight of the form

$$W = \exp\left[-\frac{\beta\mu}{4\pi} I^2 \sum_{i,j} \oint_{\Gamma_i} \mathrm{d}\mathbf{x}_i \oint_{\Gamma_j} \mathrm{d}\mathbf{x}_j \frac{1}{|\mathbf{x}_i - \mathbf{x}_j|}\right]. \tag{3.40}$$

In Eq. 3.40 i and j are indexes for different *current loops*, all carrying the same current I. Γ_i is the *path* along loop i, and $\mathrm{d}\mathbf{x}_i$ is a line element along Γ_i. It can be shown [17] that the Boltzmann weigh tEq. 3.40 can be written as a functional integral over an auxiliary gauge field $\mathbf{h}$, coupled to the current distribution from the loops,

$$W = \int \mathcal{D}\mathbf{h}\Phi\left[\mathbf{h}\right] \exp\left[-\frac{1}{T}\int \mathrm{d}\mathbf{x} \frac{1}{2\mu}\left(\nabla \times \mathbf{h}\right)^2 - iI \sum_i \oint_{\Gamma_i} \mathrm{d}\mathbf{x}_i \mathbf{h}(\mathbf{x}_i)\right]. \tag{3.41}$$

Now we will turn to the free field theory Eq. 3.37, and see how this theory can be modified to take the long range interactions into account. Going back to the fundamental quantity $P(\mathbf{x}, \mathbf{y}, N)$ it is clear that there are *many different paths* connecting $\mathbf{x}$ and $\mathbf{y}$, and a *path integral* representation seems quite natural. Omitting the intermediate steps we get the following path integral representation of the complete partition function Eq. 3.37

$$\Xi = \sum_N \frac{1}{N!} \prod_{i=1}^{N} \int_0^\infty \frac{\mathrm{d}s_i}{s_i} e^{-\beta f s_i/a} \int \mathcal{D}\mathbf{x}_i \mathcal{D}\mathbf{p}_i \exp\left[\int_0^{s_i} \mathrm{d}s_i' \left(i\mathbf{p}_i(s_i')\dot{\mathbf{x}}_i(s_i') - \frac{\mathbf{p}_i^2(s_i')}{2M}\right)\right]. \tag{3.42}$$

Now the crucial point is that in the formulation Eq. 3.42 the long range forces, i.e. the coupling between loop-coordinates and a fluctuating gauge field, can be incorporated by following simple prescription:

1. Replace $\mathbf{p}_i(s) \to \mathbf{p}_(s) - q\mathbf{h}(\mathbf{x}_(s))$, or in real-space $\nabla \to \nabla - q\mathbf{h}$, i.e. the well known *minimal coupling*.

2. Add an additional field energy $\frac{1}{2\mu}\left(\nabla \times \mathbf{h}\right)^2$, and integrate over the auxillary field $\mathbf{h}$.

In conclusion the final field theory for a grand canonical ensemble of interacting loops, with both steric repulsion and long range interactions, is given by the following field theory

$$\boxed{\Xi = \int \mathcal{D}\phi\mathcal{D}\mathbf{h} \exp\left[-\int \mathrm{d}\mathbf{x}\left\{m_\phi^2 |\phi|^2 + |(\nabla - iq\mathbf{h})\,\phi|^2 + u_\phi |\phi|^4 + \frac{1}{2}\left(\nabla \times \mathbf{h}\right)^2\right\}\right].} \tag{3.43}$$

Interpreting the interacting loop gas

Up to now the loops in this section have been completely arbitrary, but of course at this stage it is natural to identify the loops with the vortex loops of the previous section, and the field theory Eq. 3.43 with the dual theories in table 3.2. The advantage of the present derivation is that it highlights the physical content of the various terms in the dual field theory. In particular that the $|\phi|^4$ term represents steric repulsion, when the prefactor u_ϕ changes sign this turns into a short range attractive interaction, and this is a possible picture of the change from type-II to type-I superconductivity in the dual description [61]. Further interpretation of the dual matter field will be given in the next section.

3.5.3 Geometric exponent relations

Another advantage with the loop gas derivation in the previous section is that we get a connection between the geometric properties of the loops, and the critical properties of the corresponding field theory. Specifically we will in this section derive a scaling relation relating η_ϕ of the (dual) field theory, the exponent[13] α characterizing the loop size distribution and the fractal dimension D_{H} of the loops at the critical point. We will again go back to the probability $P(\mathbf{x}, \mathbf{y}, N)$, but now the focus shifts to the perimeter N, and not on the particular points $\mathbf{x}$ and $\mathbf{y}$. Let $D(N)$ be the density of loops with perimeter N:

$$D(N) \propto \frac{1}{N} \sum_{\mathbf{x}} P(\mathbf{x}, \mathbf{x}, N) \ \propto N^{-\alpha}. \tag{3.44}$$

The important point with Eq. 3.44 is that we know from the polymer literature [70, 71] that in a critical loop tangle $D(N)$ should scale with $N^{-\alpha}$ as indicated. All the contributions in Eq. 3.44 are equal, and to proceed we pick an arbitrary $\mathbf{x}$ and invert

$$P(\mathbf{x}, \mathbf{x}, N) \ \propto N P(N, \mathbf{z}) \propto N^{1-\alpha}. \tag{3.45}$$

In addition we have the following scaling ansatz for $P(\mathbf{x}, \mathbf{y}, N)$

$$P(\mathbf{x}, \mathbf{y}, N) \propto \frac{1}{N^{d\Delta}} F\left(\frac{|\mathbf{x}-\mathbf{y}|}{N^{\Delta}}\right). \tag{3.46}$$

This ansatz is motivated by the exact result for the case of random loops [70], and gives explicit exponent values for this case. $F(z)$ is a general scaling function, the exponent Δ in the argument is called the *wandering exponent*, and indicates how much the path from $\mathbf{x}$ to $\mathbf{y}$ "wiggles". By turning the argument around we find that the number of links in a path of linear extent L scales as

$$N \propto L^{\frac{1}{\Delta}} = L^{D_{\mathsf{H}}}, \tag{3.47}$$

[13] α should *not* be confused with the exponent regulating the divergence in the specific heat.

and as indicated in Eq. 3.47 Δ^{-1} corresponds to the *fractal dimension* of the loop [70]. Regarding the function $F(z)$ we will be interested in the limit $z \to 0$. For self avoiding walks[14] $F(z) \propto z^{\gamma}$ in this limit, whereas in our case $\lim_{z\to 0} F(z) = C$. By combining Eq. 3.45 and 3.46 we find the scaling relation $d\Delta = \alpha - 1$.

At the critical point the two point correlation function $G(r)$ scales with an anomalous scaling dimension η_ϕ. At the same time we know from the way the ϕ field was introduced in Eq. 3.37 that $G(\mathbf{x}, \mathbf{y})$ is proportional to the probability to get from $\mathbf{x}$ to $\mathbf{y}$ on a connected vortex tangle,

$$G(\mathbf{x}, \mathbf{y}) = \langle \phi(\mathbf{x}) \phi^*(\mathbf{y}) \rangle \propto \sum_N P(\mathbf{x}, \mathbf{y}, N). \tag{3.48}$$

The sum over N in Eq. 3.48 can not be done, but if we focus on long loops/distance the discrete nature of N becomes unimportant, and we can replace $\sum_N$ with $\int \mathrm{d}n$

$$G(\mathbf{x}, \mathbf{y}) \sim \int \mathrm{d}n \frac{1}{n^{d\Delta}} F\left(\frac{|\mathbf{x} - \mathbf{y}|}{n^{\Delta}} \right) = \frac{1}{|\mathbf{x} - \mathbf{y}|^{d - \frac{1}{\Delta}}} \mathsf{C}. \tag{3.49}$$

In Eq. 3.49 C is numerical constant. By combining the power of $|\mathbf{x} - \mathbf{y}|$ with the usual scaling of $G(\mathbf{x}, \mathbf{y})$ we find the scaling relation $\eta_\phi + \Delta^{-1} = 2$. All in all this section can be summed up with the relations:

$$\boxed{\frac{d}{D_{\mathsf{H}}} = \alpha - 1, \quad \eta_\phi + D_{\mathsf{H}} = 2.} \tag{3.50}$$

When Eq. 3.50 is applied to vortex loops it is important to realize that the anomalous scaling dimension η_ϕ belongs to the *dual field*. So by performing simulations on the 3DXY model, identifying the vortex loops of this model and calculating α from Eq. 3.44 we can calculate $\eta_\phi \approx -0.30$ of the dual to the 3DXY model, and not $\eta_{XY} \approx 0.034$ [72].

The final connection between the vortex loops and the dual field-theory is the quantity $\mathsf{O_L}$ [51,52]. If there is *at least* one vortex path connecting the opposite sides of the system $\mathsf{O_L} = 1$, otherwise $\mathsf{O_L} = 0$. Clearly $\mathsf{O_L}$ measures whether the ϕ field has condensed, and we get the following correspondence:

$$\lim_{|\mathbf{x}-\mathbf{y}|\to\infty} \langle \phi(\mathbf{x}) \phi^*(\mathbf{y}) \rangle = \begin{cases} \mathsf{C} & \leftrightarrow & \mathsf{O_L} & = & 1 \\ 0 & \leftrightarrow & \mathsf{O_L} & = & 0 \end{cases} \tag{3.51}$$

The scaling relations Eq. 3.50 and the connection Eq. 3.51 touches the fascinating field of the geometry of phase transitions. In the early 1970's Kastelyn and Fortuin [73] developed a link/cluster representation of the partition function for the Ising model and some other similar models. In 1980 Coniglio and Klein showed that the Kastelyn-Fortuin clusters percolate at the Ising critical point, and the exponents characterizing the

[14] These walks are not allowed to form closed loops.

geometric properties of this cluster coincide with the thermal Ising exponents. Later this has been expanded to more advanced models [74], and quite recently A. M. Schakel [75] derived the relations Eq. 3.50. The distinction between these references and our result is that in our case the geometric objects are well defined in terms of the original spin-model, whereas in these other approaches the geometric objects are purely the results of a transformation. Nevertheless it would be *very interesting* to relate our results closer to the framework of Fortuin and Kastelyn.

3.5.4 Discussion of geometric results

In Paper II we have calculated the exponent α which characterizes the loop size distribution, both for charged and neutral condensates. The results are summarized numerically in table 3.3, and "visually" in Fig. 3.8[15].

Exponent	Gaussian	$e = 0$	$e \neq 0$	Limit		
$\boldsymbol{\alpha}$	$\mathbf{5/2}$	$\mathbf{2.312 \pm 0.003}$	$\mathbf{2.56 \pm 0.03}$	$\boldsymbol{\alpha}$	$>$	$\mathbf{2}$
D_{H}	2	2.287 ± 0.004	1.92 ± 0.04	D_{H}	$<$	3
Δ	$1/2$	0.437 ± 0.001	0.52 ± 0.01	Δ	$>$	$1/3$
η_ϕ	0	-0.287 ± 0.004	0.08 ± 0.04	η_ϕ	$>$	-1

Table 3.3: Value of the loop-size distribution exponent, as determined from simulations. The remaining exponents have been calcualated using scaling relations Eq. 3.47 and 3.50. Gaussian results are exact, and confirmed for the different exponents independently.

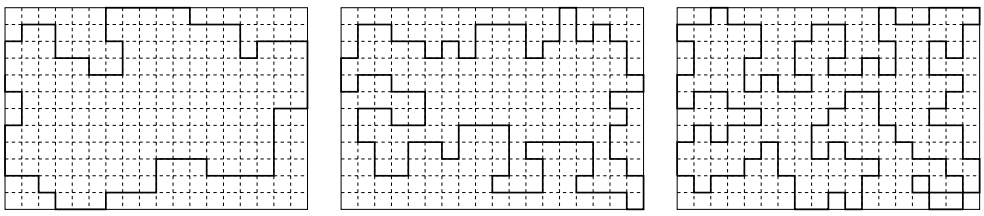

Figure 3.8: A *schematic* illustration of the three cases in table 3.3. The three fractal dimensions are ordered according to: $D_{\mathsf{H}}(e \neq 0) < D_{\mathsf{H}}^{\mathsf{G}} < D_{\mathsf{H}}(e = 0)$, where $D_{\mathsf{H}}^{\mathsf{G}}$ is the fractal dimension corresponding to a Gaussian field theory, i.e. random loops. Qualitively the three loops are *self-avoiding*, *random* and *self-seeking*.

The precise numerical values are not of major importance, however there are several qualitative aspects which are worth considering. The Gaussian results in table 3.3

[15] Observe that Fig. 3.8 is somewhat misleading, the duality transformation presented in section 3.4 applies *only* in $d = 3$, in $d = 2$ the topological excitations are *points* and not loops.

come from random closed loops, corresponding to the free field theory Eq. 3.37, these results are excact. Compared to Eq. 3.37 the interacting theory Eq. 3.43 contains t w o competing terms, the $|\phi|^4$ term is a steric repulsion term. Conseqently we expect that the v ortex tangle from a charged theory, i.e. dual neutral, has a vortex tangle which is *less compact* than random loops, i.e. $D_{\mathsf{H}}(e \neq 0) < D_{\mathsf{H}}^{\mathsf{G}}$, and from table 3.3 we see that this is correct.

On the other hand the gauge-field $\mathbf{h}$ in Eq. 3.43 mediates long range attractive interactions which counteract the effect of the $|\phi|^4$ term, and w eexpect the vortex tangle from a neutral theory, i.e. dual charged, to be more compact than the neutral tangle, i.e. $D_{\mathsf{H}}(e = 0) > D_{\mathsf{H}}(e \neq 0)$. Actually table 3.3 shows that the v ortex tangle from a neutral theory is more compact than the random loops, i.e. the long interactions *over-compensate* the steric repulsion. However the steric repulsion term prevents a complete collaps of the vortex tangle.

That the v ortex tangle from a neutral theory is more compact than that originating from a charged theory has direct physical explanation. Due to the presence of a fluctuating gauge field, the vortex-vortex interactions in the charged system are screened, and the v ortex tangle is *compressible*. How ev er in the originally neutral system the v ortices in teract through long range interactions, and the vortex tangle is incompressible. By generating a large amount of compact vortex loops the system tries to become compressible by self-screening vortex loops.

A vortex tangle with $D_{\mathsf{H}} > 2$ is opaque. If a magnetic field is applied to such a vortex tangle the thermal vortex loops will be devoured by the field induced lines, how ev er the magnetic field lines ha v ea cross sectional area that scales as L^2, and with D_{H} there remains a vortex tangle which can undergo a vortex loop blow out in the liquid phase, as suggested by Ngyuen [52].

3.6 RG Flow

The full GL model has three nontrivial fixed points in addition to the Gaussian fixed point. Starting along the neutral $e = 0$ line the Gaussin fixed point G is unstable, and a finite value of u will flow tow ards the 3DXY fixed point under renormalization. This fixed point determines the critical exponents for a neutral superfluid like ^{4}He and the 3DXY and $|\phi|^4$ models.

The 3DXY fixed point is unstable in the charge direction, and for a finite charge the system will flow to the SC fixed point which is *distinct* from the 3DXY fixed point [62]. The shaded region in Fig. 3.9 corresponds to a region of runaw ay trajectories; thisis interpreted as a first order transition in accordance with Halperin, Lubsenky and Ma [43]. The tricritical point T seperates the critical point SC from a first order transition, and the line connecting G and T is a separatrix. In Paper III we argue that this line corresponds to the line separating type-I and type-II superconductivity.

The duality transformation betw eencharged and neutral theories which w e have de-

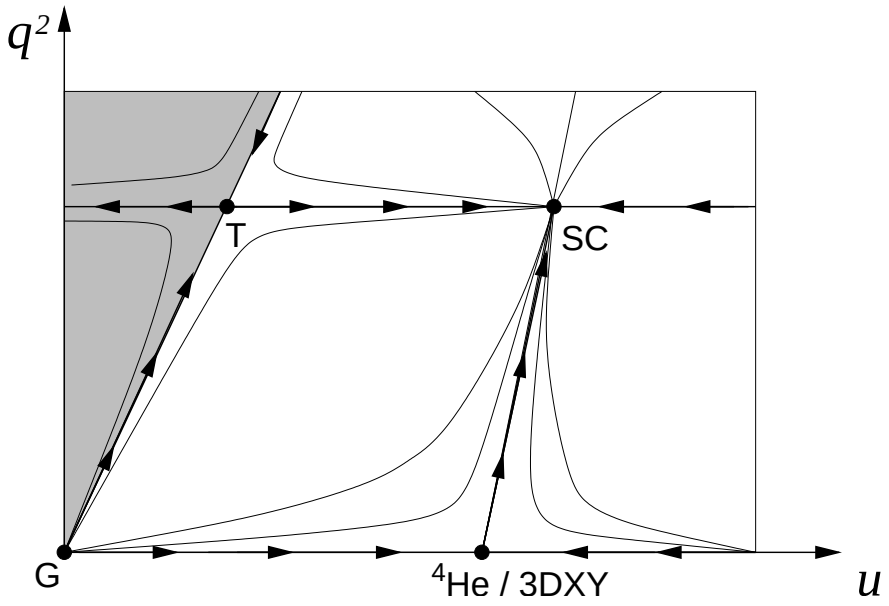

Figure 3.9: A RG flow diagram for the GL model, the various fixed points are SC: charged superconductor fixed point, 3DXY: neutral 3DXY/^{4}He fixed point, G: Gaussian fixed point and Ttricritical point. In the shaded region there is no fixed point, i.e. first order. The couplings on the axis are the rescaled charge and self coupling from Eq. 3.5.

scribed in the preceeding sections, i.e. Fig. 3.5, corresponds to moving up and down along the line connecting 3DXY and SC. Since a duality transformation only affects the *description* of a particular phase transition, the invariant subgroups in Eq. 2.21 must connect the exponents of the SC and 3DXY fixed points. Observe that in the case of a *massive* gauge field the topology of the phase diagram changes, and in particular the flow direction between 3DXY and SC is reversed.

It is often claimed in the literature that the phase transition in High T_c superconductors like YBCO and LaSCO is in the same universality class as ^{4}He, but if we consider Fig. 3.9 it is clear that this cannot be the case. These superconducting condensates *are charged* and the ultimately stable fixed point is the SC fixed point. However the charge is "small", and when we approach the critical point we will observe 3DXY critical behavior for $|t| \lesssim t_{\mathsf{XY}}$, this will pertain until we reach a *crossover* [18] temperature $t^* \ll t_{\mathsf{XY}}$. Finally for $|t| \lesssim t_{\mathsf{SC}} \ll t^*$ the critical properties will be governed by the true charged SC fixed point. However due to the narrowness of the true critical region, and the duality arguments relating the 3DXY and SC fixed points, it is probably difficult differentiate e.g. YBCO behavior from ^{4}He behavior experimentally.

3.7 Lattice version

In Paper III we calculated the tricritical x_{tri} separating the first order and second order transition, this is not a *universal* quantity, and care must be taken to not introduce spurious lattice artifacts, in particular one must take finite a effects explicitly into account, and the final answers must be evaluated in the limit $a \to 0$. This is covered quite thoroughly in Paper III and references therein.

The model can be parameterised in many different ways. The parametrisation presented below is marginally different from the one used in Paper III.

$$\begin{aligned} S = \beta_G \sum_{\mathbf{x},i<j} \frac{1}{2}\alpha_{ij}^2(\mathbf{x}) - \frac{2}{\beta_G} \sum_{\mathbf{x},i} \mathsf{Re}\left[\phi^*(\mathbf{x}) U_i(\mathbf{x}) \phi(\mathbf{x}+\hat{\imath})\right] \\ + \beta_2 \sum_{\mathbf{x}} \phi^*(\mathbf{x})\phi(\mathbf{x}) + \frac{x}{\beta_G^3} \sum_{\mathbf{x}} \left|\phi^*(\mathbf{x})\phi(\mathbf{x})\right|^2 \end{aligned} \tag{3.52}$$

The gauge field has been discretised according to:

$$\begin{aligned} \alpha_i(\mathbf{x}) &= aqA_i(\mathbf{x}) \\ \alpha_{ij}(\mathbf{x}) &= \alpha_i(\mathbf{x}) + \alpha_j(\mathbf{x}+\hat{\imath}) - \alpha_i(\mathbf{x}+\hat{\jmath}) - \alpha_j(\mathbf{x}) \\ U_i(\mathbf{x}) &= e^{i\alpha_i(\mathbf{x})} \end{aligned}$$

The couplings β_G and β_2 are related to the lattice constant a, and the continuum

parameters x and y as:

$$\beta_G = \frac{1}{q^2 a}$$

$$\beta_2 = \frac{1}{\beta_G}\left[6 + \frac{y}{\beta_G^2} - \frac{3.1759115\,(1+2x)}{2\pi\beta_G} - \frac{\left(-4+8x-8x^2\right)(\ln 6\beta_G + 0.09) - 1.1 + 4.6x}{16\pi^2\beta_G^2}\right].$$

4 The tools of the trade

Phase transitions are probably the most intriguing aspects of statistical mechanics, and as already mentioned in chapter 2 they correspond to singular behavior in the derivatives of the Free Energy. When the points of interest correspond to mathematical singularities it is obvious that a mathematical description will be challenging. In this chapter we will describe the Monte Carlo method, which has been our approach to study phase transitions, but first we will very briefly mention some other techniques which are widely used in statistical physics.

Analytical solutions

Some, exceptionally few, lattice models have exact analytical solutions, where the 2D Ising model solved by Lars Onsager [76] is the most prominent example. Exact solutions to some other models like the *Potts-model* and *Vertex-model* can be found in [77]. Although these solutions are the result of impressing mathematical vigor, they are very specialized and provide limited possibility for generalizing to other models. The most important use of these exact solutions is to serve as a benchmark for the validity of more general approximate methods.

Mean-field theory

Mean-field theory, can in general always be applied. The fundamental approximation of the mean-field theory is to *ignore spatial fluctuations*, and treat the original many-particle problem as an effective one-particle problem [13, 26]. This can provide a good overall structure of the phase diagram, but close to the critical point we know what *fluctuations are important*, and the mean-field predictions will generally be incorrect. In some cases the *order* of the transition will be incorrectly predicted, and in the case of continuous transitions the critical exponents will be wrong[1]. The temperature range where mean-field theory fails is called the *critical regime*, and the width of this regime is given by the Ginzburg criterion [13, 26, 78]. In some cases, like conventional type-I superconductors, this regime is so narrow that experiments will never reveal anything

[1] The critical exponents calculated in mean-field theory are called *classical*, not to be confused with classical/QM.

but mean-field behavior, whereas in other transitions like high T_c superconductors and ^{4}He the critical regime is wide and true critical behavior is observed in experiments.

Spatial dimension is important for the properties of phase transitions, this also applies to mean-field approximations. The higher the spatial dimension the stronger the influence of interacting neighbors, and consequently the importance of fluctuations is reduced with increasing dimension. For $d = 4$ mean-field theory is correct up to logarithmic corrections, and for this reason $d = 4$ is called the *upper critical dimension*. That an exact result can be found in $d = 4$ has led to the $\varepsilon = 4 - d$ expansion where $d = 3$ results are obtained by doing perturbation theory around the $d = 4$ result, with ε as expansion parameter. Combined with RG this is a major sport in statistical field theory with good numerical results, however the method provides limited insight into the qualitative properties of the transition [11, 21, 23].

Perturbation series

Perturbation theory in terms of low and high temperature[2] expansions make it possible to study various thermodynamic quantities analytically, expansions of various models in statistical physics can be found in [17, 79]. The inherent problem with these expansions is that they can never get the critical properties correct, and the same expansion can *not* be used on both sides of the critical point[3]. This is really no surprise since the critical points correspond to mathematical singularities, which generally limit the usefulness of a perturbative approach.

Simulations

When all else fails, one must turn to the computer for help. The essence of simulations in statistical physics is to let a state ψ evolve in phase space, and as ψ evolves we make *measurements* We can not assume to sample the entire phase space, but the hope is that the states we visit are *representative* There are *many* different methods to do computer simulations [80], three much used methods are:

Molecular dynamics, the most "brute-force" way, where the equations of motion for a large number of particles are integrated in time - quite simply. For a classical system the state of the system then evolves according to

$$\psi_i(t + \Delta t) = \psi_i(t) + \Delta t \dot{\psi}_i(t) - (\Delta t)^2 \frac{\partial H(\{\psi\})}{\partial \psi_i}. \tag{4.1}$$

The result is generally deterministic when the initial condition is specified [81].

[2] Corresponding to strong coupling and weak coupling in terms of field theory.

[3] Prior to Lars Onsager exact solution of the $2D$ Ising model, some people thought one had to employ *two different* partition functions, one below and above the critical point.

Langevin dynamics is a variation of Molecular Dynamics based on a first order equation of motion, and an additional noise term representing the properties of a thermal bath

$$\psi_i(t + \Delta t) = \psi_i(t) - \Gamma \Delta t \frac{\partial H(\{\psi\})}{\partial \psi_i} + \Delta t \eta_i(t). \tag{4.2}$$

$\eta_i(t)$ is the noise term, and Γ is a constant representing coupling to the *dissipative modes* of the system. Without the noise term Eq. 4.2 describes dissipative dynamics, which will lead the system straight into the closest local minimum in energy. If we set $\Gamma = \Delta t$ in Eq. 4.2 we see that Langevin Dynamics can be interpreted as Molecular Dynamics with random velocities. Antunes et.al. [82] have used Langevin dynamics to study the distribution of vortices and vortex loops, very similar to Paper I and Paper II in this thesis.

Monte Carlo is *not* á priori based on dynamics like the two other methods. Instead it is based on selecting configurations ψ_α randomly, this can of course be done in *many* different ways, and the resulting dynamics depends on the details of the simulations [83]. For local algorithms it is probably possible to relate Monte Carlo time to "real time" [85].

If we go through the three approaches listed above, the focus of the algorithms shifts continuously from details to universal quantities. In Molecular Dynamics the simulations are performed so that the final answers can be compared with experiments on a quantitive level; the results are reported with dimensionful pressure and temperature etc. For Monte Carlo simulations only the qualitative behaviour is expected to reproduce the real world, consequently Monte Carlo is mostly used to access *universal* properties. We have used the Monte Carlo method exclusively, and the rest of the current chapter is devoted describing this method.

In section 4.1 we present the Monte Carlo method, the importance sampling, and finally the *Metropolis algorithm* Section 4.2 is devoted to data analysis, and especially how to calculate the *error* in the measurements, in section 4.3 we present *reweighting* which is a very powerful method to extract more information from a simulation. All simulations are necessarily performed with a finite system size, in section 4.4 we discuss how this affects the results, and how we can use *finite size effects* to gather information about the critical properties. Finally we conclude the chapter with some considerations for Lattice Gauge theories in section 4.5.

4.1 Monte Carlo - a crash course

Monte Carlo (MC) is a very general method, applicable to a wide variety of problems. Common for all these problems is that phase space is very large, prohibiting an exhaustive search. In physics MC is in particular used to study equilibrium properties in statistical physics and lattice gauge theory. If combined with an annealing scheme [86]

MC can be used to find approximate solutions to hard optimizing problems like "the traveling salesman problem", design of integrated circuits, organizing the timetable for a public transport company and image restoriation. A naive MC simulation is quite simple and straightforward to implement, however it should nevertheless be a last resort, since it is a costly method in terms of computer time.

A note on notation

For the remaining part of this chapter we will use the following notation:
True values:

$$\text{Expectation values:} \qquad \langle O \rangle = \frac{1}{Z} \sum_i O_i e^{-\beta E_i} \tag{4.3}$$

$$\text{Fluctuations/statistical variance:} \qquad \sigma_O^2 = \langle O^2 \rangle - \langle O \rangle^2 \tag{4.4}$$

Of course the true values Eq. 4.3 and 4.4 require knowledge of the full partition function, and we must be contentwith *estimators*, generally we will use $\Omega_\alpha[\cdot]$ to indicate an estimator, the index on the estimator indicates how the rawdata have been sampled, see page 49. Typically we want to estimate expectation values, i.e. we use an estimator $\Omega_\alpha[\langle O \rangle]$. In addition to the estimate $\Omega_\alpha[\langle O \rangle]$ itself we also want an indication of how *reliable* this estimate is, i.e. the *variance of the estimator*. The following notation is used for estimators and their accompanying errors:

$$\text{Estimator of expectation value:} \qquad \Omega_\alpha[\langle O \rangle] \tag{4.5}$$

$$\text{Error in estimate:} \qquad \Omega_\alpha\left[\sigma^2_{\Omega_\alpha[\langle O \rangle]}\right] = \delta\left[\langle O \rangle\right] \tag{4.6}$$

Where the notation $\delta\left[\langle O \rangle\right]$ is introduced to simplify. Consequently a numerical value is according to Eq. 4.5 and 4.6 given as the value of $\Omega_\alpha[\langle O \rangle] \pm \delta\left[\langle O \rangle\right]$.

4.1.1 The generic statistical physics problem

The most naive approach is to pick N states ψ_α randomly, and then use the estimator

$$\Omega_i[\langle O \rangle] = \frac{\sum_{k=1}^N O_k e^{-\beta E_k}}{\sum_{k=1}^N e^{-\beta E_k}}. \tag{4.7}$$

The estimator Eq. 4.7 is unbiased, i.e. its expectation value coincides with the true expectation value, nevertheless this is generally a *very* poor approach. At a given temperature T the partition function and expectation values are heavily dominated by states with $E \simeq \langle E \rangle$, these states typically constitute only a small fraction of the total

number of states, and the general random state will give a small contribution to the averages[4]. Consequently a large part of the computing time will be wasted on states which only contribute a vanishing amount to the final answer.

Instead of the random sampling, we will use what is called *importance* sampling. The key point about importance sampling is that instead of jumping about in phase space completely at random, we devise a random walk, where consecutive steps in the walk represent states which are "thermodynamically close". The walk is constructed such that the probability to visit a state is proportional to its Boltzmann weight. This way the walker is ensured to spend most of its time on states with $E \approx \langle E \rangle$, and consequently little computing resources are wasted on the states which give a very limited contribution. The walk is devised so that the probability $\mathsf{P}(\alpha)$ to be in state α *only* depends on the state α' in the previous step, and not on the preceding states. A random sequence with this property is called a *Markov chain* [89].

Because the states are visited with a frequence proportional their Boltzmann weight, it might seem that an implementation requires knowledge of the density of states, $\Omega(E)$, however as we shall see below it is possible to construct such a walk if we only know the *ratio* between the probabilities $\mathsf{P}(\alpha)$ and $\mathsf{P}(\alpha')$. When the occurence frequency of the states is proportional to the Boltzmann distribution, we do not need the Boltzmann weights in the estimators:

$$\Omega_\alpha[\langle O \rangle] = \frac{1}{N} \sum_{\alpha=1}^{N} O_\alpha. \tag{4.8}$$

Observe the use of greek indices's in Eq. 4.8 compared to the latin in Eq. 4.7. For the remaining part of this chapter greek indices's will be used to indicate timeseries which have been sampled using importance sampling.

4.1.2 Building the Markov chain

In the following we will use $\mathsf{W}(\alpha|n)$ to denote the probability distribution of α after n steps of the walk through phase space, furthermore $\mathsf{P}(\alpha)$ denotes the target[5] distribution which $\mathsf{W}(\alpha|n)$ should converge towards in the $n \to \infty$ limit. We start the system in a particular state α, then we consider the set of states $\alpha' \in \{\alpha_1, \alpha_2, \cdots, \alpha_N\}$ *which can be reached* from α, and the transition probabilites $\mathcal{P}(\alpha \to \alpha')$. The transition probabilities are key ingredients in this scheme, and must satisfy the following requirements:

Normalisation:

$$\sum_{\alpha'} \mathcal{P}(\alpha \to \alpha') = 1, \tag{4.9}$$

[4] At $\beta = 1.1$ only seven out of totally 512 states provide 99.9% of the contribution to the partition function of a 3×3 Ising system [13]

[5] In our case the target distribution will of course be the Boltzmann distribution, but the analysis has general applicability.

Detailed balance:

$$\mathsf{P}(\alpha)\mathcal{P}\left(\alpha \to \alpha'\right) = \mathsf{P}(\alpha')\mathcal{P}\left(\alpha' \to \alpha\right). \tag{4.10}$$

Accessibility:
The transition probabilities must be such that all of phase space is accessible, i.e. given two arbitrary states α_1 and α_2 it must be possible to evolve from α_1 to α_2 in a finite number of steps.

Observe that the actual transition probabilites are still left unspecified, nevertheless, given that they actually satisfy Eq. 4.9 and 4.10 we can show that the *actual* distribution $\mathsf{W}(\alpha|n)$ converges towards $\mathsf{P}(\alpha)$. Let us introduce D_n as a "difference" between the distributions $\mathsf{P}(\alpha)$ and $\mathsf{W}(\alpha|n)$

$$D_n = \sum_{\alpha} \left|\mathsf{W}(\alpha|n) - \mathsf{P}(\alpha)\right|. \tag{4.11}$$

We will show that $\mathsf{W}(\alpha|n)$ indeed converges towards the target distribution $\mathsf{P}(\alpha)$ by showing that $D_{n+1} < D_n$.

$$\begin{aligned} D_{n+1} &= \sum_{\alpha} \left|\mathsf{W}(\alpha|n+1) - \mathsf{P}(\alpha)\right| \\ &= \sum_{\alpha} \left| \sum_{\alpha'} \mathsf{W}(\alpha'|n)\mathcal{P}\left(\alpha' \to \alpha\right) - \mathsf{P}(\alpha) \right| \\ &= \sum_{\alpha} \left| \sum_{\alpha'} \left(\mathsf{W}(\alpha'|n)\mathcal{P}\left(\alpha' \to \alpha\right) - \mathsf{P}(\alpha)\right) \right| \\ &= \sum_{\alpha} \left| \sum_{\alpha'} \left\{\mathsf{W}(\alpha'|n) - \mathsf{P}(\alpha')\right\} \mathcal{P}\left(\alpha' \to \alpha\right) \right|. \end{aligned} \tag{4.12}$$

Since it is a probaility we must have $\mathcal{P}\left(\alpha' \to \alpha\right) \geq 0$, if we apply the triangle inequality[6] to Eq. 4.12 we get

$$\begin{aligned} D_{n+1} &\leq \sum_{\alpha\alpha'} \left|\mathsf{W}(\alpha'|n) - \mathsf{P}(\alpha')\right| \mathcal{P}\left(\alpha' \to \alpha\right) \\ &= \sum_{\alpha'} \left|\mathsf{W}(\alpha'|n) - \mathsf{P}(\alpha')\right| \sum_{\alpha} \mathcal{P}\left(\alpha' \to \alpha\right) \\ &= D_n \end{aligned} \tag{4.13}$$

What we have essentially proved with Eq. 4.12 and 4.13 is that provided the two conditions Eq. 4.9 and 4.10 are satisfied, the *actual* distribution $\mathsf{W}(\alpha|n)$ will converge

[6] Triangle inequality $|x + y| \leq |x| + |y|$.

towards the wanted distribution $\mathsf{P}(\alpha)$. So far this has been quite general, now we must specify the transition probabilities $\mathcal{P}(\alpha \to \alpha')$, it is by specifying these probabilities the target distribution is determined. Consider the detailed balance condition Eq. 4.10 slightly rewritten

$$\frac{\mathcal{P}(\alpha \to \alpha')}{\mathcal{P}(\alpha' \to \alpha)} = \frac{\mathsf{P}(\alpha')}{\mathsf{P}(\alpha)}. \tag{4.14}$$

The individual probabilities $\mathsf{P}(\alpha)$ and $\mathsf{P}(\alpha')$ require knowledge of the full partition function and are clearly unknown, but their ratio $\mathsf{P}(\alpha')/\mathsf{P}(\alpha)$ *is known*

$$\frac{\mathsf{P}(\alpha')}{\mathsf{P}(\alpha)} = e^{-\beta(E_{\alpha'} - E_\alpha)}, \tag{4.15}$$

and we can use this to devise transition probabilities which will ensure that $\mathsf{W}(\alpha|n)$ converges towardsthe Boltzmann distribution. Eq. 4.15 still leavesquite a lot of arbitrariness and the eventual choice is mostly a matter of computational convenience, the Metropolis algorithm described in the next section is probably the most common.

4.1.3 The Metropolis algorithm

The Metropolis algorithm wasfirst introduced by Metropolis et.al. in 1953 [90][7] . Propose a change in the system state $\alpha \to \alpha'$ and calculate the change in energy $\Delta E = E_{\alpha'} - E_\alpha$. If $\Delta E < 0$ the proposed change is accepted, otherwise it is only accepted with a probability $\exp(-\beta \Delta E)$, ie

$$\mathcal{P}(\alpha \to \alpha') = \begin{cases} \frac{1}{N_\alpha} & \Delta E < 0 \\ \frac{e^{-\beta \Delta E}}{N_\alpha} & \Delta E > 0 \end{cases} \tag{4.16}$$

In Eq. 4.16, N_α is the number of states reachable from the state α - it must be included to satisfy the normalisation constraint in Eq. 4.9, but plays no further role. How to perform simulations with the Metropolis algorithm is schematically shown in Fig. 4.1.

Many other algorithms are used. *Heat Bath*, where the transition probabilities are changed to $\mathcal{P}(\alpha \to \alpha') = (1 + \exp(\beta \Delta E))^{-1}$, is another general purpose algorithm, and in addition several specialized algorithms which for instance respect particular symmetries, havebeen developed [91]. In our simulations we have used the Metropolis algorithm, along with *overrelaxation*, which is briefly mentioned in section 4.5.

[7] The title of the paper was: "Equation of State Calculations by Fast Computing Machines"

1. Prepare an initial configuration α_0.
2. Propose a new state α' randomly, and calculate $\Delta E = E_{\alpha'} - E_{\alpha}$.
3. Accept the new state α' with probability $P = \min(1, e^{-\beta \Delta E})$, this is practically done by drawing a uniformly distributed random rumber $r \in [0, 1]$, and accepting the new state if $r < P$.
4. Make measurements on the current state α.
5. Reedo from 2 above until sufficient accuracy has been obtained.

Figure 4.1: The Metropolis algorithm

4.2 Data analysis

4.2.1 Temporal correlations

Compared to the naive random sampling we have increased the efficiency of the simulations considerably by employing the importance sampling method, but it comes with a price. The consecutive states in the Markov chain are highly correlated, and only states separated by several sweeps through the lattice are truly independent. To test for independence we can study a normalised autocorrelation function

$$\phi(t) = \frac{\langle O(t)O(0)\rangle - \langle O\rangle^2}{\langle O^2\rangle - \langle O\rangle^2} \simeq e^{-t/\tau}. \tag{4.17}$$

As indicated in Eq. 4.17 the autocorrelation function decays roughly as an exponential function with a characteristic time scale τ. The problem with temporal correlations is specially severe around phase transitions.

4.2.2 Statistical errors

Averages are calculated from the naive formula Eq. 4.8, and the errors in these measurements are given by the standard error of this estimator. For independent measurements the standard error can be estimated simply from

$$\delta\left[\langle O\rangle\right] = \frac{1}{N(N-1)} \sum_{k}^{N} \left(O_k - \langle O\rangle\right)^2, \tag{4.18}$$

i.e. the squared standard error is given by the *variance* of the original data divided by the number of measurements. However this formula can not be applied directly to

MC rawdata because they are not truly independent. To circumvent this we group the measurements together in bins to form new stochastic variables, and these bin variables are assumed to be independent.

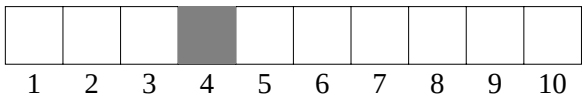

Figure 4.2: The full timeseries has been divided in ten different bins, and averages are calculated for each bin. These averages are then used as new, *independent* random variables.

We denote the *full timeseries* of N measurements as $\{\Psi\}$, then we divide this series into J independent timeseries $\{\psi_1, \psi_2, \psi_3, \ldots, \psi_\mathsf{J}\}$, and calculate the averages X_i

$$X_i = \frac{\mathsf{J}}{N} \sum_{\alpha \in \psi_i} O_\alpha \tag{4.19}$$

for each bin independently. Observe that although X_i in Eq. 4.19 represents an average over a subset of the data we will consider it as a stochastic variable with $\langle X_i \rangle = \langle O \rangle$ and unknown variance. Now we can use these new variables to express $\langle O \rangle$ as

$$\Omega_\alpha[\langle O \rangle] = \frac{1}{\mathsf{J}} \sum_{i=1}^{\mathsf{J}} X_i. \tag{4.20}$$

Although the original measurements were highly correlated the new variables $X_1, X_2, \ldots, X_\mathsf{J}$ are independent, and we can estimate the variance in the estimator Eq. 4.20 as

$$\delta[O] = \frac{1}{\mathsf{J}(\mathsf{J}-1)} \sum_{i=1}^{\mathsf{J}} \left(X_i - \langle O \rangle\right)^2. \tag{4.21}$$

When we wish to estimate a *nonlinear* function $f(O_\alpha)$ of the MC data, we use the estimator

$$\Omega_\alpha[f(\langle O \rangle)] = f\left(\Omega_\alpha[\langle O \rangle]\right) = f\left(\frac{1}{N} \sum_\alpha O_\alpha\right), \tag{4.22}$$

i.e. $\langle O \rangle$ is estimated first. Applying the estimator Eq. 4.22 is straightforward, but it is difficult to get a reliable estimate for the error $\delta[f(\langle O \rangle)]$, this is done using *Jack-Knife* estimators [92,93]. We go back to Fig. 4.2 and the variables X_i from Eq. 4.19 and form the new variables

$$Y_i = \frac{1}{\mathsf{J}-1} \sum_{k \neq i} X_k, \quad f_i = f(Y_i), \tag{4.23}$$

i.e. in terms of Fig. 4.2 the variable Y_4 is the average over all the "white blocks", and f_i is function evaluation of this average. Then the following Jack-Knife estimators are

used to estimate $f(\langle O\rangle)$ and $\delta[f(\langle O\rangle)]$

$$\Omega^{\mathsf{J}}[f(\langle O\rangle)] = \frac{1}{N}\sum_{i=1}^{N} f_i \tag{4.24}$$

$$\delta^{\mathsf{J}}[f(\langle O\rangle)] = \frac{N-1}{N}\sum_{i=1}^{N}\left(f_i - \frac{1}{N}\sum_{k=1}^{N} f_k\right)^2. \tag{4.25}$$

The important content of this technique is Eq. 4.23 where the variable set (Y_i, f_i) is formed. What we essentially do here is to apply the estimators Eq. 4.20 and 4.22 to a dataset with one variable missing, and then repeating with a new dataset missing until all possibilities have been exhausted. In this way all the data are sampled $(\mathsf{J}-1)$ times, and the technique is an example of *resampling* [93].

4.3 Reweighting techniques

During the simulations the probability to find the system with energy E can be approximated by recording a histogram $H(E)$,

$$P(E) = \frac{N(E)e^{-\beta E}}{Z(\beta)} \simeq \frac{H(E)}{\int \mathrm{d}E H(E)}, \tag{4.26}$$

and in the limit of an infinitely long simulation this will approach the true probability given on the right hand side of Eq. 4.26. The important point with Eq. 4.26 is that we have factored out the temperature *independent* density of states $N(E)$, and we can write

$$N(E) \simeq P(E,\beta)e^{\beta E}Z(\beta). \tag{4.27}$$

Eq. 4.27 should apply equally well irrespective of the temperature, and we can write

$$\begin{aligned} P(E,\beta_1)e^{\beta_1 E}Z(\beta_1) &= P(E,\beta_0)e^{\beta_0 E}Z(\beta_0) \\ P(E,\beta_1) &= P(E,\beta_0)e^{-\Delta\beta E}\frac{Z(\beta_0)}{Z(\beta_1)}, \end{aligned} \tag{4.28}$$

where $\Delta\beta = \beta_1 - \beta_0$. Eq. 4.28 contains the unknown quantities $Z(\beta_0)$ and $Z(\beta_1)$, but if we require that $P(E,\beta_1)$ be normalized to unity we can write

$$P(E,\beta_1) = \frac{P(E,\beta_0)e^{-\Delta\beta E}}{\int \mathrm{d}E P(E,\beta^0)e^{-\Delta\beta E}}. \tag{4.29}$$

If we now use Eq. 4.26 to approximate $P(E,\beta_0)$ we can calculate $P(E,\beta_1)$ from Eq. 4.29. In this way we can calculate thermodynamical properties at the coupling constant β_1 from rawdata obtained at the coupling constant β_0. This process is called *reweighting*.

Often we are not interested in the probabilities $P(E,\beta)$ themselves, but rather how a general expectation value $\langle A\rangle$ varies with β. If we multiply Eq. 4.29 with A and sum over all A we get

$$\langle A\rangle(\beta) = \frac{\int \mathrm{d}A P(A,\beta_0) A e^{-\Delta\beta E}}{\int \mathrm{d}A P(A,\beta^0) e^{-\Delta\beta E}} = \frac{\sum_\alpha A_\alpha e^{-\Delta\beta E_\alpha}}{\sum_\alpha e^{-\Delta\beta E_\alpha}}, \tag{4.30}$$

where $\sum_\alpha$ is a sum over the complete *time-series* of the quantity A. In the final step of Eq. 4.30 we have used

$$\langle A\rangle(\beta) = \int \mathrm{d}A P(A,\beta) A = \frac{1}{N}\sum_\alpha A_\alpha. \tag{4.31}$$

Eq. 4.30 requires that we store the complete time series of the simulations, but the advantage is that no ambiguity is introduced by binning the rawdata in histograms. If we consider a general field theory like in section 4.5 where the action can be written

$$S = \beta_1 H_1 + \beta_2 H_2 \tag{4.32}$$

the exponent in Eq. 4.30 must be generalized to $e^{-\Delta\beta_i H_{\alpha_i}}$, and the timeseries of H_1 and H_2 must be stored individually. A demonstration of reweighting is given in Fig. 4.3.

4.3.1 Ferrenberg Swendsen reweighting

Ferrenberg Swendsen reweighting is the most succesful example of *Multi Histogram Methods* [91]. The method consist of combining the rawdata from simulations at *several* different values of the coupling constant, and then reweight the complete dataset. This method allows for reweighting to a much broader range of coupling constants. For Paper III reweighting was absolutely essential[8] to find the critical coupling constants.

The original formula as given by Ferrenberg and Swendsen [94] is given in terms of histograms. Given N histograms $H_i(E,A)$ of energy and an arbitrary operator A sampled at N different coupling constants β_i, the probability distribution reweighted to coupling constant β is given by

$$P_\beta(E,A) = \frac{\sum_{i=1}^N g_i^{-1} H_i(E,M) e^{-\beta E}}{\sum_{j=1}^N n_j g_j^{-1} e^{-\beta_j E + f_j}}, \tag{4.33}$$

here n_j is the length of timeseries j, $g_j = 1 + 2\tau_j$ is a weight factor determined by the autocorrelation time and f_j is free-energy like quantity which must be determined self-consistently from

$$e^{-f_j} = \sum_{E,A} P_{\beta_j}(E,A). \tag{4.34}$$

[8] We used a software package kindly donated to us by Kari Rummukainen at Nordita to do Ferrenberg Swendsen reweighting.

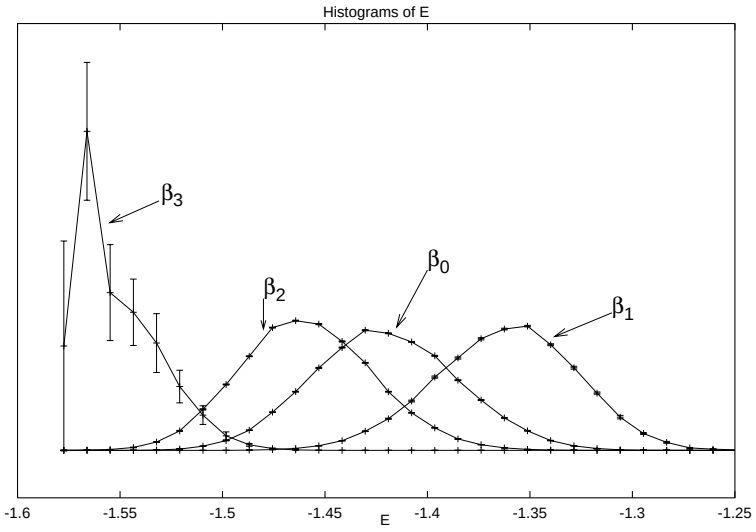

Figure 4.3: This figure shows histograms of E for the 2D Ising model. The simulation has been performed at $\beta_0 = \beta_c \approx 0.44069$, and the rawdata have subsequently been reweighted to $\beta_1 = 0.436$, $\beta_2 = 0.444$ and $\beta_3 = 0.456$. The histograms reweighted to β_1 and β_2 overlap quite nicely with the original histogram and the errors are small. β_3 is too fa r from β_0, and the dominating weight of this histogram is in a region where the original histogram has negligible support, consequently the errors grow dramatically large and this histogram is *not* reliable.

The use of Eq. 4.33 requires that 2-dimensional histograms $H(E, A)$ are stored during the simulations, this is impractical and an implementation in terms of the timeseries (E_α, A_α) is preferable. In this case the expectation value of A reweighted to β is given by [95]:

$$\langle A \rangle (\beta) = \frac{\sum_{i=1}^{N} \sum_{\alpha_t=1}^{n_i} A_i(\alpha_t) P_i(\alpha_t, \beta)}{\sum_{i=1}^{N} \sum_{\alpha_t=1}^{n_i} P_i(\alpha_t, \beta)}. \tag{4.35}$$

Where $P_i(\alpha_t, \beta)$ and f_i are given by a self consistent solution of the set:

$$P_i(\alpha_t, \beta) = \frac{g_i^{-1} e^{-\beta E_i(\alpha_t)}}{\sum_{j=1}^{N} n_j g_j^{-1} e^{-\beta_j E_j(\alpha_t) + f_j}} \tag{4.36}$$

$$e^{-f_j} = \sum_{i=1}^{N} \sum_{\alpha_t=1}^{n_i} P_i(\alpha_t, \beta_j). \tag{4.37}$$

4.4 Finite size effects

As mentioned in section 2.2 an infinite system size is essential to get a true phase transition. Obviously simulations must be performed with a finite system size, and this will inevitably affect the results.

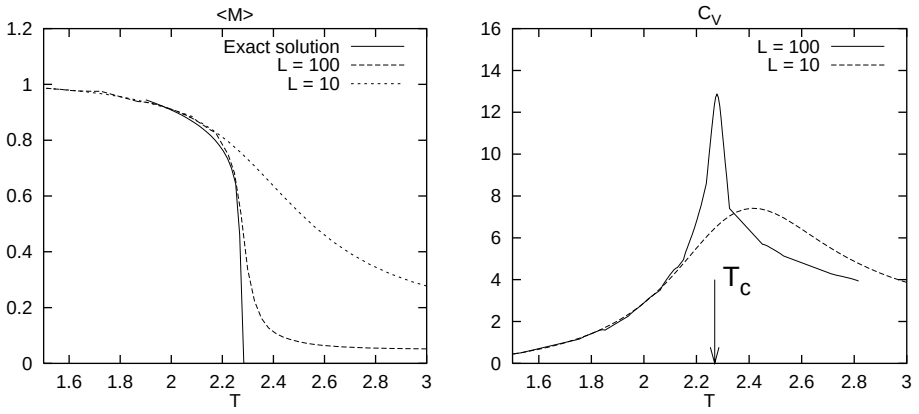

Figure 4.4: Simulation results on the 2D Ising model. The left part shows the magnetization as a function of temperature, the right part shows C_V for $L = 10$ and $L = 100$.

[8] The pseudocritical temperature in this case is the location of the maximum in the spesific heat.

From Fig. 4.4 we can see how the phase transition[9] is affected by finite size. In general all *singularities will be rounded*, in particular this means that

1. Response functions like C_V and χ attain finite values instead of diverging at the critical point, they will also be broadened. This is illustrated in the right part of Fig. 4.4.
2. Functions which should be excactly zero will generally have a finite tail, as the magnetisation above T_C, shown to the left in Fig. 4.4.
3. Discontinous *jumps* across first order transitions will be smeared out to narrow regions with large slope, and be superficially continous.

In addition critical couplings will be shifted. These shifts can generally be both ways, and the *pseudo*critical couplings will be different for different quantites. These effects always take place, in addition there can be other finite size effects which are more specific for the model/observable in question, for instance a quite exotic finite size effect for loop size distribution is discussed in [71].

The microscopic origin of finite size effects is that the correlation length ξ is bounded by the system size. In true critical phenomena $\xi = |t|^{-\nu} \to \infty$ at the critical point, whereas in finite systems ξ can not exceed L:

$$\xi_0(T) = |T - T_c|^{-\nu}, \quad \xi(T) = \begin{cases} \xi_0 & \xi_0 < L \\ L & \xi_0 > L \end{cases}. \tag{4.38}$$

If we go back to the critical scaling presented in section 2.4.1 we can replace $|t|^{-\nu}$ with L, and in that way we can find how the quantities vary with system size

$$C_V \propto |t|^{-\alpha} = \left(|t|^{-\nu}\right)^{\alpha/\nu} \Rightarrow C_V \propto L^{\alpha/\nu} \tag{4.39}$$

$$m \propto |t|^{\beta} = \left(|t|^{-\nu}\right)^{-\beta/\nu} \Rightarrow m \propto L^{-\beta/\nu} \tag{4.40}$$

$$\chi \propto |t|^{-\gamma} = \left(|t|^{-\nu}\right)^{\gamma/\nu} \Rightarrow \chi \propto L^{\gamma/\nu} = L^{2-\eta}. \tag{4.41}$$

In Eq. 4.41 we have used the scaling law Eq. 2.17 to get an expression involving *only* η, and not ν. Utilizing the finite size effects in this manner is falled *Finite Size Scaling* (FSS) and is the most commonly used method to calculate critical exponents from MC data. A good introduction to FSS can be found in [96], and an extremely elaborate FSS see [72].

In addition to calculating exponents, finite size effects can be applied to many other things. In Paper III finite size effects were used to differentiate between first and second

[9] Of course, in a finite system it is not a true phase transition, we will nevertheless talk about it as a phase transition.

order phase transitions, and in Paper IV we studied the finite size behaviour of the vortex-vortex distance to determine whether a particular superconductor was type-I or type-II.

4.4.1 A first order transition?

The most naive way to determine the order of a phase transition is to look for a discontinuous jump in the order parameter, or other thermodynamic quantities. This method detects *strong* first order transitions, but a weak transition, combined with unavoidable finite size rounding, will be impossible to detect this way. In the late 1980's Lee and Kosterlitz [97] devised a method based on finite size scaling and coexistence at first order transitions, to differentiate between first and second order transitons, the use of this method was essential in Paper III.

At a first order transition we have coexistence of two different phases, we call them *symmetric* and *broken* and use ψ_{S} and ψ_{B} to denote the two *pure* states. In addition we will use the symbol $\psi_{\mathrm{S+B}}$ to denote a mixed state containing *both* symmetric matter *and* broken matter. According to the definition of coexistence, the two states ψ_{B} and ψ_{S} have the same free energy, but in going from one state to the other we have to form an interface, and due to interface tension there is a free energy barrier ΔF between the two pure states.

During the simulation we build up a histogram $H(O)$ of the operator $\hat{O}$, for a first order transition the critical histogram will typically look like the right part of Fig. 4.5, with a double peak structure corresponding to the pure states ψ_{B} and ψ_{S} and a valley in between corresponding to the mixed state $\psi_{\mathrm{S+B}}$ which is less probable to find.

The probability that an operator X has the particular value X_1 can be written:

$$P(X = X_1) = \frac{\sum_{\{\alpha | X_i = X_1\}} e^{-\beta E_\alpha}}{Z(\beta)} = e^{-\beta A(X_1, L)} \tag{4.42}$$

In Eq. 4.42 $A(X_1, L)$ is a *free energy like* quantity, it differs from the true free energy by a temperature dependent additive quantity, but the difference ΔA between two states X_1 and X_2 is the same as for the free energy

$$A(X_1, L) - A(X_2, L) = F(X_1, L) - F(X_2, L) = \Delta F(L). \tag{4.43}$$

Combining Eq. 4.42 and 4.43 we find that the free energy gap separating the two pure states is given by

$$\Delta F(L) = \frac{1}{\beta} \ln \left(\frac{P_+}{P_-} \right), \tag{4.44}$$

where P_+ denotes the probability to find either one of the pure states, and P_- denotes the probability to find the mixed state in the bottom of the well of Fig. 4.5. Now to

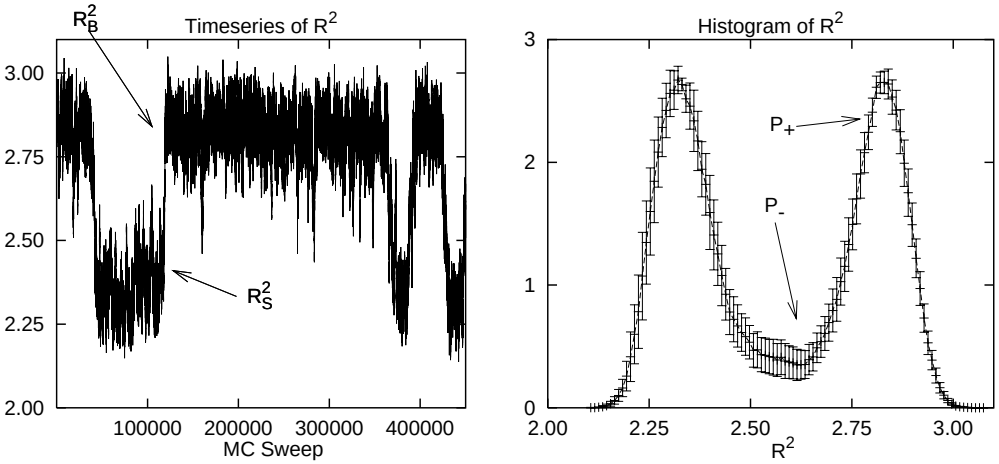

Figure 4.5: The left part shows rawdata of the quantity R^2, we can clearly identify two stable states, indicated with arrows as R^2_B and R^2_S in the figure. The right part shows a histogram of R^2, and the probabilities P_+ and P_- referenced in Eq. 4.44 are indicated with arrows. The histogram shows a slightly *reweighted* (see section 4.3) version of the rawdata. The reweighting has been done to get two *equally high* peaks.

finally determine the order of the phase transition we consider the scaling of $\Delta F(L)$ from Eq. 4.44 with L:

$$\Delta F(L) \propto L^{d-1} \quad \Rightarrow \quad \text{First order transition} \tag{4.45}$$

$$\Delta F(L) \propto L^{0} \quad \Rightarrow \quad \text{Second order transition} \tag{4.46}$$

The power $d-1$ in Eq. 4.45 corresponds to a flat interface between the two pure states. To get proper $d-1$ scaling of $\Delta F(L)$ requires quite large systems/strong transitions, in Paper III we generally concluded that transitions with $\Delta F(L) \propto L^{\kappa}, \kappa > 0$ were first order.

4.5 Simulations of the full GL model

Monte Carlo simulations on Lattice Gauge Theories is in principle not different from standard statistical mechanics simulations; however there are some conceptual differences it is important to be aware of:

1. There is *no heat bath* - i.e. there is no natural factorization of the action in terms of $[\beta] = J^{-1}$ and $[H] = J$ - instead we only have a complete action S which has dimension $[S] = 1$, and instead of the coupling β to an external thermal reservoir there are only the "internal couplings" of the field theory.

2. The Metropolis acceptance probability $P = \min(1, e^{-\beta\Delta E}) \to \min(1, e^{-\Delta S})$.

3. Because of the points mentioned above one quite often has to abondon the "common sense" one has developed for T dependence e.t.c. from conventional statistical physics simulations.

However these differences do not present any serious difficulties compared conventional statistical mechanics. The rest of this section will be devoted to *overrelaxation*, which is a method designed to speed up Lattice Gauge simulations.

4.5.1 Overrelaxation

Section 4.4.1 was devoted to the free energy barrier between the two coexisting states in a first order transition, and how the height of this barrier could be used to determine the order of the transition. Unfortunately this barrier also complicates the simulations significantly. If we look at the rawdata to the left in Fig. 4.5 we see that the system moves very infrequently between the two coexisting phases, the characteristic timescale diverges as $\tau \propto e^{\Delta F}$, and the resulting statistics is poor. To reduce this problem *overrelaxation* has been essential[10].

The idea of overrelaxation is to calculate a new state ψ'_α which "deviates much" from the original state ψ_α, but nevertheless is accepted with high probability. This way the correlations between consecutive states are reduced. The algorithm we have used [99– 101] consists of two steps:

We start with writing the scalar potential in Eq. 3.52 as

$$V(\psi(x)) = -\mathbf{a}\cdot\mathbf{F} + \beta_2 |\psi(\mathbf{x})|^2 + \frac{x}{\beta_G^3} |\psi(\mathbf{x})|^4 \tag{4.47}$$

where

$$\mathbf{a} = |\psi(\mathbf{x})| \begin{pmatrix} \cos[\arg(\psi(\mathbf{x}))] \\ \sin[\arg(\psi(\mathbf{x}))] \end{pmatrix} \tag{4.48}$$

and

$$\mathbf{F} = \frac{2}{\beta_G} \begin{pmatrix} \sum_\mu |\psi(\mathbf{x}\pm\hat{e}_\mu)| \cdot \cos[\arg(\psi(\mathbf{x}\pm\hat{e}_\mu)) + \alpha_\mu(\mathbf{x})] \\ \sum_\mu |\psi(\mathbf{x}\pm\hat{e}_\mu)| \cdot \sin[\arg(\psi(\mathbf{x}\pm\hat{e}_\mu)) + \alpha_\mu(\mathbf{x})] \end{pmatrix}. \tag{4.49}$$

$\mathbf{F}$ is proportional to an average of $\psi(\mathbf{x})$ at the neighboring points. Using $\mathbf{a}$ and $\mathbf{F}$ we introduce the new variables

$$X = \mathbf{a}\cdot\mathbf{f} \quad , \quad \mathbf{f} = \frac{\mathbf{F}}{|\mathbf{F}|} \tag{4.50}$$

[10] We have focused on rather *weak* first order transitions, if the phase transitions in question are strongly first order *Multicanonical* simulations is essential [98].

and

$$\mathbf{Y} = \mathbf{a} - X\mathbf{f} \tag{4.51}$$

and rewrite the scalar potential Eq. 4.47 in terms of $X, \mathbf{Y}$ and $|\mathbf{F}|$,

$$\bar{V}(X, Y^2, |\mathbf{F}|) = X^4 \frac{x}{\beta_G^3} + X^2 \underbrace{\left(\beta_2 + \frac{2xY^2}{\beta_G^3}\right)}_{B} - X|\mathbf{F}| + Y^2\beta_2 + Y^4\frac{x}{\beta_G^3}. \tag{4.52}$$

The actual updates are performed on the new variables X and Y with Eq. 4.52 as the starting point. As we can see $\bar{V}$ in Eq. 4.52 only depends on Y^2, so changing $\mathbf{Y} \to \mathbf{Y}' = -\mathbf{Y}$ leaves the action invariant. In terms of the original variables this corresponds to reflecting the phase of $\psi(\mathbf{x})$ around the direction of $\mathbf{f}$

$$\arg(\psi(\mathbf{x})) = \arctan\frac{2Xf_2 - a_2}{2Xf_1 - a_1}. \tag{4.53}$$

The updating of X is more complicated. Naively we would just solve the equation $\bar{V}(X) = \bar{V}(X')$, but the problem with this is that for an unsymmetric potential the interval $\mathrm{d}X$ is mapped to $\mathrm{d}X'$

$$\mathrm{d}X' = -\mathrm{d}X \underbrace{\left[\frac{\partial V(X)}{\partial X}\right]\left[\frac{\partial V(X')}{\partial X'}\right]^{-1}}_{P(X\to X')}, \tag{4.54}$$

as illustrated in Fig. 4.6. This leads to a violation of detailed balance, which can be corrected by the use of an accept/reject step with the probiblity $P(X \to X')$ indicated in Eq. 4.54. Consequently the algorithm for overrelaxation update of X consists of two steps:

1. Find the X' which solves the equation

$$\bar{V}(X) = \bar{V}(X'). \tag{4.55}$$

2. Accept the new state X' with probability

$$P(X \to X') = \left[\frac{\partial V(X)}{\partial X}\right]\left[\frac{\partial V(X')}{\partial X'}\right]^{-1}. \tag{4.56}$$

When we have calculated a new X', and determined to accept it, the new value of $\psi(\mathbf{x})$ is calculated from

$$\begin{aligned} |\psi(\mathbf{x})| &= \sqrt{X'^2 + Y'^2} \\ \arg(\psi(\mathbf{x})) &= \arctan\frac{Y_2' + X'f_2}{Y_1' + X'f_1}. \end{aligned} \tag{4.57}$$

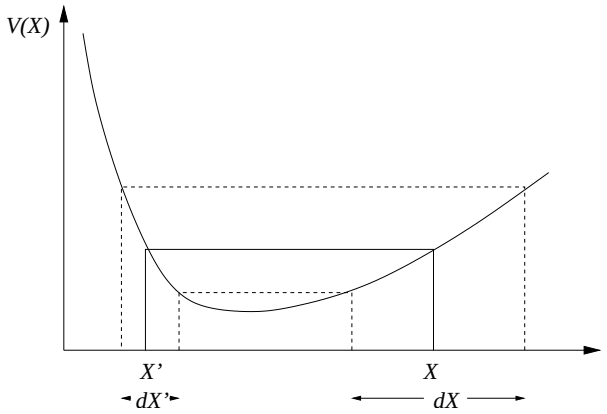

Figure 4.6: A demonstration of how $\mathrm{d}X$ maps to $\mathrm{d}X'$ with an unsymmetric potential.

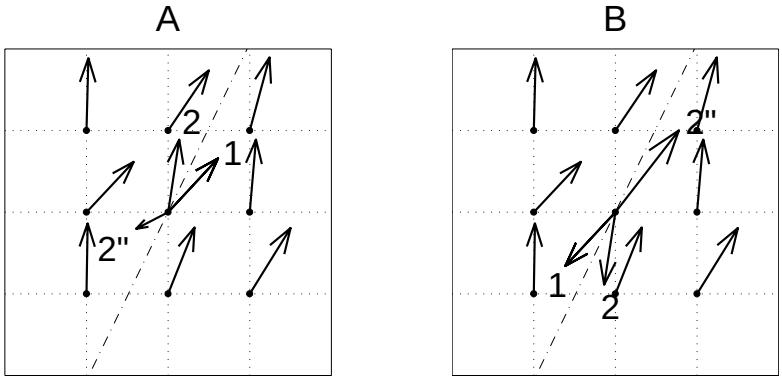

Figure 4.7: A 2D visualization of the overrelaxation update of the central "spin". The position marked as *1* is the initial state of ψ, the dashed line is parallel to $\mathbf{F}$. The $\mathbf{Y}$ update consists in reflecting the spin around this line to position *2*. Finally the position 2" is the final configuration from Eq. 4.57. See the text for the difference betw een figure A and B.

The phase transition in this model is schematically between an ordered state characterized by relatively large values of the amplitude, and gauge invariant phase differences close to zero, and a disordered state which is opposite in the sense that the average amplitude is small, and the gauge invariant phase differences are close to random.

Now, if we consider the overrelaxation scheme as visualized in Fig. 4.7 we see that the algorithm is designed to facilitate faster changes between ordered and disordered states. Both figure A and B in Fig. 4.7 show a "quite ordered" state. In figure A the central spin is aligned parallel to the neighboring spins, and in the final overrelaxed state it is anti parallel to its neighbors, and with much reduced amplitude. Hence both $\arg(\psi(\mathbf{x}))$ and $|\psi(\mathbf{x})|$ have been updated cooperatively to aid in *disordering* the system. In figure B the situation is opposite, in the final overrelaxed state both $\arg(\psi(\mathbf{x}))$ and $|\psi(\mathbf{x})|$ have been updated to *order* the system.

Bibliography

[1] M. Tinkham, *Introduction to Superconductivity*, McGraw-Hill, (1996).

[2] J. Bardeen, L. N. Cooper and J. R. Schrieffer, *Phys. Rev.* **108**, 1175 (1957).

[3] L. P. Gorkov, *Sov. Phys. JETP* **9**, 1364 (1959).

[4] A. A. Abrikosov, *Zh. Eksperim. i Teor. Fiz.* **32**, 1442 (1957).

[5] G. Bednorz and K. A. Müller, *Z. Phys. B* **64**, 189 (1986).

[6] http://www.conductus.com/pressReleases/press76.html

[7] http://www.detnews.com/2001/business/0105/22/b01-227761.htm

[8] C. C. Tsuei, J. R. Kirtley, C. C. Chi, L. S. Yu-Jahnes, A. Gupta, T. Shaw, J. Z. Sun and M. B. Ketchen, *Phys. Rev. Lett.* **73**, 593 (1994).

[9] D. J. V. Harlingen, *Rev. Mod. Phys.* **67**, 515 (1995).

[10] J. Orenstein and A. J. Millis, *Science* **228**, 468 (2000).

[11] H. Kleinert, *Phys. Lett. A* **277**, 205 (2000)[cond-mat/9906107].

[12] S. Elitzur, *Phys. Rev. D* **12**, 2455 (1974).

[13] J. J. Binney, N. J. Dowrick, A. J. Fisher and M. E. J. Newman, *The theory of critical phenomena*, Clarendon Press, (1992).

[14] G. S. Rushbrooke, *J. Chem. Phys.* **39**, 842 (1963).

[15] B. Widom, *J. Chem. Phys.* **43**, 3892 (1965).

[16] L. P. Kadanoff, *Physica* **2**, 263 (1966).

[17] H. Kleinert, *Gauge Fields in Condensed Matter*, World Scientific Publishing, (1989).

[18] J. Cardy, *Scaling and Renormalization in Statistical Physics*, Cambridge University Press, (1997).

[19] M. E. Fisher, *Rev. Mod. Phys.* **70**, 653 (1998).

[20] H. E. Stanley, *R ev. Mod. Phys.* **71**, 359 (1999).

[21] C. Itzykson and J. -. Drouffe, *Statistic al Field Theory*, Cambridge University Press, (1991).

[22] N. Goldenfeld, *L ectures on phase transitions and the renormalization group*, Addison-Wesley Publishing Company, (1992).

[23] J. Zinn-Justin, *Quantum field theory and critical phenomena*, Clarendon, (1989).

[24] L. P. Kadanoff, *A nn. Phys.***100**, 359 (1976), A. A. Migdal, *Z. Eksper. T eroet. Fiz.* **69**, 810 (1975).

[25] R. H. Swendsen, *Phys. Rev. Lett.* **42**, 859 (1979).

[26] P . M. Chaikin and T. C. Lubensky *Principles of condensed matter physics*, Cambridge University Press, (1995).

[27] Selected examples include the Higgs mechanism in particle physics, [28] phase transitions in liquid crystals, [29, 30] crystal melting, [31] the quantum Hall effect, [32, 33] and it is also used as an effective field theory describing phase transitions in the early Universe. [34]

[28] S. Coleman and E. Weinberg, *Phys. Rev. D* **7**, 1988 (1973).

[29] P . G. de Gennes,*Solid State Commun.* **10**, 753 (1972).

[30] T. C. Lubensky and J.-H. Chen, *Phys. Rev. B* **17**, 366 (1978).

[31] H. Kleinert, *Gauge Fields in Condensed Matter*, World Scientific Publishing, (1989).

[32] X. G. Wen and Y. S. Wu, *Phys. Rev. Lett.* **70**, 1501 (1993).

[33] L. Pryadko and S. C. Zhang, *Phys. Rev. Lett* **73**, 3282 (1994).

[34] A. Vilenkin and E. P .S. Shellard, *Cosmic strings and other topolo gical defects*, Cambridge University Press, (1994).

[35] V. L. Ginzburg and L. D. Landau, *Zh. Eksp. Teor. Fiz.* **20**, 1064 (1950).

[36] P .-G. de Gennes,*Superconductivity of Metals and Alloys*, Addison-Wesley, (1989).

[37] A. A. Abrikoso v, L. P. Gorkov and I. E. Dzyaloshinski, *Methods of quantum field theory in statistical physics*, Dover, (1975).

[38] J. W. Negele and H. Orland, *Quantum Many-Particle Systems*, Addison-Wesley , (1988).

[39] P. W. Anderson, *Phys. Rev.* **130**, 439 (1963).

[40] P. W. Higgs, *Phys. Rev.* **145**, 1156 (1966).

[41] K. Kajantie, M. Laine, T. Neuhaus, A. Rajantie and K. R. , hep-lat/0110062 (2001).

[42] H. Kleinert and V. Schulte-Frohlinde, *Critical properties of ϕ^4 theories*, World Scientific, (2001).

[43] B. I. Halperin, T. C. Lubensky and S. K. Ma, *Phys. Rev. Lett.* **32**, 292 (1974).

[44] C. Dasgupta and B. I. Halperin, *Phys. Rev. Lett.* **47**, 1556 (1981).

[45] C. W. Garland and G. Nounesis, *Phys. Rev. E* **49**, 2964 (1994).

[46] H. Kleinert, *Nuovo Cimento* **35**, 405 (1982).

[47] J. Bartholomew, *Phys. Rev. B* **28**, 5378 (1983).

[48] R. Folk and Y. Holovatch, cond-mat/9807421 (1998).

[49] A. Rajantie, hep-ph/0108159 (2001).

[50] J. M. Kosterlitz and D. J. Thouless, *J. Phys. C* **5**, L124 (1972), J. M. Kosterlitz and D. J. Thouless, *J. Phys. C* **6**, 1181 (1973) and J. M. Kosterlitz and D. J. Thouless, *J. Phys. C* **7**, 1024 (1974).

[51] A. K. Nguyen and A. Sudbø, *Phys. Rev. B* **60**, 15307 (1999).

[52] A. K. Nguyen and A. Sudbø, *Euro. Phys. Lett.* **46**, 780 (1999).

[53] H. B. Nielsen and P. Olesen, *Nucl. Phys. B* **61**, 45 (1973).

[54] H. A. Kramers and G. H. Wannier, *Phys. Rev. B* **60**, 252 (1941).

[55] R. Savit, *Rev. Mod. Phys.* **52**, 453 (1980).

[56] F. Wegner, *J. Math. Phys* **12**, 2259 (1971).

[57] P. R. Thomas and M. Stone, *Nucl. Phys. B* **144**, 513 (1978).

[58] M. Peskin, *Ann. Phys.* **113**, 122 (1978).

[59] M. Kiometzis, H. Kleinert and A. M. J. Schakel, *Phys. Rev. Lett.* **73**, 1975 (1994)[cond-mat/9503019].

[60] M. Kiometzis, H. Kleinert and A. M. J. Schakel, *Fortschr. Phys.* **43**, 697 (1995)[cond-mat/9508142].

[61] S. Mo, J. Hove and A. sudbø, *Phys. Rev. B* **65**, 104501 (2002)[cond-mat/0109260].

[62] J. Hove and A. Sudbø, *Phys. Rev. Lett.* **84**, 3426 (2000).

[63] P. Olsson and S. Teitel, *Phys. Rev. Lett.* **80**, 1964 (1998).

[64] J. Lidmar, M. Wallin and C. Wengel, *Phys. Rev. B* **58**, 2827 (1998).

[65] J. Lidmar and M. Wallin, *Phys. Rev. B* **59**, 1999 (8451).

[66] A. K. Nguyen, A. Sudbø and R. E. Hetzel, *Phys. Rev. L ett.***77**, 1592 (1996).

[67] I. F. Herbut, *J. Phys. A* **30**, 423 (1997).

[68] C. de Calan and F. S. Nogueira, cond-mat/9903247 (1999).

[69] N. Nagaosa, *Quantum Field Theory in Condensed Matter Phyiscs*, Springer Verlag, (1999).

[70] P.-G. de Gennes, *Scaling Consepts in Polymer Physics*, Cornell University Press, (1979).

[71] D. Austin, E. J. Copeland and R. J. Rivers, *Phys. Rev. D* **49**, 4089 (1994).

[72] M. Campostrini, M. Hasenbusch, A. Pelissetto, P. Rossi and E. Vicari, *Phys. Rev. B* **63**, 214503 (2001)[cond-mat/0010360].

[73] P. W. Kastelyn and C. M. Fortuin, *Physica* **57**, 536 (1972), P. W. Kastelyn and C. M. Fortuin, *Physica* **58**, 393 (1972), P. W. Kastelyn and C. M. Fortuin, *Physica* **59**, 545 (1972).

[74] S. Fortunato, hep-lat/0012006 (2000).

[75] A. M. J. Schakel, *Phys. Rev. E* **63**, 026115 (2001)[cond-mat/0008443].

[76] L. Onsager, *Phys. Rev.* **65**, 117 (1944).

[77] D. A. Lavis and G. M. Bell, *Statistical Mechanics of Lattice Systems 1*, Springer Verlag, (1999).

[78] H. Kleinert, cond-mat/9908239 (1999).

[79] G. Parisi, *Statistic al Field Theory*, Addison-Wesley Publishing Company, (1988).

[80] J. M. Thijssen, *Computational Physics*, Cambridge University Press, (1999).

[81] D. C. Rapaport, *The Art of Molecular Dynamics Simulation*, Cambridge University Press, (1997).

[82] N. D. Antunes, L. Bettencourt and M. Hindmarsh, *Phys. Rev. L ett.***80**, 908 (1998), N. D. Antunes, L. Bettencourt and M. Hindmarsh, *Phys. Rev. Lett.* **81**, 3083 (1998).

[83] For instance the dynamical critical exponent for the 2D ising model is $z \approx 2$ for single site update, and $z \approx 0$ for Wolff [84] cluster update. This example also shows that dynamic universality classes are *less universal* than static.

[84] U. Wolff, *Phys. Rev. Lett.* **62**, 361 (1989).

[85] P. Meakin, H. Metiu, R. G. Petschek and D. J. Scalapino, *J. Chem. Phys.* **79**, 1948 (1983).

[86] An annealing scheme corresponds to gradually reducing the temperature in the simulations, so that the system will eventually end up in the groundstate. Compared to more naive steepest descent algorithms the chance of beeing trapped in a local minima is greatly reduced, see Refs. [87] and [88].

[87] S. Kirkpatrick, C. D. G. Jr and M. P. Vecchi, *Science* **220**, 671 (1983).

[88] W. H. Press, B. P. Flannery, S. A. Teukolsky and W. T. Vetterling, *Numerical Recipes*, Cambridge University Press, (1986).

[89] J. Honerkamp, *Statistical Physics*, Springer Verlag, (1998).

[90] Metropolis, N., A. W. Rosenbluth, M. N. Rosenbluth, A. H. Teller and E. Teller, *J. Chem. Phys.* **21**, 1087 (1953).

[91] D. P. Landau and K. Binder, *A Guide to Monte Carlo Simulations in Statistical Physics*, Cambridge University Press, (2000).

[92] B. A. Berg, *Computer Physics Communications* **69**, 7 (1992).

[93] B. Efron, *The Jackknife, the Bootstrap, and Other Resampling Plans*, Society for Industrial and Applied Mathematics, (1982).

[94] A. M. Ferrenberg and R. H. Swendsen, *Phys. Rev. Lett.* **63**, 1195 (1989).

[95] E. P. Müngner and M. A. Novotny, *Phys. Rev. B* **43**, 5773 (1991).

[96] K. Binder and D. W. Heermann, *Monte Carlo Simulations in Statistical Physics*, Springer Verlag, (1997).

[97] J. Lee and J. M. Kosterlitz, *Phys. Rev. Lett.* **65**, 137 (1990).

[98] B. A. Berg, cond-mat/9909236 (1999).

[99] P. Dimopoulos, K. Farakos and G. Koutsoumbas, *Eur. Phys. J. C* **16**, 489 (2000)[hep-lat/9911012].

[100] K. Kajantie, M. Laine, K. Rummukainen and M. Shaposhnikov, *Nucl. Phys. B* **466**, 189 (1996)[hep-lat/9510020].

[101] Private communication from Kari Rummukainen at Nordita.

[102] J. Villain, *J. Phys. (Paris)* **36**, 581 (1977).

URN:NBN:no-2110

A Details of duality transformation

The problem with Eq. 3.18 is the cos function, which is difficult to handle analytically. The final approximation is the *Villain* approximation [102], which consist in replacing the cos with a "forced periodic" harmonic potential in the following way

$$e^{\beta \cos\theta} \approx R_{\mathrm{V}}(\beta) \sum_{n=-\infty}^{n=\infty} e^{-\beta_{\mathrm{V}}(\beta)/2(\theta-2\pi n)^2}. \tag{A.1}$$

In Eq. A.1 $\beta_{\mathrm{V}}(\beta)$ is a modified bending energy and $R_{\mathrm{V}}(\beta)$ is a normalization constant, with the special choice

$$\beta_{\mathrm{V}}(\beta) = -\frac{1}{2}\left(\ln\left(\frac{I_1(\beta)}{I_0(\beta)}\right)\right)^{-1} \quad \text{and} \quad R_{\mathrm{V}}(\beta) = \sqrt{2\pi\beta_{\mathrm{V}}(\beta)} I_0(\beta) \tag{A.2}$$

the Villain approximation Eq. A.1 is quantitativ ely correct ov er the whole temperature range [17]. How ev er the *critical* properties of the XY model will be correctly reproduced even if w eset $\beta_{\mathrm{V}}(\beta) = \beta$ and $R_{\mathrm{V}}(\beta) = 1$, and w ewill generally be content with the approximation

$$e^{\beta \cos\theta} \sim \sum_{n=-\infty}^{n=\infty} e^{-\beta/2(\theta-2\pi n)^2}. \tag{A.3}$$

Basically this approximation amounts to approximating the cosine with a harmonic approximation, and then introducing the new *integer valued* field n to enforce the *perio dic* behavior of the cosine. Since the vortices are a consequence of the *perio dic* nature of cos, the n field is essential.

Now we are ready to embark on the actual duality transformation in section A, apart from the approximations described in this section, the actual transformation is *exact*. The duality transformation is performed with the gauge field present, but for simulations w eoften go back to Eq. 3.18 and omit the gauge field altogether. Then w eare left with the 3DXY model, which is a thoroughly investigated model in statistical physics. Physically , omitting the gauge field amounts to "turning off" the charge in the problem, i.e. as if the condensate w ere *neutral*. These aspects are discussed further in section 3.4.3.

In this section we will perform the duality transformation from the original GL model to a grand canonical set of interacting vortex loops. In the derivation we will make repeated use of the Poisson summation formula [17]

$$\sum_{n=-\infty}^{\infty} e^{2\pi i n A} = \sum_{a=-\infty}^{\infty} \delta(A-a) \tag{A.4}$$

to shift between integer fields and real fields, and the Hubbard-Stratonovich (HS) decoupling [26] is repeatedly used to linearize quadratic exponents at the price of an auxiliary field. This process involves a great number of different fields - it is important to realize that at each step equivalence is *only* in terms of the partition function, i.e. the sum over all field configurations for the different fields, and not between the different fields. In other words it is not possible to transform uniquely from a state specified by one set of fields to the same state specified by another set of fields[1].

$$Z_V(\beta) = \int \mathcal{D}\theta\mathcal{D}\mathbf{A} \sum_{\mathbf{n}=-\infty}^{\infty} \exp\left[\sum_{\mathbf{x}}\left\{\sum_{\mu}\frac{\beta}{2}\left(\partial_\mu\theta - 2\pi n_\mu - eA_\mu\right)^2 + \frac{1}{2}\left(\nabla\times\mathbf{A}\right)^2\right\}\right] \tag{A.5}$$

The first operation on Eq. A.5 is to HS decouple the kinetic term. This introduces an auxiliary vector field $\mathbf{B}(\mathbf{x})$ which must be integrated over, but the advantage is that the coupling between the integer $\mathbf{n}$ field and the θ and $\mathbf{A}$ fields is linearised. If we temporarily ignore the gauge field, the Hubbard Stratonvich decoubled partition function is[2]

$$\tilde{Z}_V(\beta) = \int \mathcal{D}\theta\mathcal{D}\mathbf{B} \sum_{\mathbf{n}=-\infty}^{\infty} \exp\left[\sum_{\mathbf{x},\mu}\left\{\frac{1}{2\beta}B_\mu^2(\mathbf{x}) + iB_\mu(\mathbf{x})\left(\partial_\mu\theta - 2\pi n_\mu\right)\right\}\right]. \tag{A.6}$$

The next step is to use Poisson summation formula Eq. A.4 on the coupling between $B_\mu(\mathbf{x})$ and n_μ, this forces the auxiliary field $\mathbf{B}(\mathbf{x})$ to take only integer values, this integer valued field will be denoted by $\mathbf{b}(\mathbf{x})$. Subsequently we perform a partial integration of the term involving $\partial_\mu\theta$

$$\prod_{\mathbf{x}}\int \mathrm{d}\theta(\mathbf{x}) e^{\sum_\mu ib_\mu\partial_\mu\theta} \to \prod_{\mathbf{x}}\int \mathrm{d}\theta(\mathbf{x}) e^{-i\theta\sum_\mu\partial_\mu b_\mu} = \prod_{\mathbf{x},\mu}\delta(\nabla\mathbf{b}(\mathbf{x})), \tag{A.7}$$

i.e. the constraint $\nabla\cdot\mathbf{b}(\mathbf{x}) = 0$ is enforced uniformly in space. Physically this means

[1] In addition we will also ignore the prefactors arising from the various Gaussian integrals, this will not affect the critical properties, but as the prefactors will generally be T - dependent the high and low temperature properties will be incorrect.

[2] In Eqns. A.6 - A.9 we denote the partition function with $\tilde{Z}_V$ to indicate the absence of the $\mathbf{A}$ field.

that $\mathbf{b}(\mathbf{x})$ describes a set of *closed loops*. At this stage the theory looks like[3]

$$\tilde{Z}_V(\beta) = \sum_b{}' \exp\left[\sum_{\mathbf{x}} \frac{1}{2\beta}\mathbf{b}^2(\mathbf{x})\right]. \tag{A.8}$$

The constraint $\nabla \cdot \mathbf{b} = 0$ in Eq. A.8 is *essential*, without this constraint the partition function would have factorized in spatially independent Jacobi Θ functions with no phase transition. However the constraint leads to spatial couplings and a nontrivial theory *with* a phase transition.

The next step is to solve the constraint $\nabla \cdot \mathbf{b} = 0$ explicitly by introducing a new integer valued field $\mathbf{K}$, and writing $\mathbf{b} = \nabla \times \mathbf{K}$. In addition we relax the integer value constraint on $\mathbf{K}$, and instead introduce the real valued field $\mathbf{h}$ along with an integer valued field $\mathbf{m}$ by using Eq. A.4 backwards

$$\tilde{Z}_V(\beta) = \int \mathcal{D}\mathbf{A}\mathcal{D}\mathbf{h} \sum_{\mathbf{m}}{}' e^{-S(\mathbf{A},\mathbf{h},\mathbf{m})}, \tag{A.9}$$

$$S(\mathbf{A},\mathbf{h},\mathbf{m}) = \sum_{\mathbf{x}} \left\{ \frac{1}{2\beta}\left(\nabla \times \mathbf{h}\right)^2 + 2\pi i \mathbf{m}\cdot\mathbf{h} - i\left(\nabla\times\mathbf{h}\right)\cdot e\mathbf{A} + \frac{1}{2}\left(\nabla\times\mathbf{A}\right)^2 \right\}.$$

In Eq. A.9 we have reinserted the gauge field $\mathbf{A}$. The $\mathbf{m}$ objects in Eq. A.9 are the vortices. In order to get a pure vortex theory we must integrate over the gauge fields $\mathbf{h}$ and $\mathbf{A}$, this can be done quite simply. The first step is to use the vector identity[4] $(\nabla\times\mathbf{A})^2 = \nabla^2\mathbf{A}^2 - (\nabla\mathbf{A})^2$ to rewrite the field energies. We work in the gauge[5] $\nabla\mathbf{A} = \nabla\mathbf{h} = 0$. Finally we express the action in terms of Fourier components

$$S(\mathbf{A},\mathbf{h},\mathbf{m}) = \sum_{\mathbf{q}} \left\{ \frac{1}{2\beta}\left|\mathbf{Q_q}\mathbf{h_{-q}}\right|^2 + \pi i\left(\mathbf{m_q}\mathbf{h_{-q}} + \mathbf{m_{-q}}\mathbf{h_q}\right) - \right.$$
$$\left. \frac{ie}{2}\left[A^\mu_{\mathbf{q}}\left(\mathbf{Q_q}\times\mathbf{h_{-q}}\right)_\mu + A^\mu_{\mathbf{-q}}\left(\mathbf{Q_{-q}}\times\mathbf{h_q}\right)_\mu\right] + \frac{1}{2}\left|\mathbf{Q_q}\mathbf{A_{-q}}\right|^2 \right\}. \tag{A.10}$$

The next step is to form complete squares. We introduce the new variables

$$\mathbf{A}^+ = \frac{1}{2}\left(\mathbf{A_q} + \mathbf{A_{-q}}\right), \quad \mathbf{A}^- = \frac{1}{2i}\left(\mathbf{A_q} - \mathbf{A_{-q}}\right) \tag{A.11}$$

and

$$\mathbf{\Gamma}^+_0 = \frac{ie}{2}\left(\mathbf{Q_q}\times\mathbf{h_{-q}} + \mathbf{Q_{-q}}\times\mathbf{h_q}\right), \quad \mathbf{\Gamma}^-_0 = \frac{e}{2}\left(\mathbf{Q_q}\times\mathbf{h_{-q}} - \mathbf{Q_{-q}}\times\mathbf{h_q}\right). \tag{A.12}$$

[3] The symbolic notation $\sum_b{}'$ is used as $\sum_b{}' = \prod_{\mathbf{x}}\sum_{b(\mathbf{x})=-\infty}^{\infty}\delta(\nabla\mathbf{b})$, i.e. a sum over closed integer loops.

[4] The general identity is $(\mathbf{A}\times\mathbf{B})\cdot(\mathbf{C}\times\mathbf{D}) = (\mathbf{AC})(\mathbf{BD}) - (\mathbf{BC})(\mathbf{AD})$.

[5] For the $\mathbf{A}$ - field this is a choice based on computational convenience, in the case of $\mathbf{h}$ there is really no choice, remember that the fields $\mathbf{K}$ and subsequently $\mathbf{h}$ were introduced to explicitly solve the constraint $\nabla\mathbf{b} = 0$.

Then the $\mathbf{A}$ part of the action can be written with completed squares as

$$S(\mathbf{A}) = \frac{1}{2}\sum_{\mathbf{q}} \Bigg\{ |\mathbf{Q_q Q_{-q}}| \Bigg(\underbrace{\mathbf{A}^+ + \frac{\mathbf{\Gamma}_0^+}{|\mathbf{Q_q Q_{-q}}|}}_{\tilde{\mathbf{A}}^+} \Bigg)^2 + |\mathbf{Q_q Q_{-q}}| \Bigg(\underbrace{\mathbf{A}^- + \frac{\mathbf{\Gamma}_0^-}{|\mathbf{Q_q Q_{-q}}|}}_{\tilde{\mathbf{A}}^-} \Bigg)^2 - \underbrace{\frac{1}{|\mathbf{Q_q Q_{-q}}|}\left(\left(\mathbf{\Gamma}_0^+\right)^2 + \left(\mathbf{\Gamma}_0^-\right)^2 \right)}_{e^2 \mathbf{h_q h_{-q}}} \Bigg\}. \tag{A.13}$$

The integrals over $\tilde{\mathbf{A}}^+$ and $\tilde{\mathbf{A}}^-$ are Gaussian and can be readily performed, and we are left with the final term $e^2\mathbf{h_q h_{-q}}/2$ in Eq. A.13. The prefactors arising from the Gaussian integrals will be ignored. For the remaining part of the theory we see that the effect of the integral over the $\mathbf{A}$ field is to produce a mass term $e^2\mathbf{h_q h_{-q}}/2$, i.e. fluctuations in $\mathbf{A}$ produce a mass term in $\mathbf{h}$, which means *screening* of the vortex-vortex interactions. At this stage the theory looks like

$$S(\mathbf{h},\mathbf{m}) = \sum_{\mathbf{q}} \left\{ \pi i \left(\mathbf{m_q h_{-q}} + \mathbf{m_{-q} h_q}\right) + \frac{1}{2\beta}\mathbf{Q_q Q_{-q} h_q h_{-q}} + \frac{e^2}{2}\mathbf{h_q h_{-q}} \right\}. \tag{A.14}$$

The $\mathbf{h}$ field is integrated over in the same manner as the $\mathbf{A}$ field. With the convenience variables

$$\mathbf{h}^+ = \frac{1}{2}\left(\mathbf{h_q} + \mathbf{h_{-q}}\right), \quad \mathbf{h}^- = \frac{1}{2i}\left(\mathbf{h_q} - \mathbf{h_{-q}}\right), \tag{A.15}$$

$$\Omega_0^+ = \frac{\pi i}{2}\left(\mathbf{m_q} + \mathbf{m_{-q}}\right), \quad \Omega_0^- = \frac{\pi}{2}\left(\mathbf{m_q} - \mathbf{m_{-q}}\right) \tag{A.16}$$

and

$$\xi^2 = \frac{1}{2}\left(e^2 + \frac{\mathbf{Q_q Q_{-q}}}{\beta}\right), \tag{A.17}$$

we can write the action with completed squares as

$$S(\mathbf{h},\mathbf{m}) = \frac{1}{2}\sum_{\mathbf{q}} \left\{ \xi^2 \Bigg(\underbrace{\mathbf{h}^+ + \frac{\mathbf{\Omega}_0^+}{\xi^2}}_{\tilde{\mathbf{h}}^+} \Bigg)^2 + \xi^2 \Bigg(\underbrace{\mathbf{h}^- + \frac{\mathbf{\Omega}_0^-}{\xi^2}}_{\tilde{\mathbf{h}}^-} \Bigg)^2 - \frac{1}{\xi^2}\left(\left(\mathbf{\Omega}_0^+\right)^2 + \left(\mathbf{\Omega}_0^-\right)^2 \right) \right\}. \tag{A.18}$$

Again only the last term in Eq. A.18 gives a contribution, and the final theory of interacting vortices is given by

$$S(\mathbf{m}) = \beta \sum_{\mathbf{q}} \frac{\mathbf{m_q m_{-q}}}{e^2\beta + \mathbf{Q_q Q_{-q}}}. \tag{A.19}$$

$$H(\mathbf{m}) = -2\pi^2 J_0 \sum_{\mathbf{x_1},\mathbf{x_2}} \mathbf{m}(\mathbf{x_1}) V(\mathbf{x_1}-\mathbf{x_2}) \mathbf{m}(\mathbf{x_2}), \tag{A.20}$$

$$V(\mathbf{x}) = \sum_{\mathbf{q}} \frac{e^{-i\mathbf{q}\cdot\mathbf{x}}}{4\sum_\mu \sin^2\left(\frac{q_\mu}{2}\right) + \lambda^{-2}}\,. \tag{A.21}$$

A.1 Generating functional

By adding source terms $\mathbf{J}\cdot\mathbf{A}$ and $\mathbf{K}\cdot\mathbf{h}$ to the action we can calculate the *generating functional* $Z(\mathbf{J},\mathbf{K})$, and then eventually the correlation functions $\langle \mathbf{A_q A_{-q}}\rangle$ and $\langle \mathbf{h_q h_{-q}}\rangle$ by differentiation. The derivation of the generating functional is completely analogous to the derivation Eqns. A.10 - A.19, but the presence of source terms complicates the algebra.

We start by going back to Eq. A.10 and add an additional term

$$\frac{1}{2}\sum_{\mathbf{q}} \left(\mathbf{J_q A_{-q}} + \mathbf{J_{-q} A_q}\right) \tag{A.22}$$

to the action. Then we proceed in the same manner as to Eq. A.13, but with

$$\mathbf{\Gamma}^+ = \mathbf{\Gamma}_0^+ - \frac{1}{2}\left(\mathbf{J_q} + \mathbf{J_{-q}}\right), \quad \mathbf{\Gamma}^- = \mathbf{\Gamma}_0^- - \frac{1}{2i}\left(\mathbf{J_q} - \mathbf{J_{-q}}\right) \tag{A.23}$$

and

$$\frac{1}{\mathbf{Q_q Q_{-q}}}\left(\left(\mathbf{\Gamma}^+\right)^2 + \left(\mathbf{\Gamma}^-\right)^2\right) = e^2 \mathbf{h_q h_{-q}} - \frac{1}{\mathbf{Q_q Q_{-q}}}\left[\mathbf{J_q J_{-q}} - i\left(\mathbf{\Gamma}^0_{\mathbf{q}} \mathbf{J_{-q}} + \mathbf{\Gamma}^0_{\mathbf{-q}} \mathbf{J_q}\right)\right] \tag{A.24}$$

Then we are ready to start on the $\mathbf{h}$ integration, with the new quantities $\mathbf{\Omega}^\pm$,

$$\mathbf{\Omega}^+ = \mathbf{\Omega}_0^+ + \frac{ie}{4\mathbf{Q_q Q_{-q}}}\left(\mathbf{J_{-q}} \times \mathbf{Q_q} + \mathbf{J_q} \times \mathbf{Q_{-q}}\right) \tag{A.25}$$

$$\mathbf{\Omega}^- = \mathbf{\Omega}_0^- - \frac{e}{4\mathbf{Q_q Q_{-q}}}\left(\mathbf{J_{-q}} \times \mathbf{Q_q} - \mathbf{J_q} \times \mathbf{Q_{-q}}\right). \tag{A.26}$$

The final generating functional is given b y

$$Z(\mathbf{J_q},\mathbf{J_{-q}}) = \sum_{\mathbf{m_q m_{-q}}} \exp\left[-\sum_{\mathbf{q}} \left\{\mathbf{m_q} G(\mathbf{q}) \mathbf{m_{-q}} - F\left(\mathbf{J_q},\mathbf{J_{-q}}\right)\right\}\right]. \tag{A.27}$$

$$\begin{aligned} F(\mathbf{J_q},\mathbf{J_{-q}}) = & \frac{\mathbf{J_q J_{-q}}}{2\mathbf{Q_q Q_{-q}}\xi^2} \\ & - \frac{e^2}{4\xi^2\left(\mathbf{Q_q Q_{-q}}\right)^2}\left[\left(\mathbf{J_q J_{-q}}\right)\left(\mathbf{Q_{-q} Q_q}\right) - \left(\mathbf{Q_{-q} J_{-q}}\right)\left(\mathbf{J_q Q_q}\right)\right] \\ & - \frac{e\pi}{\xi^2 2\mathbf{Q_q Q_{-q}}}\left[\mathbf{J_{-q}}\left(\mathbf{Q_q}\times\mathbf{m_q}\right) + \mathbf{J_q}\left(\mathbf{Q_{-q}}\times\mathbf{m_{-q}}\right)\right]. \end{aligned} \tag{A.28}$$

Finally the correlation function can be found by differentiation,

$$\begin{aligned} \langle A^\mu_{\mathbf{q}} A^\nu_{\mathbf{-q}}\rangle = & \frac{1}{Z(0,0)}\frac{\partial^2}{\partial J^\mu_{\mathbf{q}} \partial J^\nu_{\mathbf{-q}}} Z(\mathbf{J_q},\mathbf{J_{-q}})\Big|_{\mathbf{J_q}=\mathbf{J_{-q}}=0} \\ = & \frac{1}{Z(0,0)} \sum_{\mathbf{m_q m_{-q}}} \left(\frac{\partial^2 F}{\partial J^\mu_{\mathbf{q}} \partial J^\nu_{\mathbf{-q}}} + \frac{\partial F}{\partial J^\mu_{\mathbf{q}}}\frac{\partial F}{\partial J^\nu_{\mathbf{-q}}}\right)\exp[\ldots]\Big|_{\mathbf{J_q}=\mathbf{J_{-q}}=0}. \end{aligned} \tag{A.29}$$

Calculating $\langle \mathbf{h_q h_{-q}}\rangle$ is done in much the same manner, but of course Eq. A.22 is replaced by

$$\frac{1}{2}\sum_{\mathbf{q}} \left(\mathbf{K_q h_{-q}} + \mathbf{K_{-q} h_q}\right). \tag{A.30}$$

In conclusion, the final formulas relating the vortex correlation function $\langle \mathbf{m_q m_{-q}}\rangle$ and the gauge field correlation functions $\langle \mathbf{A_q A_{-q}}\rangle$ and $\langle \mathbf{h_q h_{-q}}\rangle$ are

$$\boxed{\begin{aligned} \langle \mathbf{A_q A_{-q}}\rangle &= \frac{1}{|\mathbf{Q}|^2 + m_0^2}\left(1 + \frac{4\pi^2\beta m_0^2 \langle \mathbf{m_q m_{-q}}\rangle}{|\mathbf{Q}|^2\left(|\mathbf{Q}|^2 + m_0^2\right)}\right) \\ \langle \mathbf{h_q h_{-q}}\rangle &= \frac{2\beta}{|\mathbf{Q}|^2 + m_0^2}\left(1 - \frac{2\beta\pi^2\langle \mathbf{m_q m_{-q}}\rangle}{|\mathbf{Q}|^2 + m_0^2}\right). \end{aligned}}$$

Anomalous scaling dimensions and stable charged fixed-point of type-II superconductors

J. Hove and A. Sudbø
Department of Physics
Norwegian University of Science and Technology, N-7491 Trondheim, Norway
(July 9, 2004)

The critical properties of a type-II superconductor model are investigated using a dual vortex representation. Computing the propagators of gauge field $\mathbf{A}$ and dual gauge field $\mathbf{h}$ in terms of a vortex correlation function, we obtain the values $\eta_{\mathbf{A}} = 1$ and $\eta_{\mathbf{h}} = 1$ for their anomalous dimensions. This provides support for a dual description of the Ginzburg-Landau theory of type-II superconductors in the continuum limit, as well as for the existence of a stable charged fixed point of the theory, not in the $3DXY$ universality class.

PACS numbers: 74.60.-w, 74.20.De, 74.25.Dw

Determining the universality class of the phase-transition in a system of a charged scalar field coupled to a massless gauge field, such as a type-II superconductor, has been a long-standing problem[1]. Analytical and numerical efforts have recently focused on the use of a *dual* description of the Ginzburg-Landau theory (GLT) of type-II superconductors, pioneered by Kleinert[2], in investigating the character of a proposed novel *stable* fixed point of the theory for a charged superconducting condensate, in which case the $3DXY$ fixed point of the neutral superfluid is rendered unstable[3–6]. The dual formulation has also been employed to investigate the possibility of novel broken symmetries in the vortex liquid phase of such systems in magnetic fields[4,5].

The GLT is defined by a complex matter field ψ coupled to a massless fluctuating gauge field $\mathbf{A}$ with a Hamiltonian

$$H_{\psi,\mathbf{A}} = m_{\psi}^2 \left|\psi\right|^2 + \frac{u_{\psi}}{2}\left|\psi\right|^4 + \left|\left(\nabla - i2e\mathbf{A}\right)\psi\right|^2 + \frac{1}{2}\left(\nabla\times\mathbf{A}\right)^2. \qquad (1)$$

Here, e is the electron charge, and $H_{\psi,\mathbf{A}}$ is invariant under the local gauge-transformation $\psi \rightarrow \psi\exp(i\theta)$, $\mathbf{A} \rightarrow \mathbf{A} + \nabla\theta/2ie$. The GLT sustains stable topological objects in the form of vortex lines and vortex loops, the latter are the critical fluctuations of the theory[4,5]. These objects are highly nonlocal in terms of ψ, but a dual formulation offers a local field theory for them. The continuum dual representation of the topological excitations, (in $D = 3$ only), consists of a complex matter field ϕ coupled to a *massive* gauge field $\mathbf{h}^2$, with coupling constant given by the dual charge e_d, and with dual Hamiltonian

$$H_{\phi,\mathbf{h}} = m_{\phi}^2 \left|\phi\right|^2 + \frac{u_{\phi}}{2}\left|\phi\right|^4 + \left|\left(\nabla - ie_d\mathbf{h}\right)\phi\right|^2 + \frac{1}{2}\left(\nabla\times\mathbf{h}\right)^2 + \frac{1}{2}\left(\nabla\times\mathbf{A}\right)^2 + ie\left(\nabla\times\mathbf{h}\right)\cdot\mathbf{A}. \qquad (2)$$

The massiveness of $\mathbf{h}$ reduces the symmetry to a global $U(1)$-invariance. For details on how to obtain this dual Hamiltonian, we refer the reader to the thorough exposition of this presented in the textbook of Kleinert[7]. For $e \neq 0$ the original GLT in Eq. 1 has a local gauge symmetry, the dual theory in Eq. 2 has a global $U(1)$ symmetry. In the limit $e \rightarrow 0$, $\mathbf{A}$ decouples from ψ in Eq. 1, H_{ψ} describes a *neutral superfluid*, and the symmetry is reduced to global $U(1)$. The dual Hamiltonian $H_{\phi,\mathbf{h}}$ describes a charged superfluid coupled to a massless gauge field $\mathbf{h}$ with coupling constant e_d, and the global symmetry is extended to a local gauge symmetry. Hence, when $e \rightarrow 0$, *the dual of a neutral superfluid is isomorphic to a superconductor*. Integrating out the $\mathbf{A}$ field in Eq. 2 produces a mass-term $e^2\mathbf{h}^2/2$, where an exact renormalization-group equation for the mass of $\mathbf{h}$ is given by $\partial e^2/\partial \ln l = e^2$[8]. Therefore, when $e \neq 0$, then $e^2 \rightarrow \infty$ as $l \rightarrow \infty$. This supresses the dual gauge field, and the resulting dual theory is a pure $|\phi|^4$-theory. Hence, in the long-wavelength limit, *the dual of a superconductor is isomorphic to a neutral superfluid*[2].

In this paper, we obtain the anomalous scaling dimensions $\eta_{\mathbf{A}}$ of the gauge field[3,9], as well as $\eta_{\mathbf{h}}$ of the dual gauge field, not previously considered, directly from large-scale Monte-Carlo simulations. At a $3DXY$ critical point,$\eta_{\mathbf{A}} = \eta_{\mathbf{h}} = 0$. We find that $(\eta_{\mathbf{A}} = 1, \eta_{\mathbf{h}} = 0)$ when $e \neq 0$, and that $(\eta_{\mathbf{A}} = 0, \eta_{\mathbf{h}} = 1)$, when $e = 0$. We also contrast the anomalous dimension of the dual mass field ϕ at the dual charged (original neutral) and dual neutral (original charged) fixed points, obtaining $\eta_{\phi} = -0.24$ in the former case, and $\eta_{\phi} = 0.04$ in the latter.

A duality transformation, to a set of interacting vortex loops, is performed on the London/Villain approximation to the GLT. In this approximation the partition function is

$$Z(\beta, e) = \int D\mathbf{A}D\theta \sum_{\{\mathbf{n}\}} \exp\left[-\sum_{\mathbf{x}}\left\{\frac{1}{2}\left(\Delta\times\mathbf{A}\right)^2 + \frac{\beta}{2}\left(\Delta\theta - e\mathbf{A} - 2\pi\mathbf{n}\right)^2\right\}\right]. \qquad (3)$$

Here, θ is the local phase of the superconducting order parameter ψ, while $\mathbf{n}$ is an integer-valued *velocity field* (not vortex field) introduced to make the Villain potential 2π-periodic. The symbol Δ denotes a lattice derivative. Amplitude fluctuations are neglected in this ap-

proach. The validity of this approximation for $3D$ systems, has recently been investigated in detail, both numerically and analytically[10].

An auxiliary velocity field $\mathbf{v}$ linearises the kinetic energy. Performing the θ-integration constrains $\mathbf{v}$ to satisfy the condition $\Delta \cdot \mathbf{v} = 0$, explicitly solved by writing $\mathbf{v} = \Delta \times \mathbf{h}$, where $\mathbf{h}$ is forced to integer values by the summation over $\mathbf{n}$. Introducing an integer-valued *vortex field* $\mathbf{m} = \Delta \times \mathbf{n}$, and using Poisson's summation formula, we find

$$S(\mathbf{A}, \mathbf{h}, \mathbf{m}) = \sum_{\mathbf{x}} \Big\{ 2\pi i \mathbf{m} \cdot \mathbf{h} + \frac{1}{2\beta} (\Delta \times \mathbf{h})^2 + ie (\Delta \times \mathbf{h}) \mathbf{A} + \frac{1}{2} (\Delta \times \mathbf{A})^2 \Big\}. \quad (4)$$

Integrating the gauge field in Eq. 4 produces a mass term $e^2\mathbf{h}^2/2$, giving an effective theory containing the vortex field $\mathbf{m}$ coupled to a *massive* gauge field $\mathbf{h}$

$$Z(\beta, e) = \int D\mathbf{h} \sum_{\{\mathbf{m}\}} \prod_{\mathbf{x}} \delta_{\Delta \cdot \mathbf{m}, 0} \exp \Big[- \sum_{\mathbf{x}} \Big\{ 2\pi i \mathbf{m} \cdot \mathbf{h} + \frac{e^2}{2} \mathbf{h}^2 + \frac{1}{2\beta} (\Delta \times \mathbf{h})^2 \Big\} \Big]. \quad (5)$$

The variables $\mathbf{m}$ in Eq. 5 describe a set of interacting vortices, where the interactions are mediated through the gauge field $\mathbf{h}$. The variables in Eq. 5 are defined on a lattice which is dual to the lattice from Eq. 3, and the behavior with respect to temperature is inverted in the new variables. The θ field in Eq. 3 describes *order*, while the $\mathbf{m}$ field represents the topological excitations of the θ field. These excitations destroy superconducting coherence, and hence quantify *disorder*[7].

Integrating out the $\mathbf{h}$ field in Eq. 5, we obtain the Hamiltonian employed in the present simulations,

$$H(\mathbf{m}) = -2\pi^2 J_0 \sum_{\mathbf{x_1}, \mathbf{x_2}} \mathbf{m}(\mathbf{x_1}) V(\mathbf{x_1} - \mathbf{x_2}) \mathbf{m}(\mathbf{x_2}), \quad (6)$$

$$V(\mathbf{x}) = \sum_{\mathbf{q}} \frac{e^{-i\mathbf{q}\cdot\mathbf{x}}}{4 \sum_\mu \sin^2 \left(\frac{q_\mu}{2} \right) + \lambda^{-2}} \ . \quad (7)$$

In Eq. 7, the charge e and lattice-spacing a have both been set to unity, and λ is the bare London penetration depth. At every MC step, we attempt to insert a loop of unit vorticity and random orientation. A new energy is calculated from Eq. 6, and the proposed move is accepted or rejected according to the Metropolis algorithm. This procedure ensures that the vortex lines of the system always form closed loops of random size and shape[5]. In all simulations, a system size of $40 \times 40 \times 40$ was used, and up to $1.5 \cdot 10^5$ sweeps over the lattice per temperature were used.

To investigate the properties of $\mathbf{A}$ and $\mathbf{h}$ at the charged critical point of the original theory, Eq. 1, we have calculated the correlation functions $\langle \mathbf{A_q} \mathbf{A_{-q}} \rangle$ and $\langle \mathbf{h_q} \mathbf{h_{-q}} \rangle$ in terms of vortex correlations, obtaining

$$\langle \mathbf{A_q} \mathbf{A_{-q}} \rangle = \frac{1}{|\mathbf{Q}|^2 + m_0^2} \left(1 + \frac{4\pi^2 \beta m_0^2 G(\mathbf{q})}{|\mathbf{Q}|^2 \left(|\mathbf{Q}|^2 + m_0^2 \right)} \right), \quad (8)$$

$$\langle \mathbf{h_q} \mathbf{h_{-q}} \rangle = \frac{2\beta}{|\mathbf{Q}|^2 + m_0^2} \left(1 - \frac{2\beta\pi^2 G(\mathbf{q})}{|\mathbf{Q}|^2 + m_0^2} \right), \quad (9)$$

where $G(\mathbf{q}) = \langle \mathbf{m_q} \mathbf{m_{-q}} \rangle$, $m_0 = \lambda^{-1}$ and $Q_\mu = 1 - e^{-i\mathbf{q}\cdot\hat{\mu}}$. All correlation functions have been calculated in the *transverse gauge* $\nabla \cdot \mathbf{A} = \nabla \cdot \mathbf{h} = 0$. Both of the fields $\mathbf{h}$ and $\mathbf{A}$ are renormalized by vortex fluctuations, albeit in quite different ways.

Invoking the standard form $\left(q^2 + m_{\text{eff}}^2 \right)^{-1}$ for the correlation functions in the immediate vicinity of the critical point in the limit $q \to 0$, we find the following expressions for the effective masses,

$$\left(m_{\text{eff}}^{\mathbf{A}} \right)^2 = \lim_{q \to 0} \frac{m_0^2}{1 + 4\pi^2 \beta G(\mathbf{q}) q^{-2}}, \quad (10)$$

$$\left(m_{\text{eff}}^{\mathbf{h}} \right)^2 = \lim_{q \to 0} \frac{m_0^2}{2\beta \left(1 - \frac{2\pi^2 \beta G(\mathbf{q})}{m_0^2} \right)}. \quad (11)$$

When $e \neq 0$ the correlation function for $\mathbf{A}$ assumes the form

$$\langle \mathbf{A_q} \mathbf{A_{-q}} \rangle \propto \frac{1}{q^{2-\eta_{\mathbf{A}}}} \quad (12)$$

at the critical point. To determine $\eta_{\mathbf{A}}$, we compute the vortex correlator $G(q)$. For $\lambda << L = 40$, we expect the following behaviour for $G(\mathbf{q})$ in the limit $q \to 0$,

$$T < T_c \Rightarrow G(\mathbf{q}) \propto q^2, \quad (13)$$

$$T = T_c \Rightarrow G(\mathbf{q}) \propto \ q^\eta, \quad (14)$$

$$T > T_c \Rightarrow G(\mathbf{q}) \propto \ C(T). \quad (15)$$

When these limiting forms are inserted in Eq. 10, we see that for $T \leq T_c$, $m_{\text{eff}}^{\mathbf{A}}$ will be finite through the Higgs Mechanism (Meissner effect). For $T \geq T_c$ we will have $m_{\text{eff}}^{\mathbf{A}} = 0$ as in the normal case of a massless photon. Assuming $G(q) \propto q^\eta$ precisely at the critical point, it is seen that η corresponds to $\eta_{\mathbf{A}}$ from Eq. 12. *We thus identify the scaling power of $G(\mathbf{q})$ at the critical point with the anomalous dimension of the massless gauge field $\mathbf{A}$.*

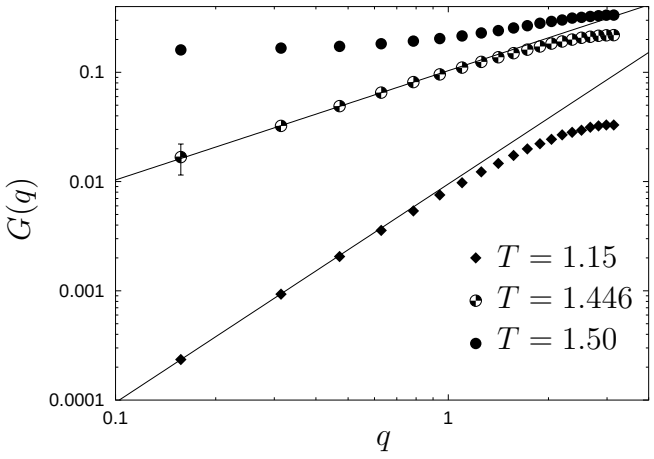

FIG. 1. log-log plot of $G(q)$ for the three alternatives in Eq. 13 - 15, with $\lambda = a/2$. For this λ, $T_c = 1.446$. Apart from the point $q = q_{\min}, T = 1.446$ the error bars are smaller than the symbols used.

All three limiting forms Eqs. 13-15 are shown in Fig. 1. The gauge field masses $m_{\rm eff}^{\mathbf{h}}$ and $m_{\rm eff}^{\mathbf{A}}$ in Eqs. 10 and 11, are shown in Fig. 2. At the critical point $G(q) \propto q$, so that $\eta_{\mathbf{A}} = 1$. Note that, while $m_{\rm eff}^{\mathbf{A}}$ vanishes at $T = T_c$, $m_{\rm eff}^{\mathbf{h}}$ is finite but non-analytic. *As a result of the vortex loop blowout, the screening properties of the vortices are dramatically increased, and* $m_{\rm eff}^{\mathbf{h}}$ *increases sharply.*

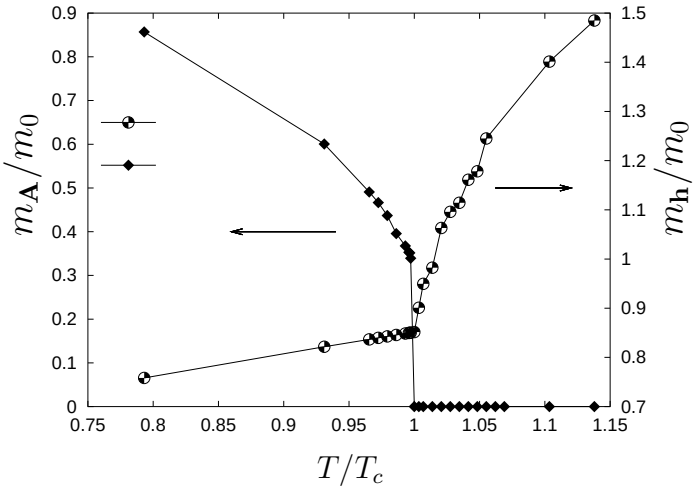

FIG. 2. $m_{\rm eff}^{\mathbf{A}}/m_0$ and $m_{\rm eff}^{\mathbf{h}}/m_0$ as functions of T.

To find $\eta_{\mathbf{h}}$ independently, we consider first the uncharged case $\lambda \to \infty$, $m_0 \to 0$. First, at an intermediate step in the transformation Eqs. 3 - 5, the action reads

$$S(\beta, e) = -\sum_{\mathbf{x}} \left\{ \frac{1}{2\beta} \mathbf{l}^2 + ei\mathbf{A}\cdot\mathbf{l} + \frac{1}{2}\left(\nabla\times\mathbf{A}\right)^2 \right\}. \quad (16)$$

Here, $\mathbf{l}$ is an integer field of closed current loops. Setting $e = 0$ in Eq. 5, the action of the dual Villain model is obtained,

$$\tilde{S}_V(\beta,\Gamma) = -\sum_{\mathbf{x}} \left\{ 2\pi i \mathbf{m}\cdot\mathbf{h} + \frac{1}{2\beta}\left(\Delta\times\mathbf{h}\right)^2 + \frac{\Gamma}{2}\mathbf{m}^2 \right\}. \quad (17)$$

Here, a term $\Gamma\mathbf{m}^2/2$ has been added, and $\tilde{S}_V(\beta,\Gamma)$ corresponds to the Villain-action in the limit $\Gamma \to 0$. However, it is physically reasonable to propose that the limit $\Gamma \to 0$ is non-singular, since the added term is short-ranged. It should therefore be an irrelevant perturbation, in renormalization group sense, to the long-ranged Biot-Savart interaction governing the fixed point, which is mediated by $\mathbf{h}$. Rescaling $\mathbf{h} \to \mathbf{h}e/2\pi$ in Eq. 17, we have[11] $Z(\beta, e) = \tilde{Z}_V\left(e^2/4\pi^2, 1/2\beta\right)\big)$, leaving Eqs. 16 and 17 interchangeable; $\eta_{\mathbf{h}}$ from Eq. 17 should have the same value as $\eta_{\mathbf{A}}$ from Eq. 16. The above is demonstrated by our simulations based on Eqs. 6-9, *which are independent of the proposed form Eq. 17.*

To determine $\eta_{\mathbf{h}}$ we study the correlation function $\langle \mathbf{h_q h_{-q}} \rangle$ (Eq. 9) in the limit $m_0 \to 0$. At the uncharged fixed point of the original theory, which is the charged fixed point of the dual theory, we have $\lim_{q\to 0} 2\pi\beta^2 G(\mathbf{q}) = (1 - C_2(T))q^2 + ..., q^2 - C_3(T)q^{2+\eta_{\mathbf{h}}} + ...$, and $q^2 - C_4(T)q^4 + ...$, for $T < T_c, T = T_c$, and $T \geq T_c$, respectively. Here, $C_2(T)$ corresponds to the helicity modulus (superfluid density)[12], $C_3(T)$ is a critical amplitude, and $C_4(T)$ is the inverse of the mass of the dual gauge field for $T \geq T_c$. Correspondingly, we have $\lim_{q\to 0} < \mathbf{h_q h_{-q}} >= 2\beta C_2/q^2$, $2\beta C_3/q^{2-\eta_{\mathbf{h}}}$, and $2\beta C_4$, for $T < T_c, T = T_c$, and $T \geq T_c$, respectively. Note that $\mathbf{h}$ is massless for $T < T_c$, while it is massive for $T > T_c$, the dual system exhibits a "dual Meissner-effect" for $T \geq T_c$. At $T = T_c$, we have $q^2 \ \langle \mathbf{h_q h_{-q}} \rangle \simeq C_3(T) q^{\eta_{\mathbf{h}}}$. A plot of $q^2 \ \langle \mathbf{h_q h_{-q}} \rangle$ is shown in Fig. 3. A linear behaviour at $T = T_c$ is found, implying that $\eta_{\mathbf{h}} = 1$ when $e = 0$. Since $\eta_{\mathbf{h}} = 1$ in the uncharged case, this provides further support for the Hamiltonian Eq. 2.

We now set $e \neq 0$. The gauge field $\mathbf{h}$ becomes massive via the term $e^2\mathbf{h}^2/2$, which appears after integrating out the $\mathbf{A}$ field in Eq. 2. In this case, $\lim_{q\to 0}\langle \mathbf{h_q h_{-q}} \rangle = 2\beta/m_0^2$ from Eq. 9, and $\mathbf{h}(r)$ would naively have the trivial scaling dimension $(2-d)/2$. However, the mass term offers us a freedom in assigning dimensions to e and $\mathbf{h}$, by introducing renormalization Z-factors, here $e' = Z_{\mathbf{h}}^{1/2} e$ and $\mathbf{h}' = Z_{\mathbf{h}}^{-1/2}\mathbf{h}$.

Prior to integrating out $\mathbf{A}$ in Eq. 2, the mass appears in the term $ie\left(\nabla\times\mathbf{h}\right)\cdot\mathbf{A}$. Integration of the ϕ field, partial or complete, can only produce $(\nabla/i - e_d\mathbf{h})$-terms. In particular, this must hold during integration of fast Fourier-modes of the ϕ field. Thus, the term $i(\nabla\times\mathbf{h})\cdot\mathbf{A}$ *is renormalisation group invariant*, i.e. its prefactor must be dimensionless. In terms of scaled fields, at the charged fixed point of the original theory, we have $\mathbf{A}' = Z_{\mathbf{A}}^{-1/2}\mathbf{A}$, with $Z_{\mathbf{A}} \propto l^{\eta_{\mathbf{A}}}$, $\eta_{\mathbf{A}} = 1$[8]. For $\mathbf{h}$, we use $Z_{\mathbf{h}} \propto l^{\Delta}$, where Δ is *not* an anomalous scaling dimension ($\mathbf{h}$ is massive, cf. Fig. 2), but rather a contribution

to the engineering dimension of $\mathbf{h}$. Inserting this into the crossterm $ie\,(\nabla\times\mathbf{h})\cdot\mathbf{A}$, we find the scaling dimension $(\eta_{\mathbf{A}}+\Delta)/2-1$, which must vanish. This gives the constraint $\Delta=1$ to avoid conflicting results for $\eta_{\mathbf{A}}$.

Remarkably, therefore, the scaling dimension of $\mathbf{h}$ at $T=T_c$ is the same in both cases $m_0=0$ and $m_0\neq 0$. The results for $\eta_{\mathbf{A}}$ and $\eta_{\mathbf{h}}$ in the previous paragraphs, are summed up in Table I.

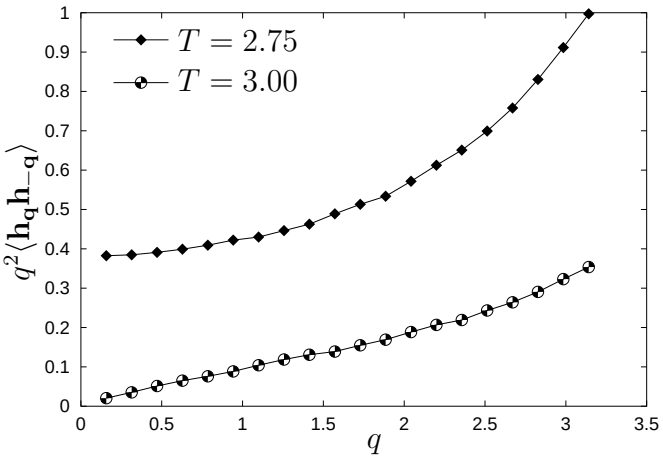

FIG. 3. $q^2\langle \mathbf{h_q}\mathbf{h_{-q}}\rangle$ for two different T. For $\lambda=\infty$, $T_c=3.00$.

We next consider the distribution of vortex loop sizes in the model Eq. 7, connecting the vortex loop distribution to the anomalous dimension of ϕ at T_c *both for the case* $e=0$ *and* $e\neq 0$. During the simulations, we sample the distribution of loop-sizes $D(p)$, where p is the perimeter of a loop. This distribution function can be fitted to the form[5,4]

$$D(p)\propto p^{-\alpha}e^{-\beta p\varepsilon(T)}, \tag{18}$$

where $\varepsilon(T)$ is an effective line-tension for the loops. Figures showing the qualitative features of $D(p)$ can be found in Ref. 5. The critical point is characterised by a vanishing line-tension, and close to the critical point we find that $\varepsilon(T)$ vanishes as $\varepsilon(T)\propto|T-T_c|^{\gamma_\phi}$.

The vortex loops are the topological excitations of the GL and 3DXY models, at the same time they are the real-space representation of the Feynman diagrams of the dual field theory. By sampling $D(p)$, we obtain information about the dual field ϕ, particularly γ_ϕ can be identified as a *susceptibility* exponent for the ϕ field[5]. Using the scaling relation $\gamma_\phi=\nu_\phi\,(2-\eta_\phi)$, and the important observation that even at the charged dual fixed point $\nu_\phi=\nu_{3DXY}$[5], this also gives us a value for the anomalous scaling dimension η_ϕ when we use the value $\nu_{3DXY}=0.673$[13].

In Ref. 5 the vortex loops of the 3DXY model have been studied meticulously, yielding the value $\eta_\phi(0)=-0.18\pm0.07$. Since the dual of this model is isomorphic to a superconductor, $\eta_\phi(0)$ should be similar to $\eta_\psi(e)$ of the original GLT.

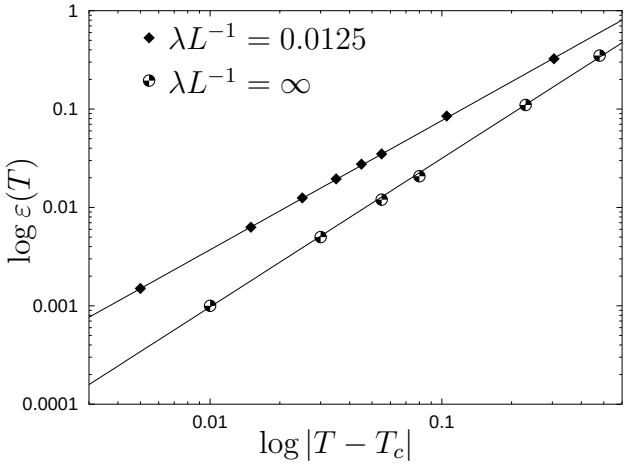

FIG. 4. $\ln\varepsilon(T)$ as a function of $\ln|T-T_c|$. The upper line shows the charged case with finite e, and the lower line shows the neutral case with $e=0$. The slopes of the two straight lines are $\gamma_\phi=1.315$ and $\gamma_\phi=1.51$, corresponding to the anomalous dimensions $\eta_\phi=-0.24$ (neutral, i.e. dual charged) and $\eta_\phi=0.04$ (charged, i.e. dual neutral), respectively.

We have studied the vortex loop distribution in both the neutral and the charged case. In the former case we find $\eta_\phi\simeq-0.24$, in good agreement with Ref. 5. In the latter case the dual theory has a $U(1)$ symmetry, and we would expect to find $\eta_\phi=\eta_{3DXY}$. The exponent η_{3DXY} has recently been determined with great accuracy to $\eta_{3DXY}=0.038$[13], whereas we find $\eta_\phi\simeq0.04$ which compares well with this value. Fig. 4 shows $\varepsilon(T)$ for both the charged and uncharged models. *It is evident that they belong to two different universality classes.*

In the case $e\neq0$, *which corresponds to the dual neutral case*, the inverse ϕ-propagator is given by $G^{-1}=q^2+\Sigma(q)$, where Σ is a self-energy, and $\Sigma(q)\sim q^{2-\eta}$ by definition. This gives a leading order behavior $G\sim1/q^{2-\eta}$ provided $\eta>0$, and we find $\eta=0.04$ for this case. On the other hand, for the case $e=0$, *which corresponds to the dual charged case*, dual gauge field fluctuations alter the physics, softening the long-wavelength ϕ field fluctuations. We obtain $G^{-1}=q^4+\Sigma(q)$, again with $\Sigma(q)\sim q^{2-\eta}$, which now gives a leading order behavior $G\sim1/q^{2-\eta}$, provided $\eta>-2$. Our result $\eta=-0.24$ for the case $e=0$ (dual charged) is consistent with this, and also with the absolute bounds $\eta>2-D=-1$, in $D=3$.

A consequence of the above is that in $D=3$ dimensions, $\lambda\sim\xi^{(D-2)/(2-\eta_{\mathbf{A}})}=\xi$ at the charged critical point, in contrast to $\lambda\sim\sqrt{\xi}$ at the $3DXY$ neutral critical point. Since our results have been obtained directly by MC simulations, they are valid beyond all orders in perturbation theory.

This work has been supported by a grant of computing time from Tungregneprogrammet, Norges Forskningsråd.

We thank Para//ab for valuable assistance in optimizing our computer codes for use on the Cray Origin 2000, and Zlatko Tešanović for many useful discussions.

[1] B. I. Halperin, T. C. Lubensky and S. K. Ma, Phys. Rev. Lett., **32**, 292 (1974); I. D. Lawrie, Nucl. Phys. **B200**, [FS 14], 1, (1982); H. Kleinert, Nuovo Cimento, **35**, 405 (1982). For a review, see I. D. Lawrie, in *Fluctuation Phenomena in High Temperature Superconductors*, Ed. M. Ausloos and A. Varlamov, Kluwer Academic Publishers, Dordrecht (1997).
[2] H. Kleinert, *Gauge Fields in Condensed Matter*, (World Scientific Publishing, Singapore, 1989).
[3] I. F. Herbut and Z. Tešanović, Phys. Rev. Lett.**76**, 4588 (1996). In this work, the existence of a stable charged fixed point was *assumed*. I. F. Herbut, J. Phys. A **30**, 423 (1997).
[4] Z. Tešanović, Phys. Rev. B**59**, 6449 (1999); A. K. Nguyen and A. Sudbø, Europhys. Lett.**46**, 780 (1999).
[5] A. K. Nguyen and A. Sudbø, Phys. Rev. **B 60**, 15307 (1999).
[6] A. Sudbø, A. K. Nguyen and J. Hove, cond-mat/**9907386**.
[7] In particular, see vol. 1, part II, Ch. 13 of Ref.[2].
[8] C. de Calan and F. S. Nogueira, Phys. Rev. **B 60**, 4255 (1999).
[9] P. Olsson and S. Teitel, Phys. Rev. Lett.**80**, 1964 (1998).
[10] See Fig. 1 of Ref.[5], and H. Kleinert, condmat/**9908239**.
[11] C. Dasgupta and B. I. Halperin, Phys. Rev. Lett.**47**, 1556 (1981).
[12] A. K. Nguyen, A. Sudbø and R. E. Hetzel, Phys. Rev. Lett.**77**, 1592 (1996).
[13] M. Hasenbusch and T. Török, J. Phys. **A 32**, 6361 (1999).

m_0	$\eta_{\mathbf{A}}$	FP, original theory	$\eta_{\mathbf{h}}$	FP, dual theory
0	0	Neutral 3DXY	1	Charged
Finite	1	Charged	0	Neutral 3DXY

TABLE I. Values of $\eta_{\mathbf{A}}$ and $\eta_{\mathbf{h}}$ at the stable neutral and charged critical points of the original and dual theories. FP is an abbreviation for fixed point.

Hausdorff dimension of critical fluctuations in abelian gauge theories

J. Hove, S. Mo, and A. Sudbø
Department of Physics
Norwegian University of Science and Technology, N-7491 Trondheim, Norway
(July 10, 2004)

The geometric properties of the critical fluctuations in abelian gauge theories such as the Ginzburg-Landau model are analyzed in zero background field. Using a dual description, we obtain scaling relations between exponents of geometric and thermodynamic nature. In particular we connect the anomalous scaling dimension η of the dual matter field to the Hausdorff dimension D_H of the critical fluctuations, *which are fractal objects*. The connection between the values of η and D_H, and the possibility of having a thermodynamic transition in finite background field, is discussed.

PACS numbers: 74.60.-w, 74.20.De, 74.25.Dw

Anderson has proposed the breakdown of a generalized rigidity associated with proliferation of defect structures in an order parameter as a general means of characterizing phase transitions[1]. In the context of three-dimensional superfluids and extreme type-II superconductors, such ideas have recently been put on a quantitative level[2,3]. It has been explicitly demonstrated that in three spatial dimensions abelian gauge theories such as the Ginzburg-Landau theory describing type-II superconductors, suffer a continuous phase transition driven by a proliferation of topological defects in the order parameter, which are closed loops of quantized vorticity[3]. These loops are induced by *transverse* phase fluctuations in a complex scalar order parameter. Such fluctuations are prominent in, for instance, doped Mott-Hubbard insulators[4,2,3].

In this paper, we investigate the non-trivial geometric properties of these critical fluctuations, and give a geometric interpretation of the anomalous scaling dimension of the condensate order parameter both for a charged and neutral condensate. In addition, we discuss the connection between the geometric properties of the zero-field critical fluctuations and the possibility of having a thermodynamic finite-field phase transition involving unbinding of loops of quantized vorticity.

We emphasize that the main results to be presented are quite general, and apply to the static critical sector of any theory of a complex scalar matter field coupled to a fluctuating gauge-field *in three spatial dimensions*[2,3,5], provided the symmetry group of the theory is abelian.

The Hamiltonian for the system is given by

$$H(q,u_\phi) = m_\phi^2 \left|\phi\right|^2 + \frac{u_\phi}{2}\left|\phi\right|^4 + \left|D_\mu\phi\right|^2 + \frac{1}{4}F^2, \qquad (1)$$

where $F^2 = F_{\mu\nu}F^{\mu\nu}$, $F_{\mu\nu} = \partial_\mu h_\nu - \partial_\nu h_\mu$, $D_\mu = \partial_\mu - iqh_\mu$, and $\phi = |\phi|\exp(i\theta)$ is a complex matter field coupled to a massless gauge field $\mathbf{h}$ with coupling constant q. The $|\phi|^4$-term mediates a short-range repulsion, while the gauge-field $\mathbf{h}$ mediates long range interactions. m_ϕ is the *mass-parameter* for the ϕ-field, and u_ϕ is a self coupling.

Consider Eq. 1 representing a $3D$ condensate with charge $q \neq 0$ sustaining stable topological objects in the form of closed vortex loops. Then the theory with $q = 0$ is a field-theoretical description of the ensemble of these stable topological objects, constituting a dual description of the original theory[5]. The theory with $q = 0$ is also a direct field-theoretical description of a neutral condensate. Thus, in $3D$, the gauge-theory $H(q \neq 0, u_\phi)$ describing a *charged* condensate has field-theoretical description of its critical fluctuations or topological defects in terms of a theory isomorphic to $H(q = 0, u_\phi)$ describing a similar but *neutral* condensate, and vice versa[5]. In this sense, a charged condensate has neutral vortices with only short-ranged steric interactions, while a neutral condensate has charged vortices with long-ranged interactions. In the former case, the long-ranged interactions between vortex segments are rendered short-ranged by fluctuations of the gauge-field in the original theory, i.e. the dual gauge-field is massive with mass given by the charge of the original problem[5].

The anomalous dimension η for the ϕ field is defined via the relation

$$G(\mathbf{x},\mathbf{y}) = \langle\phi(\mathbf{x})\phi^\dagger(\mathbf{y})\rangle = \frac{\mathcal{G}(|\mathbf{x}-\mathbf{y}|/\xi)}{|\mathbf{x}-\mathbf{y}|^{d-2+\eta}}, \qquad (2)$$

where $\mathcal{G}(z)$ is some scaling function, ξ is a correlation length, and d is the spatial dimension of the system. This correlation function has a geometric interpretation, yielding the probability amplitude of finding any particle-path connecting $\mathbf{x}$ and $\mathbf{y}$. In the present work, the particle trajectories correspond to vortex lines.

For a random walk of length N in $d = 3$, the probability of going from $\mathbf{x}$ to $\mathbf{y}$ is given by[7]

$$P(\mathbf{x},\mathbf{y};N) = \left(\frac{3}{2\pi N}\right)^{3/2} \exp\left[-\frac{(\mathbf{x}-\mathbf{y})^2}{2N}\right]. \qquad (3)$$

The correlation function $G(\mathbf{x},\mathbf{y})$ of the corresponding gaussian field theory is found by summing up $P(\mathbf{x},\mathbf{y};N)$ for all N

$$G(\mathbf{x},\mathbf{y}) = \sum_N P(\mathbf{x},\mathbf{y};N) \propto \frac{1}{|\mathbf{x}-\mathbf{y}|}. \qquad (4)$$

Comparing this with Eq. 2, we find $\eta = 0$, as expected. The random walker traces out a fractal path with Hausdorff dimension D_H. Moreover, in general the distance between two points $\mathbf{x}$ and $\mathbf{y}$ N walks apart is given by

$$\langle |\mathbf{x} - \mathbf{y}|^2 \rangle \propto N^{2\Delta}, \tag{5}$$

where Δ is the wandering exponent which for the gaussian $3D$ case is $\Delta = 1/2$. Inverting Eq. 5, we find that the total length of the random walker scales with linear size as $L^{1/\Delta}$, hence the Hausdorff dimension of the random walker is given by $D_H = 1/\Delta$. If we set $\mathbf{x} = \mathbf{y}$ in Eq. 3 we find that the unnormalized distribution $D(N)$ of *loops* of perimeter N, at the critical point, is given by

$$D(N) \propto \frac{1}{N} \sum_{\mathbf{x}} P(\mathbf{0}; N) \propto N^{-\alpha}, \tag{6}$$

with $\alpha = 5/2$ for purely random walkers. The extra factor N^{-1} in Eq. 6 comes from the arbitrariness in defining the starting position along the loop. Hence, for the case of strict random walkers in $3D$, described by a gaussian field theory $H = m_\phi^2 |\phi|^2 + |\nabla \phi|^2$, the corresponding set of values for the two geometric and one thermodynamic exponents is given by $(\Delta, \alpha, \eta) = (1/2, 5/2, 0)$.

Beyond the gaussian case, exact exponents can not be obtained analytically, however we will derive scaling relations for them. When Eq. 5 is invoked, a generalized probability function $P(\mathbf{x}, \mathbf{y}; N)$ may be written on the form

$$P(\mathbf{x}, \mathbf{y}; N) \propto \frac{1}{N^\rho} \, F\left(\frac{|\mathbf{x} - \mathbf{y}|}{N^\Delta} \right), \tag{7}$$

where $F(x)$ is a scaling function, and normalizability of P implies $\rho = d\Delta$. From Eq. 6, we find that $P(\mathbf{x}, \mathbf{y}; N)$ should scale with N as $N^{1-\alpha}$, which yields the scaling relation $\rho = \alpha - 1$. Conversely, summing over all N in Eq. 7 to find the correlation function $G(\mathbf{x}, \mathbf{y})$, we obtain

$$G(\mathbf{x}, \mathbf{y}) = \sum_N P(\mathbf{x}, \mathbf{y}; N) \propto \frac{1}{|\mathbf{x} - \mathbf{y}|^{\frac{\rho - 1}{\Delta}}}, \tag{8}$$

giving the scaling relation $\eta = \frac{\rho - 1}{\Delta} + 2 - d$. Combining the above, we find

$$\eta + D_H = 2, \quad D_H = \frac{d}{\alpha - 1}. \tag{9}$$

A computation of the *geometric* exponent α yields the *thermodynamic* exponent η and the Hausdorff dimension D_H. Note that both η and D_H are sensitive functions of α, $\partial \eta / \partial \alpha = -\partial D_H / \partial \alpha = d/(\alpha - 1)^2$, such that a precise determination of η and D_H requires great precision in the determination of α. The above reinforces the statement that a geometric transition of the vortex tangle at criticality of the gauge theory Eq. 1 can be assigned a genuine thermodynamic order parameter via a dual formulation of the original theory *in three spatial dimensions*[2,3]. The random walker is represented by a gaussian theory, Eq. 1 with $(u_\phi = 0, q = 0)$, for which $\eta = 0$. This corresponds to $D_H = 2$, such that the random walker in three dimensions traces out a path that precisely fills a cross-sectional area of the system. *Note that $D_H < 2 \leftrightarrow \eta > 0$, while $D_H > 2 \leftrightarrow \eta < 0$.*

The Hamiltonian Eq. 1 with $(u_\phi \neq 0, q \neq 0)$ has a dual field theory corresponding to Eq. 1 with $q = 0$ describing the neutral vortex tangle of a charged superconductor[5]. The $|\phi|^4$-term in Eq. 1 represents a *steric repulsion*, i.e. the vortex loops can not overlap, leading to a random walk problem with self-avoiding *links* (but not necessarily self-avoiding sites), in the sense that parallel vortex segments repel, perpendicular vortex segments can cut[8], while antiparallel vortex-segments can annihilate. Hence, this is not a standard self-avoiding path problem. However, we expect $\Delta > 1/2$ or equivalently $D_H < 2$, since steric repulsion should result in a vortex-loop tangle packing space less densely than for the non-interacting case, so that $\eta > 0$. The repulsive interaction between parallel vortex segments also leads to a more efficient suppression of long loops than for the non-interacting case, so that $\alpha > 5/2$.

Consider next Eq. 1 with $(u_\phi \neq 0, q = 0)$ for $d = 3$, which has a dual field theory corresponding to Eq. 1 with $q \neq 0$ describing the charged vortex tangle of a neutral condensate[5]. A long-ranged (anti) Biot-Savart interaction is mediated by the gauge-field. This is a relevant perturbation, in renormalization group sense, to a steric contact repulsion[9]. The geometric properties of the charged vortex tangle are a result of a balance between attractive forces mediated by the gauge field, and the steric repulsion. As the numerical simulations show, we find $\Delta < 1/2$, corresponding to $D_H > 2$ which means that the vortex tangle is more compact than the ensemble of pure random walkers, due to the fact that an attractive long-ranged Biot-Savart interaction between oppositely oriented vortex segments overcompensates the steric repulsion so as to contract the vortex-loop tangle not only compared to the pure $|\phi|^4$-case, but even compared to the noninteracting case. The tangle thus packs space so that it more than fills a cross-sectional area of the system.

The fluctuation-dissipation theorem provides a bound on η via the susceptibility $\chi_\phi = \int d^d x G(x) \sim \xi^{2-\eta}$, which is bounded by the volume L^d of the system, $L^{2-\eta} = L^d \cdot L^{2-d-\eta} < L^d$, so $\eta > 2 - d$. Eq. 9 gives a geometric interpretation of this bound. Specializing to $d = 3$, $\eta = -1$ corresponds to topological excitations with $D_H = 3$, an upper limit.

For $d = 3$, the continuous phase transition in a superfluid or extreme type-II superconductor has recently been *demonstrated* to be driven by a proliferation of vortex loops[3,5]. From the above, $\eta = -1$ means that a single vortex loop at T_c packs space completely, i.e. its perimeter N scales as $N \propto L^3$, implying that the vortex-tangle collapses on itself, rendering the transition discontinuous. This may be been seen from the standard scaling rela-

tion $\beta = \nu\ (d-2+\eta)/2$ for critical exponents. Formally, this implies that the limit $\eta \to (2-d)^+$ corresponds to the limit $\beta \to 0^+$, characteristic of a discontinuous transition. More informally, a collapse of a vortex tangle may be viewed as mediated by an effective attractive vortex interaction, a situation akin to what is known in type-I superconductors. Deep in the type-I regime, it is known that superconductors suffer a weakly discontinuous transition[10].

Monte Carlo simulations have been performed on the lattice version of Eq. 1 in the phase-only approximation, to determine precise values of α, both for $q = 0$ and $q \neq 0$. We have also performed simulations on pure random walkers described by the theory $H(q = 0, u_\phi = 0)$. They reveal that a determination of α is less fraught with finite-size effects than a determination of D_H. Thus, we focus on determining α. The model we consider is

$$H = -J \sum_{<i,j>} \cos(\theta_i - \theta_j - q_{\rm C}\ h_{ij}) + \frac{1}{2}(\nabla \times \mathbf{h})^2, \quad (10)$$

where the site-variable θ_i is the phase of the complex matter field $\phi = |\phi| \exp(i\theta)$ of Eq. 1, when the system is discretized, J is essentially a bare phase-stiffness, and the link-variable $h_{ij} = \int_i^j d\mathbf{l} \cdot \mathbf{h}$. The charge $q_{\rm C}$ is the (original) charge entering in the simulations. Up to this point we have considered a general charge q irrespective of whether it couples to the original condensate or the resulting vortex tangle. The numerical simulations are performed on the phase of the condensate, hence the concept of *original* and *dual* are fixed in terms of the numerical simulations. Consequently we introduce the charges $q_{\rm C}$ for the condensate and $q_{\rm V}$ for the vortices.

¿From the phase distributions of the matter field we can extract vortex loops[3]. These loops have charge $q_{\rm V}$ and are described by the field theory $H(q_{\rm V}, u_\phi)$[5]. Hence, we can study the critical properties of the charged field theory $H(q_{\rm V}, u_\phi)$ by considering the geometric properties of the thermally excited vortex-loop tangle at the critical temperature in the 3DXY model. Conversely, the geometric properties of the vortex tangle with $q_{\rm C} \neq 0$ yield the critical properties of the neutral field theory $H(q_{\rm V} = 0, u_\phi)$ of Eq. 1.

The simulations with $q_C = 0$ are described elsewhere[3], while for $q_C \neq 0$ the simulations proceed as follows. For every site on the lattice a phase change $\theta_i \to \theta_i'$ is attempted, and accepted or rejected according to the Metropolis algorithm. Then a change in $h_{ij} \to h_{ij} + \delta h$ is attempted, and accepted or rejected according to the Metropolis algorithm. When updating h_{ij} we update all the link variables on a randomly oriented elementary plaquette containing h_{ij} as one of its four edges. Updating of $\mathbf{h}$ in this fashion guarantees that the gauge-fixing condition $\nabla \cdot \mathbf{h} = 0$ is enforced at all times. For $q_{\rm C} = 0$, the simulations were performed for a system of size $L \times L \times L$ with $L = 180$, while those for $q_{\rm C} \neq 0$ were performed with $L = 64$.

During the simulations we have sampled the distribution function $D(N)$, Eq. **??**, obtaining α. The results are shown in Fig. 1 and listed in Table I. The value of α obtained for $q_C \neq 0$ (dual neutral), which is the hardest system to simulate, gives a value for η in good agreement with high-precision results for η of the pure ϕ^4-theory[11]. This serves as a useful benchmark on our method of extracting η. For $q_C = 0$ we have simulated much larger systems than for $q_C \neq 0$. The deviation from the gaussian value $\alpha = 5/2$ is substantial, *and of opposite sign compared to* $q_C \neq 0$. Given the size of the system we consider for $q_C = 0$, it is unlikely that this is a finite-size artifact. An $\alpha < 5/2$ guarantees $\eta < 0$ for the $q_C = 0$ (dual charged) case, contrary to the value of $\eta > 0$ for $q_C \neq 0$[11,3]. In particular, the inset of Fig. 1 lends strong support to the proposition that $\eta(q_C \neq 0) > 0$, while $\eta(q_C = 0) < 0$.

The value $\eta < 0$ obtained for the original neutral, dual charged case, is significant: It implies that $D_H > 2$ for this case. *Whether $D_H > 2$ or $D_H < 2$ is of great import to the possibility of having a genuine phase-transition driven by a vortex-loop unbinding even in the presence of a finite background field such as magnetic induction in type-II superconductors.* A vortex system accesses configurational entropy more easily if it is compressible than if it is incompressible. For the charged case the gauge-field fluctuations render the system compressible. In the neutral case, the system expands screening strings of closed vortex loops to a larger extent than for the charged case, as substitutes for the gauge-field fluctuations. This is why $D_H(q_{\rm C} = 0) > D_H(q_{\rm C} \neq 0)$. There is an infinitely larger amount of screening vortex-strings in the neutral case (dual charged) than for the charged case (dual neutral), which is the true significance of the fact that η is smaller for $q_{\rm C} = 0$ than for $q_{\rm C} \neq 0$. The possibility of the zero-field vortex-loop blowout transition surviving the presence of a finite field is much greater in a neutral superfluid or an extreme type-II superconductor, than in a charged condensate with *a priori* good screening.

Given the significance of $D_H > 2$, we elaborate on the fact that for the neutral (dual charged) case, we find $\eta < 0$. The Lehmann-representation of the Fourier transform $\tilde{G}(p)$ of Eq. 2, is sometimes used to argue that η obeys the strict inequality $\eta > 0$. The Lehmann-representation of $\tilde{G}(p)$ is given by

$$\tilde{G}(k) = \int_0^\infty d\mu^2\ \ \frac{\rho(\mu^2)}{k^2 + \mu^2}, \quad (11)$$

where $1 = \int_0^\infty d\mu^2 \rho(\mu^2)$, and $\rho(\mu^2) = Z\delta(\mu^2 - m_\phi^2) + \sigma(\mu^2)$. The propagator for the gaussian case would be $\tilde{G}(k) = 1/(k^2 + m_\phi^2)$, where m_ϕ^2 refers to the bare massparameter in Eq. 1. Thus, $\eta > 0$ follows if $0 < Z < 1$, which holds for a uniformly positive $\rho(\mu^2)$. However, in theories with a *local gauge symmetry*, the two-point correlation function is a gauge-dependent quantity. Thus, $\sigma(\mu^2)$ may in principle be made negative for certain values of μ by a gauge-transformation. This invalidates the reason-

ing leading to the strict inequalities $Z < 1$ and $\eta > 0$. A negative η, as found here and in other simulations[3,5] all representing basically exact results, agrees with a recent non-perturbative RG calculation[12], which also gives $\nu = \nu_{3DXY}$ at the *charged* critical point.

At the critical point, the relevant fluctuations are *transverse* phase-fluctuations, or vortices[2,3,5]. Ignoring amplitude fluctuations yields an effective Hamiltonian governing the transverse θ-fluctuations, whose Fourier-transform $\mathcal{F}$ we denote by $\mathbf{S}_k$, $\mathcal{F}((\nabla\theta)_T) = \mathbf{S}_k = -2\pi\ i\ (\mathbf{k}\times\mathbf{n}_k)/k^2$, where $\mathbf{n}_k$ is the Fourier-transform of the *local vorticity*. We find, after integrating out the transverse gauge-field, that $H = \Xi^2(k)\ \ \mathbf{S}_k\cdot\mathbf{S}_{-k}$, where $\Xi^2(k) = k^2/(k^2+2q^2)$. For $q=0$, we have $\Xi^2(k)=1$, while $\lim_{k\to 0}\Xi^2(k) \sim k^2$ for $q\neq 0$. The coupling to a fluctuating gauge field *softens* the transverse phase-fluctuations, providing the effective phase-stiffness with an extra power k^2 compared to the $q=0$-case. Thus, $\tilde{G}^{-1}(k,q=0) = k^2+\Sigma(k)$ and $\tilde{G}^{-1}(k,q\neq 0) = k^4+\Sigma(k)$. In both cases, the $k\to 0$-limit of the self-energy $\Sigma(k)$ is given by $\Sigma(k)\sim k^{2-\eta}$. We thus have $\lim_{k\to 0}\tilde{G}^{-1}(k) \sim k^{2-\eta}$ provided $\eta > 0$ for $q=0$ and, when invoking the absolute lower bound, $\eta > -1$ for $q\neq 0$. For a pure $|\phi|^4$-theory, the Lehmann-representation coupled with positive-definiteness of $\rho(\mu^2)$, holds.

This work was supported by the Norwegian Research Council via the High Performance Computing Program, and by Grant 124106/410 (S.M. and A.S). (J. H.) thanks NTNU for support. Communications with F. S. Nogueira and Z. Tešanović, are gratefully acknowledged.

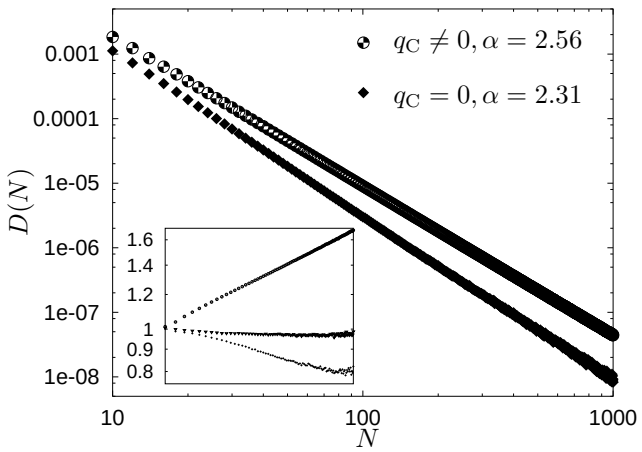

FIG. 1. The vortex-loop distribution function $D(N) \sim N^{-\alpha}$ as a function of loop-perimeter N, at the critical point for the charged ($q_C \neq 0, q_V = 0$) and neutral ($q_C = 0, q_V \neq 0$) cases. Numerical results for the exponents $(\alpha, D_H, \Delta, \eta)$ are given in Table I. The system size is $L\times L\times L$, with $L = 180$ for $q_C = 0$, and $L = 64$ for $q_C \neq 0$. Inset shows *simulation results* for $N^{5/2}D(N) \sim N^{5/2-\alpha}$ on a double-logarithmic scale. Top: $q_C = 0, L = 180$ (dual charged). Middle: Noninteracting vortex loops (gaussian case), $L = 64$. Bottom: $q_C \neq 0, L = 64$ (dual neutral). The results demonstrate that $5/2-\alpha > 0$ for $q_C = 0$ (dual charged), while $5/2-\alpha < 0$ for $q_C \neq 0$ (dual neutral). Hence, by Eq. 9, $D_H > 2, \eta < 0$ for $q_C = 0$, while $D_H < 2, \eta > 0$ for $q_C \neq 0$. The latter agrees with other high-precision results for η, see Ref. 11. Note that the gaussian result $\alpha = 5/2$ is obtained to high precision, for $L = 64$.

Exponent	Gaussian	$q_C = 0, q_V \neq 0$	$q_C \neq 0, q_V = 0$
α	5/2	2.312 ± 0.003	2.56 ± 0.03
D_H	2	2.287 ± 0.004	1.92 ± 0.04
Δ	1/2	0.437 ± 0.001	0.52 ± 0.01
η	0	-0.287 ± 0.004	0.08 ± 0.04

TABLE I. The loop distribution exponent α, as determined from Monte-Carlo simulations. The remaining exponents have been determined from Eq. 9. Symbols are explained in the text.

[1] P. W. Anderson, *Basic Notions in Condensed Matter Physics*, Benjamin Cummings, (1984). See also P. G. de Gennes, *Proceedings of the Nobel Symposium*, **24**, 112 (1973).
[2] Z. Tešanović, Phys. Rev. **B 59**, 6449 (1999).
[3] A. K. Nguyen and A. Sudbø, Phys. Rev. **B 60**, 15307 (1999); Europhys. Lett., **46**, 780 (1999).
[4] V. J. Emery and S. A. Kivelson, Nature, **374**, 434 (1995). See also H. Kleinert, Phys. Rev. Lett., **84**, 286 (2000).
[5] J. Hove and A. Sudbø, Phys. Rev. Lett., **84**, 3426 (2000).
[6] H. Kleinert, *Gauge fields in condensed matter, Vol. 1*, World Scientific, Singapore, (1989).
[7] D. Austin *et al.*, Phys. Rev. **D 49**, 4089, (1994).
[8] A. Sudbø and E. H. Brandt, Phys. Rev. Lett. **67**, 3176 (1991); C. Carraro and D. S. Fisher, Phys. Rev. **B 51**, 534 (1995).
[9] C. Dasgupta and B. I. Halperin, Phys. Rev. Lett., **47**, 1556, (1981).
[10] B. I. Halperin *et al.*, Phys. Rev. Lett., **32**, 292 (1974).
[11] M. Hasenbusch and T. Török, J. Phys. A **32**, 6361 (1999).
[12] I. F. Herbut and Z. Tešanović, Phys. Rev. Lett. **76**, 4588 (1996).

The order of the metal to superconductor transition

S. Mo,[1,*] J. Hove,[1,†] and A. Sudbø[1,2,‡]

[1] *Department of Physics*
Norwegian University of Science and Technology,
N-7491 Trondheim, Norway
[2] *Institut für Theoretische Physik*
Freie Universität Berlin
Arnimallee 15, D-14195 Berlin, Germany

(Dated: July 10, 2004)

We present results from large-scale Monte Carlo simulations on the full Ginzburg-Landau (GL) model, including fluctuations in the amplitude and the phase of the matter-field, as well as fluctuations of the non-compact gauge-field of the theory. From this we obtain a precise critical value of the GL parameter $\kappa_{\rm tri}$ separating a first order metal to superconductor transition from a second order one, $\kappa_{\rm tri} = (0.76 \pm 0.04)/\sqrt{2}$. This agrees surprisingly well with earlier analytical results based on a disorder theory of the superconductor to metal transition, where the value $\kappa_{\rm tri} = 0.798/\sqrt{2}$ was obtained. To achieve this, we have done careful infinite volume and continuum limit extrapolations. In addition we offer a novel interpretation of $\kappa_{\rm tri}$, namely that it is also the value separating type-I and type-II behaviour.

PACS numbers: 74.55.+h,74.60.-w, 74.20.De, 74.25.Dw

I. INTRODUCTION

The character of the metal to superconductor transition is an important and long-standing problem in condensed matter physics. The critical properties of a superconductor may be investigated at the phenomenological level by the Ginzburg-Landau (GL) model of a complex scalar matter field ϕ coupled to a fluctuating mass-less gauge-field $\mathbf{A}$. The GL model in d-dimensions is defined by the functional integral

$$\begin{aligned} Z &= \int \mathcal{D}A_i \mathcal{D}\phi \exp(-S(A_i,\phi)) \\ S &= \int d^d x \left[\frac{1}{4} F_{ij}^2 + |D_i \phi|^2 + m^2 |\phi|^2 + \lambda |\phi|^4 \right] \end{aligned} \tag{1}$$

where $F_{ij} = \partial_i A_j - \partial_j A_i$, $D_i = \partial_i + iqA_i$, q is the charge coupling the condensate matter field to the fluctuating gauge-field, λ is a self-coupling, and m^2 is a mass parameter which changes sign at the mean field critical temperature. This model is also used to describe a great number of other phenomena in Nature, including such widely separated phenomena as the Higgs mechanism in particle physics,[1] phase transitions in liquid crystals,[2,3] crystal melting,[4] the quantum Hall effect,[5,6] and it is also used as an effective field theory describing phase transitions in the early Universe.[7]

The GL model may conveniently be formulated in terms of two dimensionless parameters $y = m^2/q^4$ and $x = \lambda/q^2$ when all dimensionful quantities are expressed in powers of the scale q^2. Here, y is temperature-like and drives the system through a phase transition, and $x = \kappa^2$ is the well known GL parameter. These parameters are related to the standard dimensionful textbook[8] coefficients α, β of the GL model by

$$y = \frac{m^* c^2}{128\pi^2 \alpha_s^2 k_{\rm B}^2 T^2}\alpha, \quad x = \frac{1}{8\pi\alpha_s \hbar c}\left(\frac{m^* c}{\hbar}\right)^2 \beta = \kappa^2 \tag{2}$$

where α_s is the fine structure constant[35] and m^* is an effective mass parameter.

At the mean-field level Eq. 1 reduces to the well known GL-equations and the model exhibits a second order phase transition when the temperature (or y) is varied through some critical value. In a seminal paper by Halperin, Lubensky and Ma[9] it was shown that by ignoring spatial fluctuations in ϕ, and then integrating out the $\mathbf{A}$ field *exactly*, one gets a term $|\phi|^3$ in the effective ϕ action. Treating this action at the mean field level leads to the prediction of a first order transition in the charged model for any value of the charge, or equivalently for any value of the GL parameter. The first order character of the transition is most strongly pronounced for large values of the charge (small κ), but even then it is very weak. For $\kappa \ll 1$ (type-I) the neglect of spatial variation in the matter field ϕ is a reasonable approximation, whereas for $\kappa \gtrsim 1$ (type-II) fluctuations in ϕ must be taken into account. By doing a one-loop RG calculation using ε-expansion it was shown[9] that no stable infrared fixed point could exist unless the number N of components of the order-parameter was artificially extended to $N > N_c = 365$, far beyond the physically relevant case of $N = 2$. Consequently, the conclusion was that gauge field fluctuations change the order of the phase transition to first order *irrespective* of the value of κ.

These predictions were difficult to test experimentally on superconductors since the predicted jump across the first order transition is very small in *physical* units, even if the *effective* theory in Eq. 1 has a strong first order transition. See e.g. Appendix A in Ref. 10. For conven-

tional superconductors the critical region where mean-field behavior breaks down is extremely narrow, consequently it is very difficult to distinguish a small finite jump from continuous behavior. However, there exists an isomorphism between the phase transition in superconductors and the smectic-A to nematic transition in liquid crystals.[11] On the latter systems experiments can be carried out in the critical regime,[12] and second order phase transitions are found. This contradicts the ϵ-expansion argument above, and presumably indicates a breakdown of the expansion for this gauge-field theory, since $\varepsilon = 4 - d = 1$.

In Ref. 13 it was shown, using duality arguments and Monte Carlo simulations, that the GL model should have a second order transition for large κ. However, what remains true is that deep in the type-I regime, the transition *is* first order. There should therefore be a tricritical point $\kappa = \kappa_{\rm tri}$ where the transition changes order.

A first estimate for $\kappa_{\rm tri}$ was obtained by Kleinert in Refs. 14,15 by developing a disorder theory formulation from which he calculated the value

$$\kappa_{\rm tri} = \frac{3\sqrt{3}}{2\pi}\sqrt{1 - \frac{4}{9}\left(\frac{\pi}{3}\right)^4} \approx \frac{0.798}{\sqrt{2}}$$

analytically[36]. Subsequently[16] this picture of a tricritical point separating first and second order transitions was given further support by Monte-Carlo simulations, and moreover an attempt was even made to determine $\kappa_{\rm tri}$, giving $\kappa_{\rm tri} \simeq 0.4/\sqrt{2}$. However, the problem turns out to be extremely demanding even by present day supercomputing standards, and not too much emphasis can be put on the *precise numerical value* obtained in this early attempt. To our knowledge, this is the most recent attempt to find a precise value for $\kappa_{\rm tri}$ numerically, although large-scale simulations have been performed much more recently for $\kappa^2 = 0.0463$ and $\kappa^2 = 2$, giving first order and continuous transitions, respectively.[10,17]

The one-loop ε-expansion result of Halperin *et al.*[9] has subsequently been improved to two-loop order,[18] drastically reducing the value of N_c to 32, but still $N_c \gg 2$. Eventually, an infrared stable fixed point was found even for the physical case $N = 2$ by combining two-loop perturbative results with Padé-Borel resummation techniques.[19] From this latter work one can also get an estimate of the critical κ from $\kappa^* = \sqrt{u^*/6f^*} \approx 0.62/\sqrt{2}$. Since Padé-Borel techniques are rather uncontrolled, only simulations can tell if such a resummation is allowed here.

From the above we can conclude that a tricritical κ, separating first and second order transitions *exists*, however a *precise value* remains to be determined..

We would also like to mention the distinction between type-I and type-II superconductors, which is related to the response to an external magnetic field. When an external field is increased beyond a critical field H_c it enters a type-I superconductor, and superconductivity is destroyed. For type-II superconductors the magnetic field enters as *a flux line lattice* when $H > H_{c1}$, and superconductivity is still present in this mixed state. At the mean-field level type-I and type-II superconductors are differentiated by $\kappa = 1/\sqrt{2}$. However there is á priori no reason to assume that this numerical value is robust against fluctuation effects, and we will argue that the critical κ separating first and second order phase transitions coincides with the κ separating type-I and type-II superconductors at y_c.

II. THE ORDER OF THE TRANSITION

The model in Eq. 1 has a phase transition for $y = y_c$. For $y < y_c$ the system is in its superconducting (broken) phase while for $y > y_c$ it is in the normal (symmetric) phase. Note that here, broken/symmetric does not refer to a breakdown of the local gauge symmetry present in Eq. 1. Elitzur's theorem[20] states that a local symmetry can never be spontaneously broken and therefore no local order parameter (in general any non-gauge invariant order parameter) can exist. On the other hand, one can explicitly break the gauge symmetry by a gauge-fixing, thereby facilitating a meaningful definition of a local order parameter. This should nonetheless be chosen in a formally gauge-invariant manner to get gauge-independent results. In our simulations, we have chosen not to fix the gauge[37].In this case a phase transition must be found either by using *non-local*[17,21] order parameters or by looking for non-analytic behavior in local quantities,[10] as we have done. E.g. the quantity $\langle|\psi|^2\rangle$ will have a jump at a first order transition, but it will not disappear in the symmetric phase as a proper order parameter should. At a second order transition there will be no jump, but the susceptibility $\chi_{|\psi|^2}$ will still have a peak.

In principle, we could therefore decide the order by looking for a jump in some local quantity as $\langle|\psi|^2\rangle$, but in finite systems the discontinuity will be rounded. In our case this is particularly problematic since the first order transitions are very weak, giving small jumps, even in infinite systems. At a first order transition ordered and disordered phases coexist and have the same free energy. In a finite system there will therefore be oscillations between the different phases. Because of the surface energy between the two pure states the probability of finding the system in an intermediate mixed state is lower than for either of the pure states, and histograms of an arbitrary observable will show a pronounced double peak structure. This is in contrast to a second order transition where the diverging correlation length forbids coexistence since the whole system is correlated. The histograms then have a single peak. Typical histograms are shown in Fig. 2.

Thus, when these histograms have a double peak structure which becomes more pronounced when the system size increases, the transition is first order, otherwise not.[22]

More precisely, we have the following scaling for the difference in free energy between the mixed and pure

phases for sufficiently large $L > L_{\rm scaling}$

$$\Delta F(L) = \ln P(X,L)_{\rm max} - \ln P(X,L)_{\rm min} \sim L^{d-1}, \quad (3)$$

where $P(X,L)$ is the probability for a given observable X in a system of size L^d, and L^{d-1} is the cross-sectional area between the ordered and the disordered phase. Near the tricritical value of κ such scaling is difficult to achieve since we are interested in the limit of vanishingly weak first order transitions. Consequently, a very large L is required in order to observe proper scaling. Only for quite strong first order transitions have we been able to observe proper scaling as predicted by Eq. 3, however we have generally taken a monotonous increase in $\Delta F(L)$ with system size as a signature of a first order phase transition. For the weakest first order transitions $\Delta F(L)$ will typically decrease for small L and then start to increase. It is therefore important to observe monotonic behavior through several system sizes before a conclusion can be drawn from the histograms[38].

III. PHASE DIAGRAM

We are searching for the point in the (x,y) plane where a first order and a second order line meet, i.e. according to the rather loose definition[39] of Lawrie and Sarbach[23] we are looking for a *tricritical point*. At a tricritical point *two* coupling constants must be fine-tuned to nontrivial values, and consequently a tricritical theory can be described with the mean-field free energy

$$f \approx |\nabla\psi|^2 + c_1(y-y_{\rm tri})|\psi|^2 + c_2(x-x_{\rm tri})|\psi|^4 + c_3|\psi|^6. \quad (4)$$

Right at the tricritical point the coefficients in front of both $|\psi|^2$ and $|\psi|^4$ vanish *simultaneously*. The upper critical dimension for this model is $d^* = 3$ and mean-field theory should be valid (up to logarithmic corrections). When approaching the tricritical point from the first order side, mean-field theory predicts that the jump $\Delta\,|\psi|^2$ will vanish as

$$\Delta\,|\psi|^2 \sim (x_{\rm tri} - x)\,. \quad (5)$$

We will make use of the above scaling in section VI to estimate $x_{\rm tri}$. For further information about tricritical points, we refer to an extensive review by Lawrie and Sarbach.[23]

In Fig. 1 we have *assumed* that the tricritical point separating first order and second order phase transitions coincides with the point separating type-I and type-II superconductivity. In principle the line of second order transitions could extend into the type-I region, with an intermediate state of type-I superconductivity with a second order phase transition to the normal state. This would be the case if the mean field value $\kappa_{\rm I/II} = 1/\sqrt{2}$ was *not* renormalized by fluctuations. We have not focused on the aspect of type-I/II superconductivity in our simulations, we will however argue that the overall structure of the phase diagram shown in Fig. 1 is correct in the vicinity of the tricritical point.

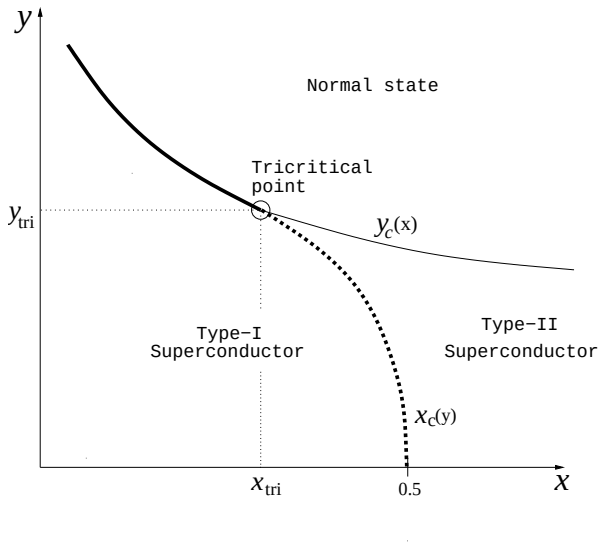

FIG. 1: A conjectured phase diagram in the (x,y) plane *in the vicinity of the tricritical point*. The thick solid line is a line of first order transitions separating type-I superconductivity and the normal (metallic) state, the thin solid line is a second order line separating type-II superconductivity from the normal (metallic) state. The dashed line separates type-I and type-II superconductivity. The dotted horizontal and vertical lines indicate the coordinates of the tricritical point $(x_{\rm tri}, y_{\rm tri}) \simeq (0.30, 0.03)$.

The microscopic difference between type-I and type-II superconductors lies in the sign of the effective vortex-vortex interaction. In $d = 3$ there exists a *dual* formulation of the GL-model which is given by a complex scalar matter-field ϕ coupled minimally to a massive gauge-field. This gauge-field can thus safely be integrated out to yield an effective *local* $|\phi|^4$-theory, where the coefficient of the $|\phi|^4$-term gives the effective vortex-vortex interaction. A positive such term signals vortex-repulsion, i.e. type-II behavior, while a negative term signals type-I behavior. *This vortex-vortex interaction term is proportional to* $\kappa - \kappa_{tri}$ where $\kappa_{\rm tri}$ is indeed to be identified with our tricritical value of κ.[14] Using the dual formulation of the GL theory, it then becomes clear that $\kappa_{\rm tri}$ is at the same time the value that separates first order and second order behavior, *and* the value that separates attractive from repulsive effective vortex-vortex interactions, i.e. type-I from type-II behavior.

An independent argument for why the transition between the normal state and type-I superconductivity *must be first order*, is based on the geometrical properties of a vortex tangle: In a recent paper[24] we have calculated the fractal dimension of vortex loops, and found the scaling relation $\beta = \nu\,(d - D_{\rm H})\,/2$, where β is the order parameter exponent, ν is the correlation length exponent and $D_{\rm H}$ is the fractal dimension of the loops. If

we formally extend this relation to the first order regime, i.e. let $\beta \to 0^+$, we find that the fractal dimension of the vortex loops $D_{\rm H} \to d$, i.e. the vortices collapse on themselves (filling space completely), rendering the transition discontinuous. This collapse is what we would expect from vortices interacting attractively (i.e. type-I), and by turning the argument above around we conclude that type-I superconductors must have a first order transition to the normal state.

We emphasize that the detailed *shape* of the line $x_c(y)$ remains to be determined. We have presented arguments above that it ends in the tricritical point $(x_{\rm tri}, y_{\rm tri})$. Moreover, deep in the broken regime, mean-field theory should apply. Consequently, we expect that the line $x_c(y)$ converges towards the mean field value $x_{\rm I/II} = 1/2$ in the $y \to -\infty$ limit.

IV. LATTICE MODEL

To perform simulations on the model in Eq. 1 we define it on a numerical lattice of size $N\times N\times N$ with lattice constant a. The *physical* volume is then $V = L^3 = (Na)^3$. By introducing a lattice field given by

$$|\phi_{\rm (cont)}|^2 = \beta_H |\psi_{\rm (latt)}|^2/2a, \tag{6}$$

where β_H so far is an arbitrary constant, Eq. 1 takes the form

$$\begin{aligned} Z &= \int \mathcal{D}A_i \mathcal{D}\psi \exp(-S(A_i,\psi)) \\ S &= \beta_G \sum_{\vec{x},i<j} \frac{1}{2}F_{ij}^2 - \beta_H \sum_{\vec{x},i} \mathsf{Re}\Big(\psi^*(\vec{x})U_i(\vec{x})\psi(\vec{x}+\hat{\imath})\Big) \\ &\quad + \frac{\beta_H}{2}\left[6+\frac{y}{\beta_G^2}\right]\sum_{\vec{x}}|\psi|^2 + \beta_R \sum_{\vec{x}}|\psi|^4 \end{aligned} \tag{7}$$

where we have defined $\alpha_i(\vec{x}) = aqA_i(\vec{x})$, $U_i(\vec{x}) = e^{i\alpha_i(\vec{x})}$, $\beta_G = 1/a_q$, $F_{ij} = \alpha_i(\vec{x}) + \alpha_j(\vec{x}+\hat{\imath}) - \alpha_j(\vec{x}) - \alpha_j(\vec{x}+\hat{\jmath})$, and $\beta_R = x\beta_H^2/4\beta_G$. F_{ij} is essentially a lattice curl of the fluctuating gauge-field, and $a_q = aq^2$ is a dimensionless lattice constant. To obtain correct continuum limit results, we will ultimately be interested in the limit $a_q \to 0$. It is furthermore possible to select a value of β_H such that the action can be written on the form

$$\begin{aligned} S = \beta_G \sum_{\vec{x},i<j} \frac{1}{2}F_{ij}^2 - \beta_H \sum_{\vec{x},i} \mathsf{Re}\Big(\psi^*(\vec{x})U_i(\vec{x})\psi(\vec{x}+\hat{\imath})\Big) \\ + \sum_{\vec{x}}|\psi|^2 + \beta_R\sum_{\vec{x}}[|\psi|^2-1]^2. \end{aligned} \tag{8}$$

This is achieved provided β_H satisfies the relation $(\beta_H/2)[6+y/\beta_G^2] + 2\beta_R = 1$.

The amplitude and gauge-invariant phase difference $\Delta = \mathsf{arg}\big(\psi^*(\vec{x})U_i(\vec{x})\psi(\vec{x}+\hat{\imath})\big)$ are coupled through the second term in Eq. 8. The ordered state is characterized by $\cos\Delta \lesssim 1$ and $|\psi|$ close to the minimum in the potential energy, whereas in the disordered state $\cos\Delta \approx 0$. In the disordered state the amplitude behavior is determined by x; for small x the coupling to Δ dominates and $|\psi|$ deviates significantly from the minimum in the potential, whereas for large x amplitude fluctuations are suppressed.

Given the fact that the theory in Eq. 1 is a continuum theory, one has to perform an ultraviolet (short-distance) renormalization, and thus $m^2 = m^2(q^2)$ has to be interpreted as a renormalized mass parameter at a given scale q^2 within a given renormalization scheme, e.g. the minimal subtraction ($\overline{MS}$) scheme. Since this continuum theory should represent the $a \to 0$ limit of the lattice theory in Eq. 8, the parameter y must be varied when a is being varied. In our case the leading terms in a can be obtained by requiring that some physical correlator calculated in both lattice and continuum perturbation theory should coincide. Thus we have to make the substitution[25,26]

$$\begin{aligned} y \to y &- \frac{3.1759115(1+2x)}{2\pi}\beta_G \\ &- \frac{\left(-4+8x-8x^2\right)\left(\ln\left(6\beta_G\right)+0.09\right) - 1.1 + 4.6x}{16\pi^2} \\ &+ \mathcal{O}(1/\beta_G) \end{aligned} \tag{9}$$

In addition, the continuum and lattice condensate matter fields are related by

$$\begin{aligned} \frac{\langle\phi^*\phi\rangle_{\rm cont}}{q^2} &= \frac{\beta_H\beta_G}{2}\langle\psi^*\psi\rangle_{\rm latt} \\ &- \frac{3.175911\beta_G}{4\pi} - \frac{\log(6\beta_G)+0.668}{8\pi^2} + \mathcal{O}(1/\beta_G). \end{aligned} \tag{10}$$

In Eq. 10 the first term comes from Eq. 6, while the second and third terms are linear and logarithmic divergences due to renormalization.

Note that the complicated counterterms in Eq. 9 merely affect the *value* of y_c separating the normal from the superconducting state for a given x, not the overall *structure* of the phase-diagram. The divergences in Eq. 10 in the continuum limit are constants that cancel when the jump in $\langle\phi^*\phi\rangle$ across a first order phase transition is calculated.

V. DETAILS OF SIMULATIONS

In order to use Eq. 8 to study the continuum theory of Eq. 1, it is necessary to carefully take two limits separately. First, the infinite volume limit $L \to \infty$ is taken, thereafter the continuum limit $a \to 0$. For reliable results one should have $a \ll \xi \ll L$, where ξ is a typical correlation length for the problem. In statistical physics, the continuum limit is usually not considered, either because the models are inherently *lattice models*, or the models are studied around a second order critical point where there exists at least one diverging length scale. Under such circumstances the short length-scale properties, like

TABLE I: The lattice sizes N^3 used for each (a_q, x)-pair. For each lattice size typically between three and eight y-values were used. The symbols are defined by:
○ Not simulated
⋆ Simulated
• Simulated and results shown in Fig. 2.

a_q	x	N									
		8	12	16	20	24	32	40	48	64	96
5.0[a]	0.10	⋆	○	○	○	○	○	○	○	○	○
	0.15	⋆	⋆	⋆	⋆	⋆	⋆	○	○	○	○
	0.16	⋆	⋆	•	•	•	•	○	○	○	○
	0.17, 0.18, 0.19	⋆	⋆	•	○	•	•	•	○	○	○
2.0	0.10	⋆	⋆	○	○	○	○	○	○	○	○
	0.15	⋆	⋆	⋆	○	○	○	○	○	○	○
	0.20	⋆	⋆	⋆	○	⋆	⋆	⋆	○	○	○
	0.22	○	○	•	○	•	•	•	○	○	○
	0.23, 0.24, 0.25	○	○	•	○	•	•	•	○	•	○
1.0	0.08	⋆	⋆	⋆	○	○	○	○	○	○	○
	0.10	⋆	⋆	⋆	⋆	○	○	○	○	○	○
	0.12, 0.13, 0.14	⋆	⋆	⋆	○	⋆	⋆	○	○	○	○
	0.15, 0.16, 0.17	○	⋆	⋆	⋆	⋆	⋆	⋆	○	○	○
	0.18, 0.20	⋆	⋆	⋆	○	⋆	⋆	⋆	⋆	○	○
	0.22	⋆	⋆	⋆	○	⋆	⋆	⋆	⋆	⋆	○
	0.24, 0.25, 0.26, 0.27	⋆	⋆	•	○	•	•	•	•	•	○
	0.30	⋆	⋆	⋆	○	⋆	⋆	⋆	⋆	○	○
	0.50	○	○	⋆	⋆	⋆	⋆	⋆	○	○	○
0.5	0.16	○	○	○	○	•	•	•	•	○	○
	0.20, 0.24	○	○	○	○	•	•	•	•	•	○
	0.26, 0.28	○	○	○	○	•	•	•	•	•	•
	0.30	○	○	○	○	•	•	•	•	•	○

[a]In Ref. 16 the lattice spacing corresponds to $a_q = 5.0$. The system sizes used were 9^3 and 15^3.

the lattice constant, are rendered irrelevant when studying universal properties. On the other hand, if one wants to study non-universal properties (such as critical coupling constants) or first order transitions without a diverging length scale, details of the system even on the shortest length scales have to be correctly taken into account in order to give reliable results.

The Monte-Carlo simulations are performed on Eq. 8, updating phases, amplitudes[40], and gauge-fields. We have used periodic boundary conditions and non-compact gauge-fields without any gauge fixing. To reduce autocorrelation times we have added global updating of the amplitude and overrelaxation of the scalar field[27,28] such that one sweep consists of: (1) conventional local Metropolis updates for phase, amplitude and gauge field, (2) global radial update by multiplying the amplitude uniformly with a common factor (acceptance according to Metropolis dynamics) and (3) 2-3 overrelaxation "sweeps" updating both the amplitude and the phase of the scalar field. The acceptance ratio in the Metropolis steps is kept between 60-70% as long as possible by adaptively adjusting the maximum allowed changes in the fields. For further details of the technical aspects of the simulations, see Refs. 27,28.

We have performed simulations for the parameters in Table I. The simulations have been done in a hierarchical manner: For a given x we have first kept a_q and N fixed, and simulated on typically three to eight y values. These runs have been combined with Ferrenberg-Swendsen[29,30] reweighting techniques, and a (pseudo)critical y has been located by requiring that the reweighted histograms have two equally high[41] peaks. Then the system size has been increased to access the *infinite volume limit*, and finally we have varied a_q to determine the *continuum limit*. At the transition the number of sweeps was chosen so that the system oscillated back and forth between the ordered and disordered state about ten times. Depending on system size and x-value (i.e. the *strength* of the first order transition) this resulted in about 10^5 to 10^6 sweeps. All computations were performed on an SGI Origin 3800 at the Norwegian High Performance Computing Center, using up to 32 nodes in parallel for the largest systems. A total of about $5{\cdot}10^4$ CPU hours were used, corresponding to $\simeq 1.5 \cdot 10^{17}$ floating point operations.

VI. RESULTS

To find $x_{\rm tri} = {\kappa_{\rm tri}}^2$ our strategy has been to start at $x \ll x_{\rm tri}$ where the transition is clearly first order, and then slowly increase x into the problematic tricritical area where $x \lesssim x_{\rm tri}$. During the simulations we have sampled the lattice amplitude

$$\overline{|\psi|^2} = \frac{1}{N^3} \sum_{\vec{x}} |\psi(\vec{x})|^2 \qquad (11)$$

and histograms of this quantity constitute the raw data for most of the subsequent analysis[42]. The connection between continuum and lattice condensates is given by Eq. 10.

Histograms reweighted to the critical y-value are shown in Fig. 2. We have used two different methods to find $x_{\rm tri}(a_q)$ from the histograms, and finally at the end of this section we have extrapolated these values to $a_q = 0$ to find the continuum limit.

A. Extrapolation of $\Delta\overline{|\psi|^2}$ to zero

The distance between the peaks of a histogram gives $\Delta\overline{|\psi|^2}(N)$, and by computing this for several different system sizes one can compute the infinite volume limit $\lim_{N\to\infty} \Delta\overline{|\psi|^2}$ of the discontinuity at the transition. Then one can (in principle) extrapolate to larger x and find the value $x_{\rm tri}$ where the discontinuity disappears. Results for $\lim_{N\to\infty} \Delta\overline{|\psi|^2}$ as a function of x are shown in Fig. 3.

For small x the curves in Fig. 3 show a distinct positive curvature, but when approaching $x_{\rm tri}$ we find that $\Delta\overline{|\psi|^2}$ vanishes as $\propto (x_{\rm tri} - x)$, in accordance with mean-field theory, Eq. 5. Also in the original attempt to locate $x_{\rm tri}$ with Monte Carlo simulations[16] this extrapolation was done, however the extrapolation was done starting from quite small x values, and the resulting $x_{\rm tri}$ was much smaller than the one we calculate.

The extrapolated results for $x_{\rm tri}$ are shown in Table II. The values found should provide a reasonable upper limit

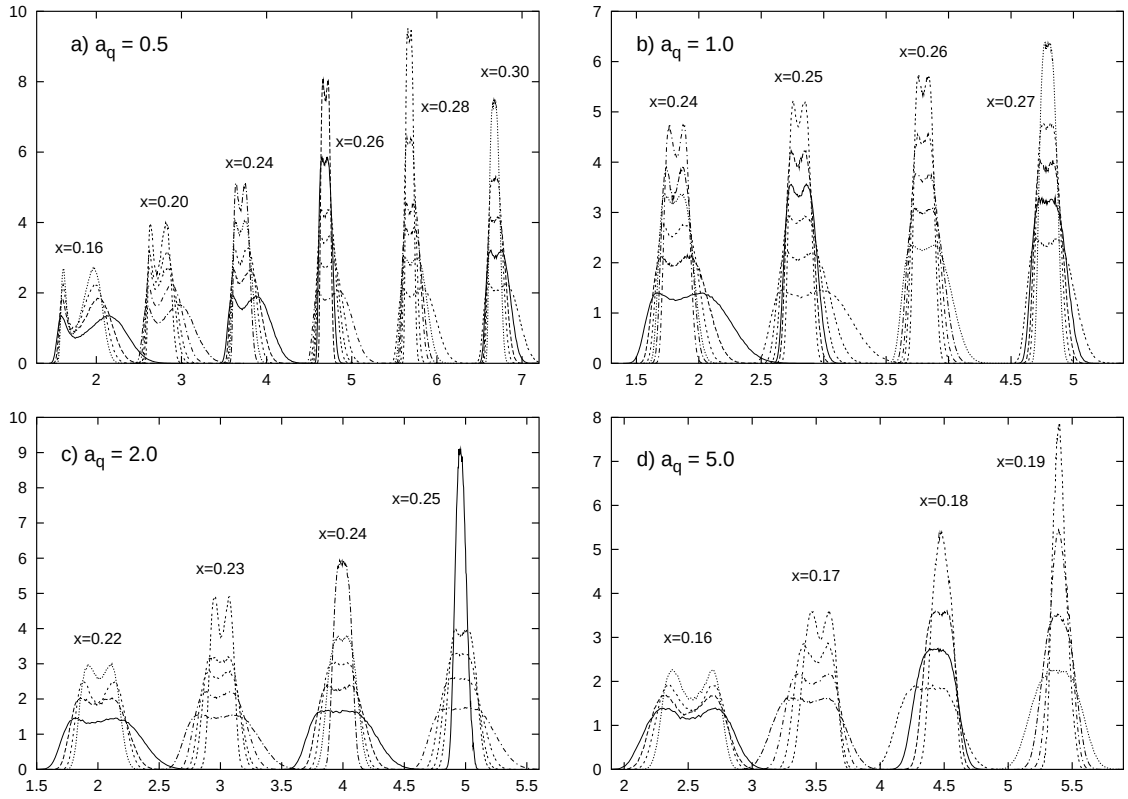

FIG. 2: Normalized histograms $P(\overline{|\psi|^2})$ as a function of $\overline{|\psi|^2}$ for a) $a_q = 0.5$, b) $a_q = 1.0$, c) $a_q = 2.0$, d) $a_q = 5.0$. For each lattice spacing the histograms for the smallest x are correctly placed horizontally. For larger x they are offset horizontally in steps of 1 for clarity. For system sizes see Table I.

TABLE II: $x_{\rm tri}$ found from extrapolation of $\lim_{N\to\infty} \Delta\overline{|\psi|^2}$ to zero and finite size scaling of $\Delta F(N)$.

a_q	$x_{\rm tri}$ (from $\Delta\overline{\lvert\psi\rvert^2}$)	$x_{\rm tri}$ (from $\Delta F(N)$)
5.0	0.174±0.002	0.175±0.005
2.0	0.246±0.002	0.235±0.005
1.0	0.286±0.010	0.260±0.010
0.5	0.294±0.005	0.280±0.020

for $x_{\rm tri}(a_q)$.

B. Finite size scaling of $\Delta F(N)$

It is also possible to study the *height* of the peaks in the histograms $[P(\overline{|\psi|^2})_{\rm max}]$ relative to the minimum between them $[P(\overline{|\psi|^2})_{\rm min}]$. This constitutes the best method of determining whether a transition is first order or not, but one cannot extrapolate to find $x_{\rm tri}$. In Fig. 4 we show some typical results for $\Delta F(N) = \ln P_{\rm max} - \ln P_{\rm min}$ as function of system size N for $a_q = 0.5$.

For $x = 0.16$ we clearly see the scaling $\Delta F(N) \propto N^2$ for $N \gtrsim 40$. This is expected since the histograms in Fig. 2 show a very pronounced double peak structure. For larger x this becomes less clear. Our estimates of $x_{\rm tri}$ for the different lattice constants are given in Table II. The results are consistently somewhat below those found with method A and give a reasonable lower limit for $x_{\rm tri}$.

C. Other methods

Finite-size scaling of the maximum in susceptibilities of the quantities $\overline{|\psi|^2}$ and $\overline{L}$ gives results that are consistent with the above conclusions.

$$\chi_S = N^d \left(\langle S^2 \rangle - \langle S \rangle^2 \right) \sim N^\sigma, \quad S \in \{\overline{|\psi|^2}, \overline{L}\} \qquad (12)$$

where $\sigma = d (< d)$ for first(second) order transitions. However, these results are more ambiguous than those from the histograms, and we have therefore chosen to work mainly with the histograms.

D. Final result for $\kappa_{\rm tri}$

It is clear that it becomes increasingly difficult to obtain good estimates of $\kappa_{\rm tri}(a_q)$ when the lattice constant is reduced. This is easy to understand since the *physical* volume $(Na_q)^3$ will be drastically reduced for the

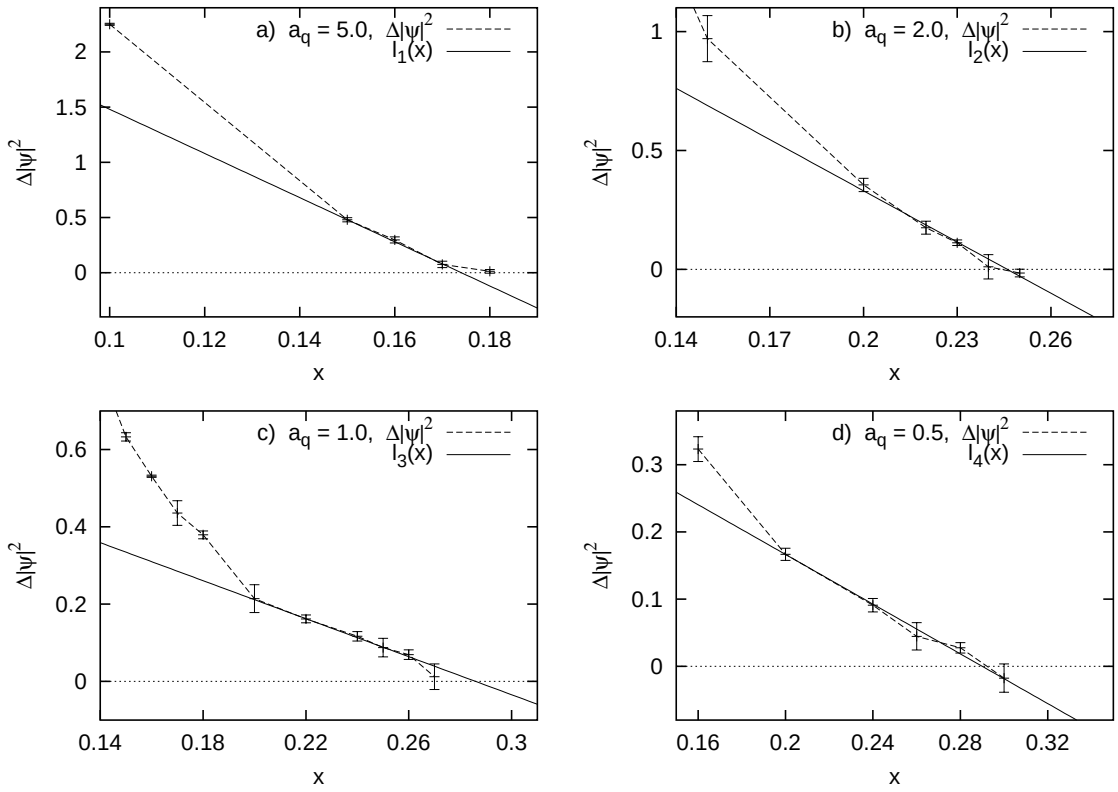

FIG. 3: $\lim_{N\to\infty} \Delta\overline{|\psi|^2}$ as a function of $x = \kappa^2$ for the lattice constants a) $a_q = 5.0$, b) $a_q = 2.0$, c) $a_q = 1.0$, d) $a_q = 0.5$. The line $l_i(x), i = 1, \ldots, 4$ is a fit to Eq. 5 where x_c is given in Table II.

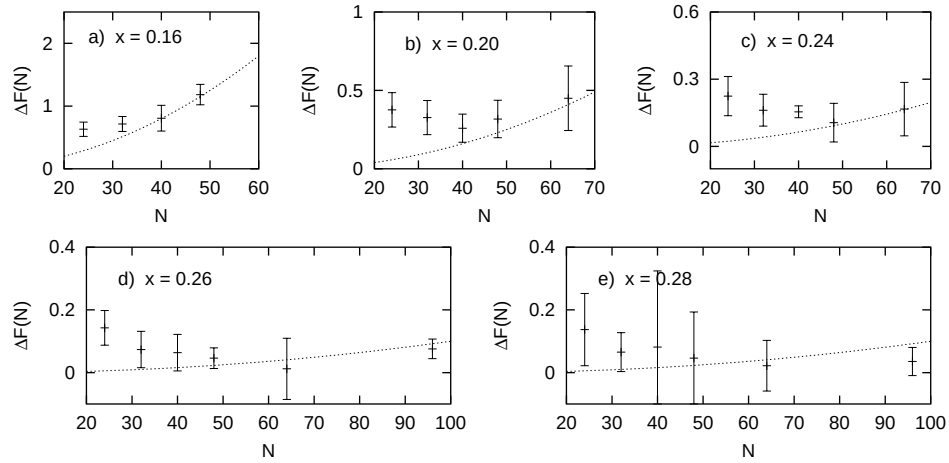

FIG. 4: $\Delta F(N) = \ln P_{\max}(N) - \ln P_{\min}(N)$ for $a_q = 0.5$. The line is $\propto N^2$ which is the scaling in Eq. 3 (for $d = 3$).

same lattice size in lattice units. The size of N necessary to access the scaling regime is (approximately) inversely proportional to the lattice constant a_q.

In Fig. 5, we show $x_{\rm tri}(a_q)$ found from extrapolation of $\Delta\overline{|\psi|^2}$ to zero and from finite size scaling of $\Delta F(N)$ as given in Table II. A linear fit to the data gives $\lim_{a_q\to 0} x_{\rm tri}(a_q) = 0.287 \pm 0.004$ with a confidence level of 25%. This is probably an underestimate of the error, since we have no particular reason to assume a linear behavior. Since the errors in $x_{\rm tri}(a_q)$ increases considerably when we reduce a_q one cannot rule out other behaviors, as quadratic. From the "worst case scenario" shown by the dotted lines in the figure we get $\lim_{a_q\to 0} x_{\rm tri}(a_q) = 0.295 \pm 0.025$. This in all likelihood gives a more realistic estimate of the error, and we therefore give our final estimate of $\kappa_{\rm tri}$ as $\lim_{a_q\to 0} \kappa_{\rm tri}(a_q) = (0.76 \pm 0.04)/\sqrt{2}$.

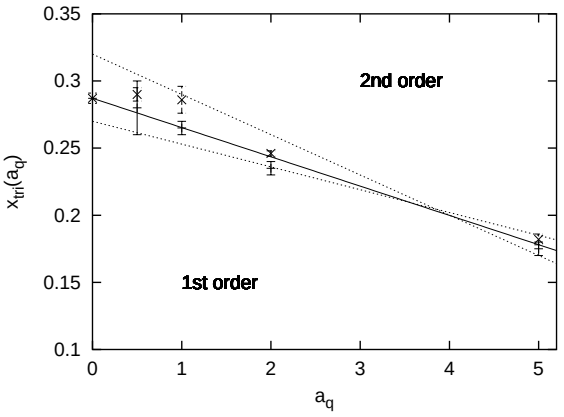

FIG. 5: Plot of $x_{\rm tri}(a_q)$ using the results from extrapolation of $\Delta\overline{|\psi|^2}$ to zero and from finite size scaling of $\Delta F(N)$ given in Table II. The solid line is a linear fit giving $\lim_{a_q\to 0} x_{\rm tri}(a_q) = 0.287\pm0.004$. The dotted lines indicate "worst case scenarios" giving $\lim_{a_q\to 0} x_{\rm tri}(a_q) = 0.295 \pm 0.025$.

VII. CONCLUSION

In summary, we have presented results from large scale Monte Carlo simulations showing that the critical value of the Ginzburg-Landau parameter that separates first order from second order behavior at the superconductor-normal metal transition point, is $\kappa_{\rm tri} = (0.76\pm0.04)/\sqrt{2}$. This is in remarkable agreement with the first estimate of $\kappa_{\rm tri}$ obtained by Kleinert[14] using a mean-field theory on the dual of the Ginzburg-Landau model, but differs almost by a factor of two from the subsequent early simulation results of Bartholomew.[16]

The reason for the remarkable agreement with our result and those of Ref. 14, is that for small to intermediate values of κ, the original problem is in the strong coupling regime and is mapped onto a weak-coupling problem in the dual formulation. The dual model is then expected to yield rather precise results at the mean-field level.[14] The dual description of the Ginzburg Landau model has recently met with considerable success in predicting the phase-structure of extreme type-II superconductors, even in magnetic fields.[31,32,33,34] We interpret the good agreement between our results and those of Ref. 14 as further support to the dual description of the Ginzburg-Landau model, now also in the intermediate-κ region.

We have also argued that this $\kappa_{\rm tri}$ coincides with the κ separating type-I and type-II superconductivity. In the superconducting regime for $\kappa \in (\kappa_{\rm tri}, 1/\sqrt{2})$ we thus predict the possibility of going from type-I to type-II superconductivity by increasing the temperature. This could in principle be possible to observe by studying the vortex structure of a superconductor with such intermediate values of κ by small-angle neutron scattering, when lowering the temperature through the line $x_c(y)$. However, more work is needed to elucidate the properties of the line $x_c(y)$ in Fig. 1.

Acknowledgments

We especially thank Dr. K. Rummukainen for generously providing us with the software for the data analysis, and for numerous helpful discussions during a visit by two of us (S.M. and J.H.) to Nordita, and later. We also thank Prof. H. Kleinert, Dr. F. Nogueira, and Prof. Z. Tešanović for useful discussions. We also thank all of the above for critical readings of the manuscript. A. S. thanks H. Kleinert and the Freie Universität Berlin for their hospitality while this work was being completed. This work was supported by the Norwegian Research Council via the High Performance Computing Program and Grant No. 124106/410 (S.M. and A.S.), and by NTNU through a fellowship (J.H.).

* Electronic address: Sjur.Mo@phys.ntnu.no
† Electronic address: Joakim.Hove@phys.ntnu.no
‡ Electronic address: Asle.Sudbo@phys.ntnu.no

[1] S. Coleman and E. Weinberg, Phys. Rev. D **7**, 1988 (1973).
[2] P. G. deGennes, Solid State Commun. **10**, 753 (1972).
[3] T. C. Lubensky and J.-H. Chen, Phys. Rev. B **17**, 366 (1978).
[4] H. Kleinert, *Gauge fields in condensed matter. Vol. 2: Stresses and defects. Differential geometry, crystal melting* (Singapore: World Scientific, 1989).
[5] X. G. Wen and Y. S. Wu, Phys. Rev. Lett. **70**, 1501 (1993).
[6] L. Pryadko and S. C. Zhang, Phys. Rev. Lett. **73**, 3282 (1994).
[7] A. Vilenkin and E. P. S. Shellard, *Cosmic strings and other topological defects* (Cambridge University Press, 1994).
[8] M. Tinkham, *Introduction to Superconductivity* (McGraw-Hill, 1996), 2nd ed.
[9] B. I. Halperin, T. C. Lubensky, and S. K. Ma, Phys. Rev. Lett. **32**, 292 (1974).
[10] K. Kajantie, M. Karjalainen, M. Laine, and J. Peisa, Nucl. Phys. B **520**, 345 (1998), hep-lat/9711048.
[11] B. I. Halperin and T. C. Lubensky, Solid State Communications **14**, 997 (1974).
[12] C. W. Garland and G. Nounesis, Phys. Rev. E **49**, 2964 (1994).
[13] C. Dasgupta and B. I. Halperin, Phys. Rev. Lett. **47**, 1556 (1981).
[14] H. Kleinert, Lett. Nuovo Cim. **35**, 405 (1982).
[15] H. Kleinert, *Gauge fields in condensed matter. Vol. 1: Superflow and vortex lines. Disorder fields, phase transitions* (Singapore: World Scientific, 1989).
[16] J. Bartholomew, Phys. Rev. B **28**, 5378 (1983).
[17] K. Kajantie, M. Karjalainen, M. Laine, and J. Peisa, Phys. Rev. B **57**, 3011 (1998), cond-mat/9704056.
[18] S. Kolnberger and R. Folk, Phys. Rev. B **41**, 4083 (1990).
[19] R. Folk and Y. Holovatch, in *Correlations, Coherence, and Order*, edited by D. V. Shopova and D. I. Uzunov (Kluwer Acadenic/Plenum Publishers, N.Y. - London, 1999), pp. 83–116, cond-mat/9807421.
[20] S. Elitzur, Phys. Rev. D **12**, 3978 (1975).

[21] K. Kajantie, M. Laine, T. Neuhaus, J. Peisa, A. Rajantie, and K. Rummukainen, Nucl. Phys. B **546**, 351 (1999), hep-ph/9809334.

[22] J. Lee and J. M. Kosterlitz, Phys. Rev. Lett. **65**, 137 (1990).

[23] I. D. Lawrie and S. Sarbarch, in *Phase Transitions and critical phenomena*, edited by C. Domb and J. L. Lebovitz (Academic Press, London, 1984), vol. 9, pp. 1–161.

[24] J. Hove, S. Mo, and A. Sudbø, Phys. Rev. Lett. **85**, 2368 (2000), cond-mat/0008112.

[25] M. Laine, Nucl. Phys. B **451**, 484 (1995), hep-lat/9504001.

[26] M. Laine and A. Rajantie, Nucl. Phys. B **513**, 471 (1998), hep-lat/9705003.

[27] P. Dimopoulos, K. Farakos, and G. Koutsoumbas, Eur. Phys. J. C **16**, 489 (2000), hep-lat/9911012.

[28] K. Kajantie, M. Laine, K. Rummukainen, and M. Shaposhnikov, Nucl. Phys. B **466**, 189 (1996), hep-lat/9510020.

[29] A. M. Ferrenberg and R. H. Swendsen, Phys. Rev. Lett. **61**, 2635 (1988).

[30] A. M. Ferrenberg and R. H. Swendsen, Phys. Rev. Lett. **63**, 1195 (1989).

[31] Z. Tešanović, Phys. Rev. B **59**, 6449 (1999).

[32] A. K. Nguyen and A. Sudbø, Europhysics Letters **46**, 780 (1999), cond-mat/9811149.

[33] A. K. Nguyen and A. Sudbø, Phys. Rev. B **60**, 15307 (1999), cond-mat/9907385.

[34] J. Hove and A. Sudbø, Phys. Rev. Lett. **84**, 3426 (2000), cond-mat/0002197.

[35] The fine structure constant is given by $\alpha_s = \frac{\mu_0 c e^{*2}}{4\pi\hbar}$ where $2e^*$ is the *effective* charge of a Cooper pair.

[36] We acknowledge Prof. H. Kleinert for pointing out this formula to us.

[37] In perturbation theory it is *necessary* to fix a gauge to avoid infinities from the infinite number of physically equivalent configurations. For simulations only the explicitly sampled configurations contribute, and no infinities arise. Finally the implementation on a parallel computer is simplest without gauge fixing.

[38] The proportionality factor between ΔF and the cross-sectional area L^{d-1} is the surface tension σ, which vanishes at $x_{\rm tri}$, but due to the difficulty in getting proper L^{d-1} scaling of ΔF, we have not considered σ.

[39] Indeed, it has been customary to describe as "tricritical" any point at which a continuous transition becomes discontinuous, irrespective of the number of phases which coexist along the first-order line or of the number of lines or surfaces of ordinary critical points which, in a suitably enlarged parameter space, may be found to meet here.

[40] Note that in the London limit, with spatially constant amplitude, one cannot access the type-I regime. The 3DXY model coupled to a gauge-field is the dual of the 3DXY-model with no gauge-field fluctuations. The latter has a critical point corresponding to the 3DXY universality class, while the former recently has been shown explicitly to have a stable infrared charged fixed point. See J. Hove and A. Sudbø, Phys. Rev. Lett., **84**, 3426 (2000).

[41] We have used equal *height* histograms instead of equal *weight*. The reason for this is that, in particular for small systems, the histograms are quite asymmetric. Then the equal weight histograms are not well defined for weak first order transitions. Both methods should give the same results in the infinite volume limit, but the convergence rate may be different.

[42] In addition to $|\psi|^2$ we have also studied other quantities, in particular

$$\overline{L} = \frac{1}{3N^3} \sum_{\mathbf{x},i} \cos\left(\mathsf{arg}\left[\psi^*(\vec{x}) U_i(\vec{x}) \psi(\vec{x}+\hat{\imath})\right]\right),$$

which varies between zero in the symmetric state and one in the broken state, quite similar to the more familiar 3DXY quantity $\langle \cos\left(\theta(\mathbf{x}) - \theta(\mathbf{x}+\hat{\imath})\right)\rangle$. However, the general picture is that the different observables give essentially the same information, and we have therefore focused mainly on Eq. 11, which has a well defined continuum limit.

Vortex Interactions and Thermally Induced Crossover from Type-I to Type-II Superconductivity

J. Hove,* S. Mo,† and A. Sudbø‡
Department of Physics
Norwegian University of Science and Technology,
N-7491 Trondheim, Norway
(Dated: July 8, 2004)

We have computed the effective interaction between vortices in the Ginzburg-Landau model from large-scale Monte-Carlo simulations, taking thermal fluctuations of matter fields and gauge fields fully into account close to the critical temperature. We find a change, in the form of what appears to be a crossover, from an attractive to a repulsive effective vortex interactions in an intermediate range of Ginzburg-Landau parameters $\kappa \in [0.76, 1]/\sqrt{2}$ upon increasing the temperature in the superconducting state. This corresponds to a thermally induced crossover from type-I to type-II superconductivity around a temperature $T_{\rm Cr}(\kappa)$, which we map out in the vicinity of the metal-to-superconductor transition. In order to see this crossover, it is essential to include amplitude fluctuations of the matter field, in addition to phase-fluctuations and gauge-field fluctuations. We present a simple physical picture of the crossover, and relate it to observations in Ta and Nb elemental superconductors which have low-temperature values of κ in the relevant range.

PACS numbers: 74.55.+h,74.60.-w, 74.20.De, 74.25.Dw

I. INTRODUCTION

The nature of the phase-transition in systems of a scalar matter field coupled to a massless gauge-field has a long history in condensed matter physics, dating at least back to the introduction of the Ginzburg-Landau (GL) theory of superconductivity[1]. At the mean-field level, ignoring spatial variations in gauge fields as well as matter fields leads to the prediction of a second order phase transition in the model, with classical mean-field exponents for all values of the GL parameter κ. The first attempt to seriously consider the role of fluctuations on the order of the metal-to-superconductor transition was made by Halperin, Lubensky, and Ma[2], who found that ignoring matter-field fluctuations entirely, and treating gauge-field fluctuations exactly, resulted in a permanent first order transition for all values of κ, since the gauge-field-fluctuations produced an extra term $\sim -|\phi|^3$ in the matter field sector of the theory in three spatial dimensions, where the complex matter field is denoted by ϕ and represents the condensate order parameter. (In the context of particle physics, Coleman and Weinberg[3] studied the equivalent problem of spontaneous symmetry breaking due to radiative corrections in the Abelian Higgs model in four space-time dimensions, finding the additional term $\phi^4 \ln(\phi^2/\phi_0^2)$, where the real matter field is denoted ϕ and represents a scalar meson.)[4]. Subsequently, Dasgupta and Halperin[5] found, using duality arguments in conjunction with Monte-Carlo simulations, that when gauge-field fluctuations and phase fluctuations of the scalar matter field are taken into account, but amplitude fluctuations are ignored, the phase transition is permanently second order[5]. Bartholomew[6] then reported results from Monte-Carlo simulations for the case when also amplitude fluctuations are taken into account, concluding that the phase transition changes from first to second order at a particular value of the GL parameter $\kappa \approx 0.4/\sqrt{2}$. As far as this numerical value is concerned, note that the problem of finding a *tricritical* value $\kappa_{\rm tri}$ separating first and second order transitions is extremely demanding even by present day supercomputing standards[7] (see below). Using ingenious duality arguments, Kleinert[8] obtained that the change from first to second order transition should occur at $\kappa \approx 0.8/\sqrt{2}$. The value of κ that separates a first order (discontinuous) transition from a second order (continuous) one, defines a tricritical point[9], and will hereafter be denoted $\kappa_{\rm tri}$. Note that to obtain the above result, it is necessary to allow for amplitude fluctuations in the superconducting order parameter, which become important for small to intermediate values of κ, but are totally negligible in the extreme type-II regime $\kappa >> 1$.

The critical properties of a superconductor may be investigated at the phenomenological level by the GL model of a complex scalar matter field ϕ coupled to a fluctuating massless gauge field $\mathbf{A}$. It is this feature of the gauge field that makes the GL model so difficult to access by the standard techniques employing the renormalisation group[2,11]. The GL model in d spatial dimensions is defined by the functional integral

$$Z = \int \mathcal{D}A_\nu \mathcal{D}\phi \exp[-\int d^d x \left[\frac{1}{4}F_{\mu\nu}^2 + |(\partial_\nu + iqA_\nu)\phi|^2 + m^2|\phi|^2 + \lambda|\phi|^4\right] \quad (1)$$

where $F_{\mu\nu} = \partial_\mu A_\nu - \partial_\nu A_\mu$, q is the charge coupling the condensate matter field ϕ to the fluctuating gauge field A_μ, λ is a self coupling, and m^2 is a mass parameter which changes sign at the mean field critical temperature. When all dimensionful quantities are expressed in powers of the scale represented by q^2, the GL model may be formulated in terms of the two dimensionless parameters $y = m^2/q^4$ and $x = \lambda/q^2$. In this case, y is temperature like and drives the system through a phase transition, and $x = \kappa^2$ is the square of the Ginzburg-Landau parameter. Depending on the value of x, the transition is either first order for $x < x_{\rm tri}$, or continuous for $x > x_{\rm tri}$[6,7,8].

In a recent paper[7], we have determined $x_{\rm tri} = 0.295 \pm 0.025$. This corresponds to a tricritical value of the GL parameter $\kappa_{\rm tri} = (0.76 \pm 0.04)/\sqrt{2}$, in rather remarkable agreement with the results of Ref. 8. *Moreover in Ref. 7 it was also argued that this value of x or κ is the demarkation value which separates type-I and type-II superconductivity, rather than the classical mean-field value* $\kappa = 1/\sqrt{2}$. The connection can be made when one realizes that *criticality* at the metal-to-superconductor transition requires that topological defects of the matter field in the form of vortex loops are stable. On the other hand, there is a connection between critical exponents and geometric properties of a tangle of such vortex loops[14]. The fractal dimension D_H of the vortex-loop tangle is connected to the anomalous scaling dimension η_ϕ[13] of the matter field in a field theory of the vortex-loop gas, a theory dual to the original GL theory[12,13] by the relation $D_H + \eta_\phi = 2$. Since the anomalous scaling dimension is connected to the order parameter exponent β of the dual matter field by the relation $2\beta = \nu(d - 2 + \eta_\phi)$[13,14], it follows that a collapse of the vortex-loop tangle implies $D_H = d$ and hence $\beta = 0$ indicative of a first order transition. Here, d is the spatial dimension of the system. Now, a collapse of the tangle in turn implies an effective attraction between vortices, or type-I behavior. On the other hand, a stable vortex-loop tangle at the critical point, with fractal dimension $D_H < d$, implies first of all type-II behavior, but also $\eta_\phi > 2 - d$ and $\beta > 0$, and hence a second order transition.

The above assertion, that the tricritical value of κ separates first order from second order metal-to-superconductor transition, and moreover also separates type-I from type-II behavior when the system is on the phase-transition line $y_c(x)$, is in contrast to the conventional wisdom that type-I and type-II superconductivity is separated by $x = 0.5$. Based on the above arguments, we have proposed the phase diagram shown in Fig. 1 of Ref. 7 which contains a new line separating type-I and type-II superconductivity. The shape of this line was inferred from the observation that far from the phase transition, mean-field estimates of the boundary between type-I and type-II should be precise, and hence this boundary should asymptotically approach $x = 0.5$ from below as the temperature is reduced.

It is the purpose of this paper to show directly, by computing the effective thermally renormalized interaction between vortices via large-scale Monte-Carlo simulations, that this quantity changes from being repulsive to attractive in the intermediate regime $\kappa \in [0.76, 1]/\sqrt{2}$. Since the sign of the vortex-interaction is the microscopic diagnostics, in terms of vortex degrees of freedom, for distinguishing type-I from type-II superconductivity, the large-scale simulations we present in this paper confirm the above conjectures and plausibility arguments of Ref. 7.

In an external field the GL model has classical solutions in terms of Abrikosov flux tubes[15], or Nielsen–Olesen vortices[16], and the concept of type-I versus type-II superconductivity is based on the interaction between these vortices. For type-I superconductors they attract each other, whereas for type-II superconductors the interaction is repulsive. Abrikosov[15] showed that at the *mean field* level type-I and type-II superconductors are separated at $\kappa = 1/\sqrt{2}$. We will refer to the value of κ separating type-I from type-II behavior at $\kappa_{\rm I/II}$, which we find varies with y. It is not a sharply defined quantity, since it represents a crossover line. The exception is at $y = y_c, x = x_{\rm tri}$, where $\kappa_{\rm I/II} = \kappa_{\rm tri}$. Elaborate calculations of vortex interactions have been carried out[17,18,19,20,21], but none of these approaches take thermal fluctuations into account. A recent overview of superconductors with κ close to $1/\sqrt{2}$ can be found in Ref. 22, see also Ref. 23.

Superconductors with $\kappa \approx 1/\sqrt{2}$ were studied extensively in the 1960s and 1970s[22], and in particular measurements on the metals Ta and Nb demonstrated that the notion of a *temperature independent* value of $\kappa_{\rm I/II}$ was incorrect[24]. At the time, this was explained with a mean-field theory involving three GL parameters[25]. Thermal fluctuations, not addressed at the mean-field level, offer an alternative and above all simpler explanation for the observations of crossovers from type-I to type-II behavior in one and the same compound as the temperature is increased.

We have performed large scale Monte Carlo (MC) simulations on the lattice version of Eq. 1, with two vortices penetrating the sample in the $\hat{z}$ direction. By measuring the interaction between these two vortices we have determined the value of $\kappa_{\rm I/II}$, in particular how this value is affected by thermal fluctuations close to the critical point.

II. MODEL, SIMULATIONS AND RESULTS

To perform simulations on Eq. 1, we have defined a discrete version as follows[27]:

$$Z = \int \mathcal{D}\boldsymbol{\alpha}\mathcal{D}\psi \exp(-S[\boldsymbol{\alpha},\psi])$$

$$S[\boldsymbol{\alpha},\psi] = \beta_G \sum_{\mathbf{x},i<j} \frac{1}{2}\alpha_{ij}(\mathbf{x})^2 - \frac{2}{\beta_G}\sum_{\mathbf{x},\hat{\imath}} \mathsf{Re}\left[\psi^*(\mathbf{x})e^{i\alpha_i(\mathbf{x})}\psi(\mathbf{x}+\hat{\imath})\right] + \beta_2 \sum_{\mathbf{x}} \psi^*(\mathbf{x})\psi(\mathbf{x}) + \frac{x}{\beta_G^3}\sum_{\mathbf{x}}\left[\psi^*(\mathbf{x})\psi(\mathbf{x})\right]^2. \quad (2)$$

In Eq. 2 $\alpha_i(\mathbf{x}) = aqA_i(\mathbf{x})$ and $\alpha_{ij} = \alpha_i(\mathbf{x}) + \alpha_j(\mathbf{x}+\hat{\imath}) - \alpha_j(\mathbf{x}) - \alpha_j(\mathbf{x}+\hat{\jmath})$. β_G and β_2 are related to the continuum parameters x and y and the lattice constant a,

$$\beta_G = \frac{1}{aq^2} \quad (3)$$

$$\beta_2 = \frac{1}{\beta_G}\left[6 + \frac{y}{\beta_G^2} - \frac{3.1759115\,(1+2x)}{2\pi\beta_G} - \frac{\left(-4+8x-8x^2\right)\left(\ln 6\beta_G + 0.09\right) - 1.1 + 4.6x}{16\pi^2\beta_G^2}\right]. \quad (4)$$

Note that β_2 contains the effect of ultraviolet renormalization in the continuum limit when the lattice constant $a \to 0$[7,26]. The model Eq. 2 is defined on a numerical grid of size $N_x \times N_y \times N_z$, corresponding to a *physical* size of $L_x \times L_y \times L_z$, with $L_i = N_i a$. All our simulations have been on cubic systems with $\beta_G = 1$.

To impose an external magnetic field[27], we modify the action Eq. 2 by changing the field energy along one stack of plaquettes located at x_0, y_0 in such a way that the action is minimized for $\alpha_{12}(x_0, y_0, z) = -2\pi n$ instead of zero, corresponding to forcing a number of n flux quanta through the system. Hence, the action $S[\alpha,\psi;n]$ for n flux-quanta forced through the system, is given by

$$S[\alpha,\psi;n] = S[\alpha,\psi;0] + \sum_z \left(2\pi n\alpha_{12}(x_0,y_0,z) + 2\pi^2 n^2\right). \quad (5)$$

The second term in Eq. 5 corresponds to forcing a flux Φ_B through the lattice in the negative z-direction

$$\frac{\alpha_{12}(x_0,y_0,z)}{q} = a^2 q\left(\nabla\times\mathbf{A}(x_0,y_0,z)\right)_z = -\frac{2\pi n}{q}. \quad (6)$$

The crucial point is that, due to periodicity, the total flux through the system *must be zero*, i.e.

$$\sum_{x,y}\alpha_{12}(x,y,z) = 0 \quad \forall z.$$

Consequently, the n flux-quanta of the total flux $2\pi n/q$ must return in the $+z$ direction. This flux returns in a manner specified by the dynamics of the theory,[27] and it is this *response* which is the topic of interest in the current paper.

The experimental situation corresponds to applying an external magnetic field H, and then study the magnetic response of the superconductor to this field. Hence, a suitable thermodynamic description is coached in terms of a potential $\Phi(H)$, which is a function of the *intensive* field variable H. In the simulations we have fixed n, which is analogous to fixing the magnetic induction, and a description based on the *extensive* field variable B is more appropriate. The two approaches are related by a Legendre transformation[27]. In principle the simulations could also be performed in an ensemble with fixed magnetic field. Technically this would be achieved by adding the term

$$HL_z 2\pi n/q$$

to the action in Eq. 1. This would promote n to a dynamical variable of the theory, and be more in accordance with the experimental situation. However, a change $n \to n \pm 1$ would require a global relaxation, and this would give very low acceptance rates, i.e. inefficient simulations.

For type-I superconductors, superconductivity vanishes for $H > H_c$. For type-II superconductors, a *flux line lattice* is formed at $H = H_{c_1}$, for smaller fields the magnetization in the sample vanishes due to the Meissner effect. By fixing n one can not study these effect directly, however it is possible to determine a corresponding field strength from n, see Ref. 27.

On the basis of simulations performed using the modified action Eq. 5, we have determined the *effec-*

tive temperature-renormalized interaction between two vortex-lines, and searched for the value of the GL parameter, or more precisely its square, $x_{\rm I/II}$, where this interaction changes character from being effectively attractive to being effectively repulsive. In section II A we have fixed $n = 2$ and studied the distance between the flux lines. In section II B we have generalized to real n, and used this to calculate a free energy difference between states containing one and two vortices. This is also a measure of the sign of the effective vortex interaction, and hence an indication of whether we have type-I or type-II behavior.

To obtain the results in Figs. 1, 2, and 5 we have performed simulations on cubic systems of size $N = 8, 12, 16, 24, 32, 48$, with $\beta_G = 1.00$. All simulations have been performed in the broken symmetry state $y < y_c$, with particular emphasis on the values $y = -0.04, -0.10, -0.20, -0.30, -0.40$. For the two largest system sizes the final datapoints are averages of approximately 10^6 sweeps, whereas approximately 10^5 sweeps have been performed for the four smallest system sizes.

The simulations leading to the results of Fig. 4 are quite different. They are performed for the fixed system parameters $N = 24$ and $\beta_G = 1.00$, and for each value of m, we have performed from $2.5 \cdot 10^4$ to $2.5 \cdot 10^5$ MC sweeps through the lattice. One sweep through the lattice consists of (1) conventional local Metropolis updates of ψ and $\mathbf{A}$, and (2) global radial updates of $|\psi|$ combined with overrelaxation[28,29] of ψ.

A. Effective vortex interaction

We first clarify what is meant by *effective vortex interaction* in this context. In the Ginzburg-Landau model at zero temperature, one may compute a pair-potential between two vortices which consists of an attractive part due to vortex-core overlap, and a repulsive part due to circulation of supercurrents (or magnetic fields) outside the vortex core. Ignoring fluctuation effects, this furnishes an adequate way of distinguishing between type-I and type-II behavior, by asking when the attractive core-contribution dominates the magnetic field contribution or vice versa. By effective interaction, we mean a thermally renormalized pair interaction which fully takes entropic contributions into account. At low temperatures the effective interaction will revert back to the standard pair-interaction described above, but will deviate as temperature is raised, and this is particularly relevant as the critical temperature is approached, as we shall see below. We also comment further on this in the Discussion section, where we elaborate on what we perceive to be a crossover between type-I and type-II behavior.

In our simulations, the value of n has been fixed to $n = 2$. This corresponds to the case of two field-induced vortices which move around in the system under the influence of their mutual effective interaction. During the simulations, we have measured the transverse position $r_\perp(z)$ of these two vortices labelled by 1 and 2, and the average distance between them.

$$\mathsf{d} = \frac{1}{N_z} \sum_z \left| r_\perp^1(z) - r_\perp^2(z) \right| . \tag{7}$$

For type-I superconductors this distance should be independent of system size, whereas for type-II we expect that this distance scales with the system size. Finite size scaling of d for various points in the (x, y) phase diagram is shown in Fig. 1.

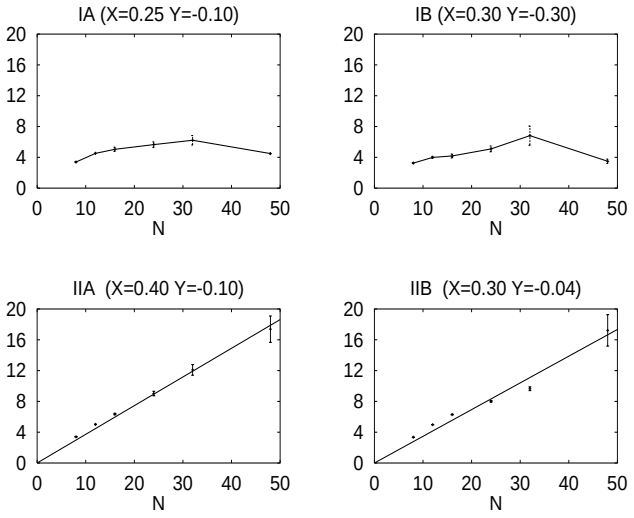

FIG. 1: The ensemble averaged separation $\langle d \rangle$ between the two vortices, as a function of system size. The two upper figures are indicative of type-I behavior, whereas the two lower ones indicate type-II behavior.

In the part of phase diagram which we focus on, namely the region defined by the dotted line in Fig.1 of Ref. 7, the vortex lines are generally directed and almost straight, well defined line objects. This can be seen either by directly taking snapshot pictures of the vortex-line configurations of the system, or by computing the mean-square fluctuations around a straight-line configuration, $\langle |r_\perp^i(z) - r_\perp^i(0)|^2 \rangle$, for *one* vortex line. This is in contrast to the situation in the vicinity of the *critical* part of $y_c(x)$ in Fig. 1 of Ref. 7, where the vortex lines loose their line tension via a vortex-loop blowout[12,13]. Consequently, we can consider the theory as an effective theory for an interacting pair of straight vortex lines which interact with the dimensionless potential $V(\mathsf{d})$. If we make this assumption, the probability of finding the vortices separated by a distance d in a system of N^3 lattice points with *periodic boundary conditions*, is given by

$$P_N(\mathsf{d}) = \frac{e^{-V(\mathsf{d})} \Omega_N(\mathsf{d})}{Z_\mathsf{d}}, \tag{8}$$

where $\Omega_N(\mathsf{d})$ is the number of configurations with a transverse vortex-vortex distance of d, and Z_d is just a

normalisation factor. $\Omega_N(\mathsf{d})$ can be calculated, either analytically in the continuum limit

$$\Omega_N(\mathsf{d}) = \begin{cases} 2\pi\mathsf{d} & \mathsf{d} < \frac{N}{2} \\ 2N\left(\frac{\pi}{2} - 2\arccos\left(\frac{N}{2\mathsf{d}}\right)\right) & \frac{N}{2} < \mathsf{d} < \frac{N}{\sqrt{2}}, \end{cases} \quad (9)$$

or by simple geometric counting in the case of a lattice. In the case of noninteracting vortices, i.e. $V(\mathsf{d}) = 0$, the expectation value of d is determined only by $\Omega_N(\mathsf{d})$, and we find the numerical value

$$\mathsf{d}_0 \equiv \langle \mathsf{d} \rangle = \frac{1}{Z_{\mathsf{d}}} \int_0^{\frac{N}{\sqrt{2}}} d\mathsf{d} \;\; \Omega_N(\mathsf{d})\mathsf{d} \approx 0.38N. \quad (10)$$

The separation d_0 defined in Eq. 10 will be used to establish a numerical value of $x_{\mathrm{I/II}}$. Namely, we can compute the averaged distance between vortices at fixed x varying y, or vice versa. In the latter case, we will use the criterion that if $\langle \mathsf{d} \rangle$ exceeds som value $c\mathsf{d}_0$ where c is some fraction, then we have type-II behavior, otherwise it is type-I. The quantity $\langle \mathsf{d} \rangle$ at fixed y will turn out to be an S-shaped curve as a function of x, increasing from small values to large values as x is increased. We interpret this as yet another manifestation of the crossover from type-I to type-II behavior, and we have chosen to locate the crossover region $x_{\mathrm{I/II}}$ at the value of x where the curves change most rapidly, which is roughly when $\langle \mathsf{d} \rangle \approx \mathsf{d}_0/2$. As we shall see (see Fig. 6), different crossover criteria give consistent results. The quantity $P_N(\mathsf{d})$ can be estimated from histograms, and then we can use Eq. 8 to determine the pair potential. Depending on whether we consider type-I or type-II superconductors we expect to see an attractive or a repulsive potential. Fig. 2 shows the potential $V(\mathsf{d})$ for the same points of the phase diagram as Fig. 1.

B. Free energy

In Eq. 5 we have used n to indicate an integer number of flux tubes, but in principle there is no reason to limit n to integer values, and we will use $S[\alpha, \psi, m]$ to denote a generalisation to real n.

We have considered the free energy difference between a state containing zero vortices, i.e. $m = 0$ and a state containing n vortices. We can not measure absolute values of the free energy, but by differentiating[27]

$$e^{-F(m)} = \mathsf{Tr} e^{-S(m)} \quad (11)$$

with respect to m, and then integrating up to n, we can calculate $\Delta F(n) = F(n) - F(0)$,

$$\frac{\Delta F(n)}{L_z q^2} = 2\pi\beta_G \int_0^n dm \underbrace{\left[2m + \frac{1}{\pi N_z} \left\langle \sum_z \alpha_{12}(x_0, y_0, z) \right\rangle_m \right]}_{\equiv W(m)}. \quad (12)$$

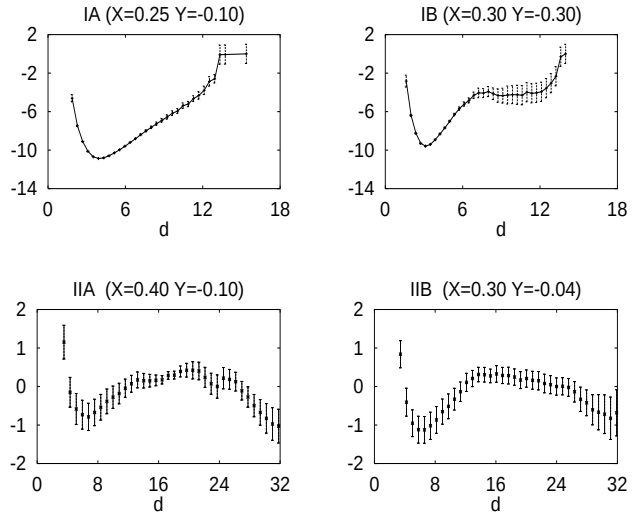

FIG. 2: The effective interaction potential between vortices $V(\mathsf{d})$ as determined from Eq. 8. Observe the difference in vertical scale, in the lower panels (type-II) the interactions are much weaker than in the upper panels (type-I). The graphs correspond to the same points in (x, y) as those in Fig. 1.

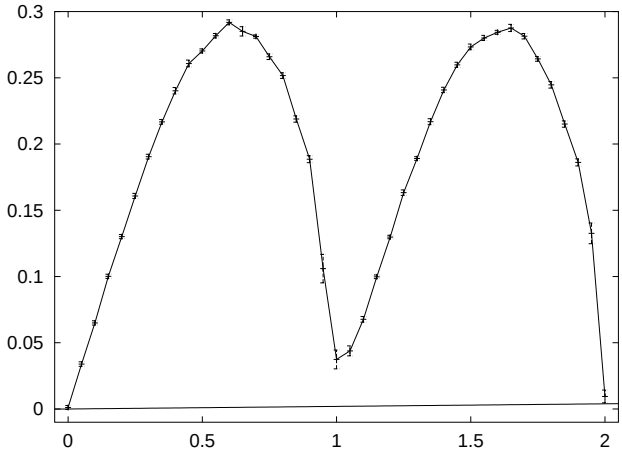

FIG. 3: $W(m)$ The straight line corresponds to $2m/N_xN_y$ which according to Eq. 13 should be satisfied for m integer.

To calculate ΔF, we have then varied m in steps of $\Delta m = 0.05$, and performed the integration in Eq. 12 numerically. Using shift symmetries, it can be shown[27] that $W(n)$ is equal to

$$W(n) = \frac{2n}{N_x N_y}, \quad (13)$$

and the behavior for intermediate real values is shown in Fig. 3. Increasing n from 0 to 1 costs a free energy $\Delta F(1)$, and adding two vortices costs an amount $\Delta F(2)$. We will *always* have $\Delta F(2) > \Delta F(1)$, but the question is whether $\Delta F(2) \gtrless 2\Delta F(1)$. We may regard $F(n+2) + F(n) - 2F(n+1)$ as the discrete second deriva-

tive of the free energy with respect to particle number, which is nothing but the inverse compressibility K^{-1} of the vortex-system. In the thermodynamic limit this quantity can never become negative. However, its vanishing signals the onset of *phase-separation* of the vortex system, which we again interpret as a lack of stability of the vortex-loop tangle, characteristic of type-I behavior.

C. Vortex compressibility, separation, and crossover

We next define a quantity ΔT by the relation

$$\Delta T = \frac{\Delta F(1)}{L_z} - \frac{\Delta F(2)}{2L_z}, \tag{14}$$

which means that ΔT measures the relative free-energy difference between adding one vortex to the system and half of that adding two vortices to the system. Intuitively it is therefore clear that it measures the sign of the vortex interactions, and hence determines whether we are in the type-I or type-II regime. $\Delta T > 0$ signals attractive interactions, i.e. type-I behavior, whereas $\Delta T \leq 0$ signals repulsive interactions, i.e. type-II behavior. We have calculated ΔT by using Eq. 12 and Eq. 14, the results are shown in Fig. 4. The main qualitative result from these simulations is again that $x_{\mathrm{I/II}}(y)$ is a declining function of y. Note also that $K^{-1} = -\Delta T$, and hence a positive ΔT clearly implies phase-separation and instability of the vortex system, characteristic of type-I behavior. This is precisely what we see for small x in Fig. 4.

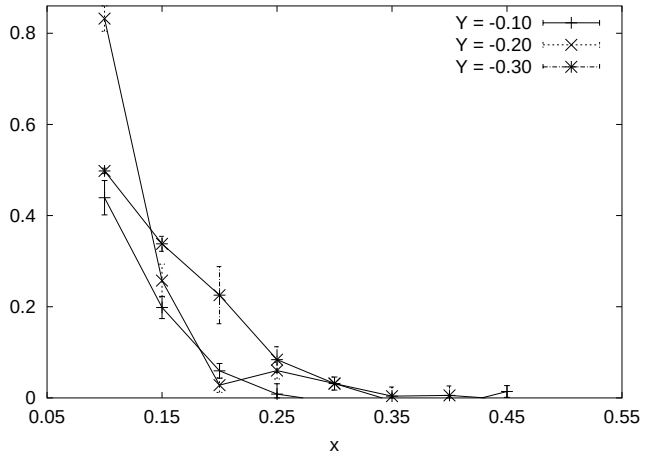

FIG. 4: $\Delta T(x)$ for different values of y. The attraction vanishes for $x_{\mathrm{I/II}} < 0.5$, and $x_{\mathrm{I/II}}(y)$ is an increasing function of $|y|$.

Finite size scaling of $\langle \mathsf{d} \rangle$ and studies of ΔT differentiate nicely between strongly type-I and type-II superconductors, but it is difficult to locate a value of $x_{\mathrm{I/II}}(y)$ with any great precision. Fig. 5 shows $\langle \mathsf{d} \rangle(x)$ for different values of y, along with a horizontal line at $\mathsf{d}_0/2$, where d_0 is the average separation between vortices had they been non-interacting. We have found that $\mathsf{d}_0 \approx 0.38N$ in our simulations. We have, rather arbitrarily, taken the interception of this horizontal line with the curve $\langle \mathsf{d} \rangle(x)$ as $x_{\mathrm{I/II}}$.

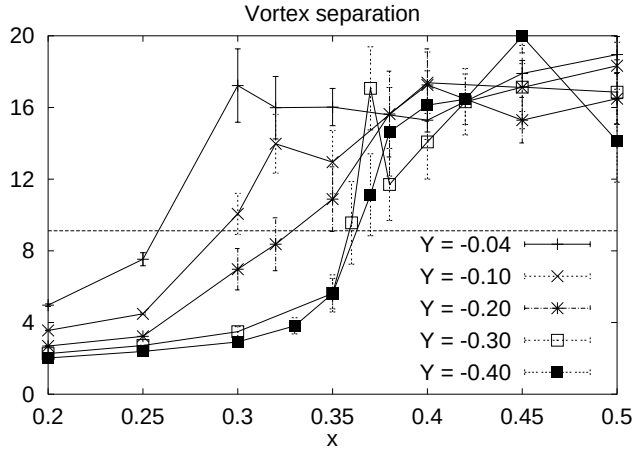

FIG. 5: The ensemble averaged distance between a pair of vortices, $\langle \mathsf{d} \rangle$, as a function of the square of the Ginzburg-Landau parameter $x = \kappa^2$, for various values of the temperature-like variable y. The horizontal line is at $\mathsf{d}_0/2$. Increasing y amounts to increasing the temperature.

The curves of $\langle \mathsf{d} \rangle(x)$ do not get significantly sharper with increasing system size, and there are no particular sharp features in $S[\alpha, \psi, 2]$ as x is increased beyond $x_{\mathrm{I/II}}$. Fig. 6 shows the intercepts from Fig. 5. Due to the features in the curves of Fig. 5, and how the results of Fig. 6 are obtained from them, we tentatively conclude that the computed line of Fig. 6, corresponding to the dashed line of Fig. 1 in Ref. 7, is a *crossover* and *not* a phase transition. However, we comment further on this in the concluding section.

As already indicated, there is some arbitrariness in the location of $x_{\mathrm{I/II}}(y)$ in Fig. 6, however the four points labelled by (IA, IB) and (IIA, IIB) clearly are in the type-I and type-II regimes, respectivly. This is demonstrated in Figs. 1 and 2.

III. DISCUSSION

From Figs. 1 and 2 we conclude that there is a crossover line separating effective attractive vortex interactions from effective repulsive ones, i.e. type-I and type-II. This line can either be crossed by changing x, i.e. IA $\rightarrow$ IIA, or by changing the temperature i.e. IB $\rightarrow$ IIB in Fig. 6. This means that for x values in a suitable range, we can have in principle have a *temperature induced* crossover from type-I to type-II superconductivity. Finally, we note that $x_{\mathrm{I/II}}(y)$ deviates significantly from the mean-field value of $x_{\mathrm{I/II}} = 0.5$.

Deep in the type-I regime, we find clear evidence of *attractive* interactions. In the type-II regime the repulsive

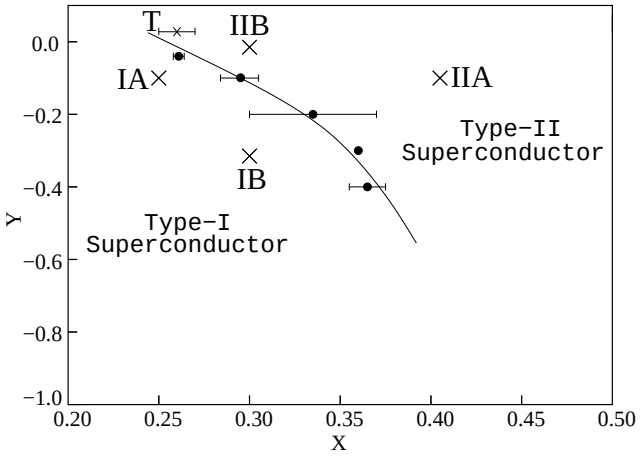

FIG. 6: The computed crossover line $y_{\rm I/II}(x)$ separating type-I and type-II superconductivity. The black circular filled points are given by the intercepts between $\mathsf{d}_0/2$ and the curves in Fig. 5. The four points labelled by (IA, IB, IIA, IIB) are the ones that were considered in detail in Figs. 1 and 2. The point marked T is the *tricritical* point in Fig. 1 of Ref. 7, see the discussion of finite size effects in section III A. The solid line connecting the points is *purely* a guide to the eye. The computed line above corresponds to the dotted line of Fig. 1 in Ref. 7 in the vicinity of $(x_{\rm tri}, y_{\rm tri})$.

interactions appear to be weak, and the results are essentially also consistent with two *randomly placed* vortex lines, i.e. not interacting, but not consistent with an attractive force between the vortices. Therefore, what the results unequivocally show is that by fixing the material parameter x and varying the temperature-like variable y, the character of the effective pair-potential is altered inside the superconducting regime, significantly away from the critical line.

A. Simulations

The simulations with $n = 2$, and the simulations with a real $m \in [0, 2]$ are quite different, and we will discuss them in turn. An important feature of *all the simulations* in the present work is *slow dynamics*.

For the $n = 2$ simulation, where we have monitored d, we find that deep in the type-I regime the simulations are quite straightforward, the vortices stay close together with only small fluctuations, and a moderate number of sweeps is sufficient to get good statistics. However when we increase x towards $x_{\rm I/II}$ the effect is *not* that d stabilises at a higher value, instead we get get fluctuations between a type-I like state where the two vortices are close together, and a type-II like state with large vortex-vortex separation. This picture persists as x is increased into the type-II regime, the only difference is that the fraction of time spent in the type-I like state state decreases. In fact the results of Fig. 1 and Fig. 2 are in the type-II region quite close to what we would get from noninteracting vortices. What makes the simulations difficult is that moving a vortex line in the transverse direction is a *global* change, and thereby very slow. Timeseries of d show characteristic time scales of 10^4 sweeps, so long simulations $\sim 10^6$ sweeps over the lattice are required to obtain acceptable accuracy. A truly high-precision determination of $x_{\rm I/II}(y)$ would surely benefit from a specialized algorithm for the MC updates.

To get good results one should take the $N \to \infty$ limit. The conclusions from the results of Fig. 1 are based on this limit, whereas those drawn from Figs. 2,5 and 6 are based on the fixed system size $N = 48$. We have not performed a systematic study of finite size effects, but the curves in Fig. 5 *do have* subject to finite size effects in them. The trend is that curves move to the right upon increasing system size, this very likely explains the apparent discrepancy between the tricritical point (where the $N \to \infty$ limit has been applied), and the remaining points in Fig. 6.

Note that Eq. 1 is a continuum field theory, and $x_{\rm I/II}(y)$ is *not* a critical point, hence the continuum limit $\beta_G \to \infty$ should be taken. Our experience from the large-scale simulations performed in Ref. 7 indicates that $\beta_G = 1.00$ provides conditions in the simulations already quite close to the continuum limit. We have therefore chosen to work with $\beta_G = 1.00$ and focused our efforts on considering large systems and long simulations.

The Monte-Carlo computations of ΔT have been even more time consuming, because we have had to do the simulations for 41 different values of m. We have therefore limited ourselves to considering only the system $L = 24, \beta_G = 1.00$, for a discussion of finite N / finite β_G effects see Ref. 27. The relaxation time for these simulations has been particularly long in the limits $m \to 1^-$ and $m \to 2^{-1}$, and we therefore have performed much longer simulations in these limits than for intermediate values of m. From Fig. 3 and Eq. 13 it is seen that $W(m)$ is a quantity of order $\mathcal{O}(N^{-2})$ whose finiteness originates in the difference between two $\mathcal{O}(1)$ quantities. Consequently, it is difficult to get numerically precise results. This has in particular been the case in the limits $m \to 1^-$ and $m \to 2^-$.

B. Crossover

The physical picture that emerges for the thermal renormalization of the vortex interactions, is the following. At low temperatures, for the κ-values we consider, the system is in the type-I region with a fairly deep minimum in the effective pair-potential between vortices at short distances, leading to an attractive interaction. At very short distances, we find a steric repulsion on the scale of the lattice constants in the system due to the large Coulomb barrier that must be overcome to occupy a link with two or more elementary vortex segments. This lenght scale represents the size of the vortex core in the problem. Upon increasing the temperature to the vicinity

of the line $y_c(x)$, we do not find large transverse meanderings of the individual vortex lines as we move along each vortex line, rather the vortex lines are essentially straight. Therefore, we believe that it is *not* entropic repulsion due to the bare steric repulsion in the problem, of the type which it seems reasonable to invoke for *strongly* fluctuating elastic strings[30,31] that renormalizes the vortex interactions in the way that is seen in Fig. 2. Rather, what appears to happen is that the vortex lines slosh back and forth in the minimum of the effective potential well as essentially straight lines. Hence, to a larger and larger extent as temperature is increased, they experience the hard wall in the interactions at small distances, and the weak attraction at large distances, effectively washing out the minimum in the potential, thus making it effectively more repulsive.

This is also seen in our simulations (not shown in any of the figures) when we monitor the transverse meandering fluctuations of each vortex line, $\langle |r_\perp(z) - r_\perp(0)|^2 \rangle$, as well as the mean square fluctuations of the intervortex distance, $\langle \mathsf{d}^2 \rangle - \langle \mathsf{d} \rangle^2$, where d is defined in Eq. (7). The former is small deep in the superconducting regime, and remains small as the line $y_c(x)$ in Fig. 1 of Ref. 7 is approached, while the latter increases dramatically as the dotted crossover line is crossed. It is precisely this fact which makes the simulations extremely time consuming.

One should however keep in mind that, since we are considering the full GL theory in our simulations, and not the linearized London limit, it is in any case a drastic simplification to view the effective interaction between vortices as a simple pair potential.

Finally, we note that, although our present simulations, which by necessity are on finite-sized systems, indicate that the change from type-I to type-II behavior is a crossover, we cannot rule out the possibility that it is elevated to a true phase-transition in the thermodynamic limit. More work is needed to clarify if this is indeed the case, but this will have to await the next generation of massive parallell computers. Questions that need to be addressed in this context, are: What is the order parameter of such a transition, and what symmetry, if any, is being broken.

IV. CONCLUSION

We have considered the effective interaction between two vortices in the full GL model, and how this effective interaction is influenced by thermal fluctuations. We have included fluctuations in the gauge fields, as well as the phase- and amplitude-fluctuations of the complex scalar matter field of the problem. We have found that the effective interaction changes from being attractive to being repulsive at $x_{\mathrm{I/II}}$. This means a change from type-I to type-II behavior. We have found that $x_{\mathrm{I/II}}$ is below the standard quoted value of 0.5, and is a function of the temperature-like parameter y. This means that at the critical point, the value of the GL parameter that separates type-I from type-I behavior is smaller than $1/\sqrt{2}$. The line $x_{\mathrm{I/II}}(y)$ appears to be a crossover, and not a true phase transition. The above seems to offer a simple explanation for the experimental observation that elemental Ta and Nb superconductors show a crossover from type-I to type-II behavior as the temperature is increased towards T_c. Previous explanations based on mean-field theories and not involving thermal fluctuations required two additional temperature dependent κ-values to be defined[25].

We acknowledge support from the Norwegian Research Council via the High Performance Computing Program (S.M.,J.H.,A.S.), and Grant Nos. 124106/410 (S.M.,A.S.) and 148825/432 (A.S.), and A.S. thanks E. H. Brandt for useful comments. J.H. also acknowledges support from NTNU via a university fellowship.

* Electronic address: Joakim.Hove@phys.ntnu.no
† Electronic address: Sjur.Mo@phys.ntnu.no
‡ Electronic address: Asle.Sudbo@phys.ntnu.no

[1] V. L. Ginzburg and L. D. Landau, Zh. Eksp. Teor. Fiz. **20**, 1064 (1950).
[2] B. I. Halperin, T. C. Lubensky, and S. K. Ma, Phys. Rev. Lett. **32**, 292 (1974).
[3] S. Coleman and E. Weinberg, Phys. Rev. D **7**, 1988 (1973).
[4] The efforts of Refs. 2 and 3 appear to be among the first to seriously adress the principle of emergent order from disorder.
[5] C. Dasgupta and B. I. Halperin, Phys. Rev. Lett. **47**, 1556 (1981).
[6] J. Bartholomew, Phys. Rev. B **28**, 5378 (1983).
[7] S. Mo, J. Hove, and A. Sudbø, Phys. Rev. B **65**, 104501, (2002), [cond-mat/0109260 (2001)].
[8] H. Kleinert, Lett. Nuovo Cimento **35**, 405 (1982).
[9] It is customary to describe as tricritical any point in a parameter space at which a continuous transition becomes discontinuous, irrespective of the number of phases which co-exist along the first-order line or surfaces of critical points which, in a suitably enlarged parameter space may be found to meet here[10].
[10] I. D. Lawrie and S. Sarbach in *Phase Transitions and critical phenomena*, eds C. Domb and M. S. Green, Academic Press, (1984).
[11] Had the gauge-field been *massive* it could have been integrated out with impunity to yield an effective $|\phi|^4$-term, and the theory would yield nicely to renormalization group treatment of the sort that has been successful for Helium IV. In fact, there exists a dual formulation of the three-dimensional Ginzburg-Landau theory which is a new Ginzburg-Landau theory with such a massive gauge-field, see Refs. 7,8,12,13.
[12] Z. Tešanović, Phys. Rev. B **59**, 6449 (1999).
[13] A. K. Nguyen and A. Sudbø, Phys. Rev. B **60**, 15307

(1999).
[14] J. Hove and A. Sudbø, Phys. Rev. Lett. **84**, 3426 (2000).
[15] A. A. Abrikosov, Sov. Phys. JETP **5**, 1174 (1957).
[16] H. B. Nielsen and P. Olesen, Nucl. Phys. B **61**, 45 (1973).
[17] E. Müller-Hartmann, Phys. Lett. **23**, 521 (1966), *ibid* 619.
[18] L. Jacobs and C. Rebbi, Phys. Rev. B **19**, 4486 (1979).
[19] L. Kramer, Phys. Rev. B **3**, 3821 (1971).
[20] E. B. Bogomol'nyi, Sov. J. Nucl. Phys. **23**, 588 (1976).
[21] E. B. Bogomol'nyi, Sov. J. Nucl. Phys. **24**, 449 (1976).
[22] I. Luk'yanchuk, Phys. Rev. B **63**, 174504 (2001).
[23] H. Kleinert and F. S. Nogueira, `cond-mat/0104573`.
[24] J. Auer and H. Ullmaier, Phys. Rev. B **7**, 136 (1973).
[25] K. Maki, Physics **1**, 21 (1964); G. Eilenberger, Phys. Rev. **153**, 584 (1967). See also Ref. 24, section III.E.
[26] M. Laine and A. Rajantie, Nucl. Phys. B **513**, 471 (1998) [`hep-lat/9705003`].
[27] K. Kajantie, M. Laine, T. Neuhaus, A. Rajantie and K. Rummukainen, Nucl. Phys. B **559**, 395 (1999)[`hep-lat/9906028`].
[28] K. Kajantie, M. Laine, K. Rummukainen, and M. Shaposhnikov, Nucl. Phys. B **466**, 189 (1996)[`hep-lat/9510020`].
[29] P. Dimopoulos, K. Farakos and G. Koutsoumbas, Eur. Phys. J. C **16**, 489 (2000)[`hep-lat/9911012`].
[30] J. Zaanen, Phys. Rev. Lett. **84**, 753 (2000).
[31] S. Mukhin, W. van Saarloos, and J. Zaanen, Phys. Rev. B **64**, 5105 (2001)[`cond-mat/0103253`].